Hypercontraction and *Drosophila*: A model system for the study of human myopathies

By

Enrico Sakai Montana

B.S. Biology: Molecular Genetics
University of Rochester, 1999

SUBMITTED TO THE DEPARTMENT OF BIOLOGY IN PARTIAL FULFILLMENT OF THE REQUIREMENT FOR THE DEGREE OF

DOCTOR OF PHILOSOPHY

AT THE
MASSACHUSETTS INSTITUTE OF TECHNOLOGY

ARCHIVES

Signature of Author: _____
Enrico Sakai Montana

Certified by: _____
J. Troy Littleton
Associate Professor of Biology
Thesis Supervisor

Accepted by: _____
Stephen P. Bell
Professor of Biology
Chairman of the Graduate Committee

Hypercontraction and *Drosophila*: A model system for the study of human myopathies

by

Enrico Sakai Montana

Submitted to the Department of Biology
on July 29, 2005 in Partial Fulfillment of the
Requirements for the Degree of
Doctor of Philosophy in Neurobiology

ABSTRACT

Currently, there are no therapeutic interventions which fully alleviate the defects associated with muscular dystrophies and cardiomyopathies. Development of model systems in which to utilize high-throughput screens for novel compounds will help in drug discovery for these diseases. In addition, genetic model systems will allow us to dissect the molecular and cellular pathways activated in response to mutations that affect muscle function, increasing our understanding of the underlying physiology of normal and diseased muscles.

Here we present work establishing *Drosophila* as a model system for human muscular dystrophies and cardiomyopathies. Characterization of hypercontraction-induced myopathy caused by mutations in *Myosin Heavy Chain* has led to a potential mechanism of hypercontraction through unregulated contraction cycles in mutant muscles. In addition, hypercontraction defects cause temperature-sensitive myogenic seizures due to an altered state of the muscle which is fundamentally different than normal and hypocontracted muscle. Analysis revealed strong parallels between the genetics of flight behavior in *Drosophila* and familial hypertrophic cardiomyopathies in humans, suggesting that the altered state in hypercontraction muscles may reflect diseased states in mammals.

Expression analysis of hypercontraction suggests a conservation of the cellular response induced in muscles which have contractile dysfunctions. This response includes the upregulation of developmentally-regulated transcripts and immune-response genes, and a downregulation of energy and metabolism genes. In addition to these parallels in transcriptional regulation in response to hypercontraction and human myopathies, a potential actin remodeling response has been uncovered. This remodeling response may be utilized in other contexts such as activity-dependent synaptic strengthening in the nervous system.

Current studies on the functional consequences of differential regulation have begun. Loss-of-function mutations in the highest upregulated transcript, *dARC1* suggests the dARC1 protein does not mediate essential roles in synaptic transmission, short-term plasticity, learning and memory of courtship, and circadian rhythms. It may be that *dARC1* underlies subtle modulation of these processes which may be inaccessible by our assays. Future studies will address its role in muscle remodeling and synaptic metaplasticity.

Acknowledgments

First and foremost, I would like to thank my parents. They have instilled in me the drive to succeed in everything with which I am involved. They have also taught me that in life, it is always better to try and fail than to not attempt something because I do not know the outcome beforehand. If I always wait until I have more experience and information, then I would wait for the rest of my life. Without the encouragement and support they have given me since the day I was born, I never would have gotten to this point, let alone succeeding through school and college. For always being there to support me emotionally, spiritually, and monetarily (in case you do not know, graduate students earn very little), I am forever grateful and will never be able to express this gratitude in words.

I would like to thank my friends. I could list them all, but I may end up doubling the length of this thesis. You know who you are, and I know who you are. Thank you for keeping me grounded to life and always reminding me that there is definitely more out there than minipreps and HL3. Thank you also for always showing interest in what I do and supporting me through this long process of education. You experienced all extremes of my personality and yet you are still there. I will always return the favor.

To my committee, thank you for your role in making this thesis something that I can be proud of. Without continual debate and challenge, any scientific inquiry quickly falls into the hazy realm of opinion. Through both your encouragement and questioning, I have done more than I could ever imagine. And though this thesis seems almost like an unfinished symphony, one big lesson I have learned is that good science does not present answers, but only presents a larger picture containing more questions. Without this lesson, one cannot appreciate the steps they have gained in the scientific endeavor.

To all the influential educators in my life that have taught me to follow my dreams—so many and so little space. I wish I could mention you all. You have taught me the importance of significant figures and carrying the ones to the necessity of music and the beauty of art. The diversity of education was essential in my development as a student, from kindergarten through graduate school.

I owe a lot thanks to my colleagues and fellow graduate students. In particular, Bill Adolfsen and Moto Yoshihara have always, ALWAYS been there to provide critical and necessary input throughout the development of this project. Even when I wanted an agreeing mind, I usually got criticism and debate. I truly think that I never would have made any progress without you two. And Bill, you were the only one dumb enough to be in the lab on a Saturday night with me. Some of

our craziest and inane ideas as well as successful ones have come about because of weekends at the lab.

Kathy Galle, well, what can I say? You put up with a lot through these past couple years and yet we make it work. Especially in the last couple of months, you have really been patient as I stressfully tried to tie up so many loose ends as I came to the end of my graduate career. Thank you for being there for me.

To Troy, I owe so much for the mentoring and training. You have been patient as I stubbornly went my own way and always there when I asked for advice and help. Your excitement in science is mind-boggling and has always been integral to me picking myself up, failed experiment after failed experiment. There have been times that I know I have been very difficult as a graduate student, you have given me the space and resources to learn something new, even if what I learned was that I was completely wrong. Thank you for everything.

And finally, though it may sound a little odd coming from a scientist, I would like to thank God. There is no proof or absolute truth when it comes to the existence of God—only faith. My faith has given me answers when nothing else could. And, admittedly, though those answers seem so counterintuitive sometimes, it works. Without faith, I probably would not have gotten through the lows of my life, and would not appreciate the highs either. And, if it weren't for God, this world would not exist for me to explore and question, and where would I be without that?

Thank you everyone in helping me get here and finishing what I started. I know you will always be there for me in the future, as I will for you.

Introduction

Introduction

Muscle Contraction

Muscular dystrophy represents a diverse group of human diseases that are characterized by a progressive degeneration and weakness of the skeletal musculature. Connective tissue accumulates with the progression of the disease, reflecting the slowly deteriorating cycle of degeneration and regeneration of the muscle. There are no current therapeutic interventions that fully alleviate the defects of these diseases. With Duchenne's Muscular Dystrophy alone affecting 1/3500 males, muscular dystrophies represent a widespread problem requiring the development of novel therapeutics (Hoffman et al., 1987b).

In order to understand how alterations in a large number of genes can lead to myopathy, an understanding of normal muscle function is required. The muscle utilizes specialized mechanisms to transform chemical energy into mechanical energy through a highly-coordinated and complex network of proteins. At the center of movement is the contractile machinery—the basal set of proteins which produce motion.

The contractile apparatus, at its basic form, consists of two, interlocked filaments, arrayed in a hexagonal pattern in parallel fibers along the axis of the muscle. The thin filament consists of a polymer of actin, whereas the thick filament consists of a polymer of myosin heavy chain (Mhc). The actin acts as a

track for the motor protein Mhc to ratchet along, shortening the length of the muscle along the axis of the filament array (Figure 1).

The basic mechanism of contraction involves an ATP-dependent process which begins with the binding of ATP to the Mhc head. The hydrolysis of ATP into ADP and P_i allows the Mhc to bind to the actin filament. Once bound, actin stimulates release of P_i, causing a conformational change in Mhc into a high-force state. Finally, Mhc is released from the actin by exchange of ADP with ATP (Figure 1). Multiple modes of regulation must occur for effective and efficient contraction.

The first level of regulation is to limit when Mhc may bind the actin filaments. This allows for concerted timing of Mhc motor activity, preventing unregulated contraction from occurring. This regulation is largely provided by a second protein that is polymerized onto the actin filament, tropomyosin (Tm). The Tm molecule serves two purposes for contraction. The first is to prevent unregulated binding of Mhc, and the second is to allosterically enhance Mhc ATP hydrolysis in order to increase the speed of contraction. In the absence of Tm, actin acts as a linear catalyst of ATPase activity in Mhc. However, in the presence of Tm, the ATPase activity becomes sigmoidal, indicating that Tm acts to create a cooperative reaction when Mhc-ATP binds the actin cytoskeleton. Therefore, Tm provides a mechanism in which actin can exist in two states (on/off). Tm regulation provides the off state in order to prevent unregulated contractions, and the on state for fast, concerted Mhc function.

Figure 1

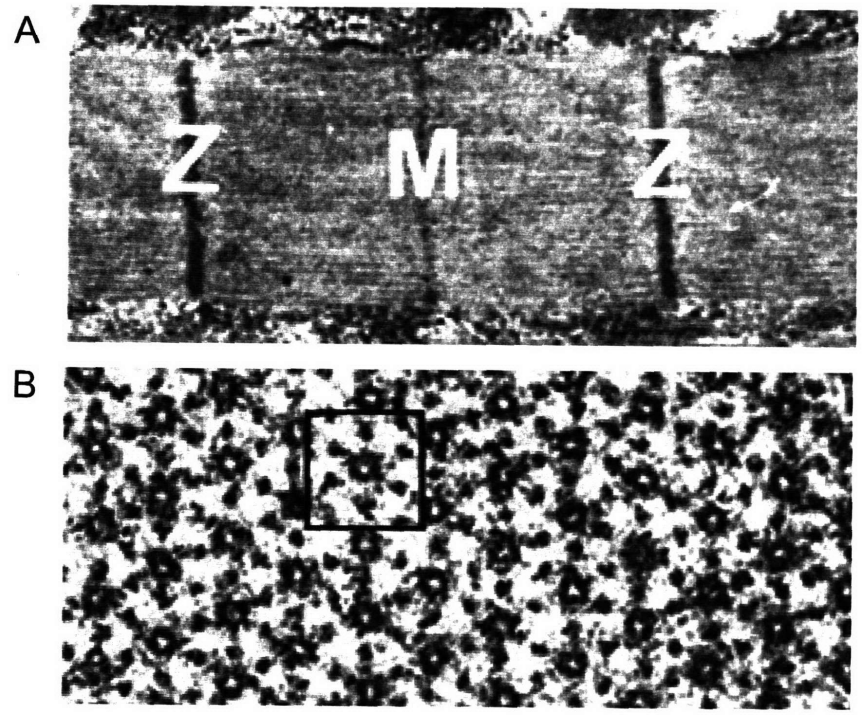

Figure 1: The General Structure of the Sarcomere (A) The longitudinal section of a *Drosophila* flight muscle illustrates how striations occur in the muscle from the ordered array of parallel fibers in the sarcomere. Z and M demarcate the location of the M-line and Z-line. (B) These fibers are arranged in a 6:1 thin:thick filament hexagonal array as seen in a transverse section. Note the box highlighting a single hexagonal array. (C) A schematic diagram illustrating the general ATPase cycle of the myosin heavy chain motor through one cycle of contraction. (A) and (B) were adapted from (Kronert et al., 1999) and (C) from (Lehrer and Geeves, 1998).

The off state induced by Tm results from a physical blockage of Mhc binding. This blockage underlies a second-order point of regulation for contraction. This regulation is mediated by the troponin (Tn) complex containing TnI, TnT, and TnC, which is bound to the thin filament. For every seven actin monomers, there is one Tm molecule and one Tn complex (Figure 2). At rest, the Tn complex keeps the actin filament in a closed state through TnI, preventing Tm from exposing the Mhc binding site. Upon muscle activation, the intracellular Ca^{2+} concentration increases, allowing Ca^{2+} to bind to TnC. Once bound, the Tn complex shifts in conformation, preventing TnI from maintaining Tm in an inhibiting state, allowing the thin filament to go into the open complex to activate contraction. Initially, only a few Mhc heads bind, as most TnI complexes remain in the closed state. However, through cooperative mechanisms, once a sufficient number of Mhc heads have bound to the thin filament, the remaining Tn complexes transition into the open state, synchronizing the binding of many Mhc heads, and contraction proceeds. Muscle contraction occurs over a distance much larger than the single ratchet motion of a Mhc motor, and thus must continue cyclically in order to gain macroscopic distances. For this to occur, not all of the Mhc molecules release the filament. Instead, several remain bound to the actin, keeping the filament in the open state for successive rounds of Mhc activity (Figure 2; Lehrer and Geeves, 1998).

The filament within the muscle can produce no force without leverage. Otherwise, the filaments will slide past each other but the membrane will remain in position. In order to contract the cell, points of architectural support provide

Figure 2

A

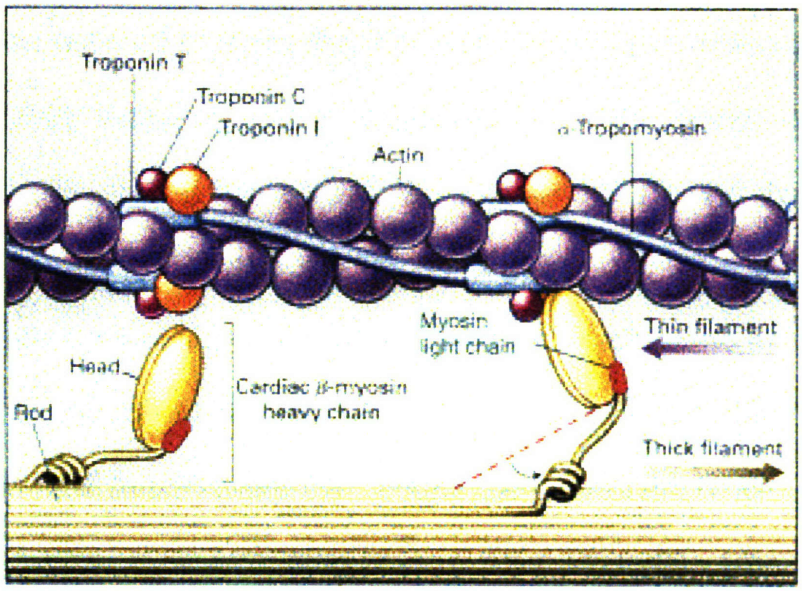

B

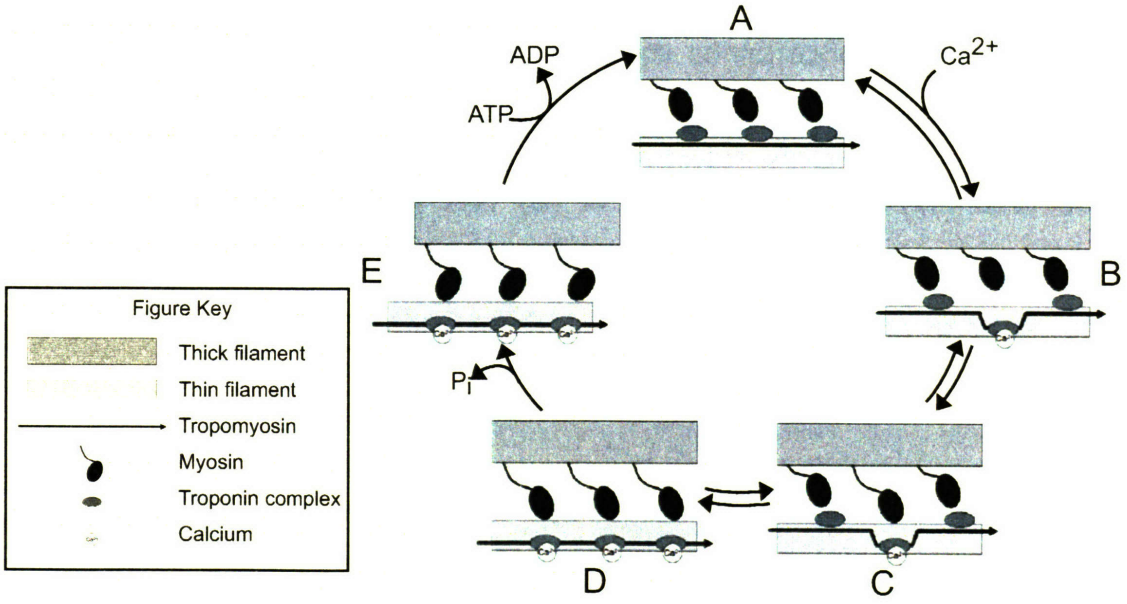

Figure 2: The contractile machinery represents a tightly regulated molecular machine (A) A schematic diagram illustrates the major components of muscle contraction, along with the regulatory components on the thin filament. For every seven actin monomers, there is one tropomyosin molecule, and one troponin regulatory complex. (B) A simplified five-state model for a single contractile cycle, illustrating the roles of Tm, troponin, Ca^{2+}, and the contractile proteins Mhc and actin. This model is based upon models in which the thin filament regulates contraction in a classical cooperative/allosteric manner. State A represents the muscle at rest, with Mhc bound to ATP and the thin filament inhibited. Upon muscle activation, Ca^{2+} enters the cytoplasm, binding troponin C and opening a limited number of Mhc binding sites (State B). Mhc binds these open sites (State C), and upon a threshold number of bound Mhc, cooperative mechanisms lead to a coincident binding of the remaining Mhc heads in State D. Release of P_i causes Mhc to enter the high-force conformation in State E, and subsequent exchange of ADP/ATP releases the Mhc. (A) is reproduced from (Seidman and Seidman, 2001) and (B) is reproduced from (Montana and Littleton, 2004).

leverage and attach the contractile machinery to the membrane as well as the extracellular matrix. These structural sites include the Z-line, nuclear membrane, plasma membrane, and the extracellular matrix. It is these sites which become critical in the overall function of the muscle, as mutating the molecular constituents of these key stress points often leads to muscular dystrophies in humans.

The Genetics of Muscular Dystrophy

Until nearly 20 years ago, the underlying genetic causes of muscular dystrophies remained a mystery. Beginning with the discovery of the dystrophin protein in 1987, identification of the genetic causes of a large and diverse number of muscular dystrophies has increased. The overall theme uniting these diseases is that mutated genes seem to normally function in providing or modulating the structural support of the contractile machinery at key stress points within the cell. However, it is unclear how disruptions of these proteins lead to degeneration of the muscle. Although many studies have been directed at determining the genetic causes of muscular dystrophy, much less is known about the downstream effects and eventual long-term changes that occur in diseased states of the muscle.

Duchenne's Muscular Dystrophy, and later Becker's Muscular Dystrophy, was found to be caused by disruptions in a large gene known as dystrophin (Hoffman et al., 1987a; Hoffman et al., 1987b; Koenig et al., 1987; Monaco et al.,

1985; Monaco et al., 1986; Ray et al., 1985). This gene spans almost 2.5Mb of genomic DNA, containing over 85 exons and encoding a 14kb transcript corresponding to a 427 kDa protein. Given its large size, it is not surprising that its mutation rate is close to 1/10000 gametes in the human population, which contributes to its relatively large prevalence (Hoffman and Dressman, 2001). The dystrophin protein plays a critical role in sarcolemma (muscle plasma membrane) stability and support, connecting the cytoskeleton to the plasma membrane.

The dystrophin complex associates the cytoskeleton with the plasma membrane *via* interactions involving the dystroglycan complex (DGC) of proteins. This complex includes α-, β-, γ-, and δ-sarcoglycan, α- and β-dystroglycan, syntrophin, and dystrobrevin (Figure 3). Underscoring the central theme of structural support underlying muscular dystrophies, mutations in these architectural proteins lead to other forms of muscular dystrophy. Limb-girdle muscular dystrophy (LGMD) type 2D, 2E, 2F, and 2C correspond to mutations in α-, β-, γ-, and δ-sarcoglycans (Bonnemann et al., 1995; Matsumura et al., 1992; Nigro et al., 1996; Roberds et al., 1994). Additionally, another protein in the sarcolemma, dysferlin, has been identified as the gene responsible for LGMD2B and distal muscular dystrophy of Miyoshi (McNally et al., 2000). Caveolin-3, a protein that is associated to the DGC and dystrophin, is mutated in LGMD1C (Minetti et al., 1998).

In addition to providing a point of support connecting the cytoskeleton to the membrane, the DGC also provides a leverage point for connections to the

Figure 3

A

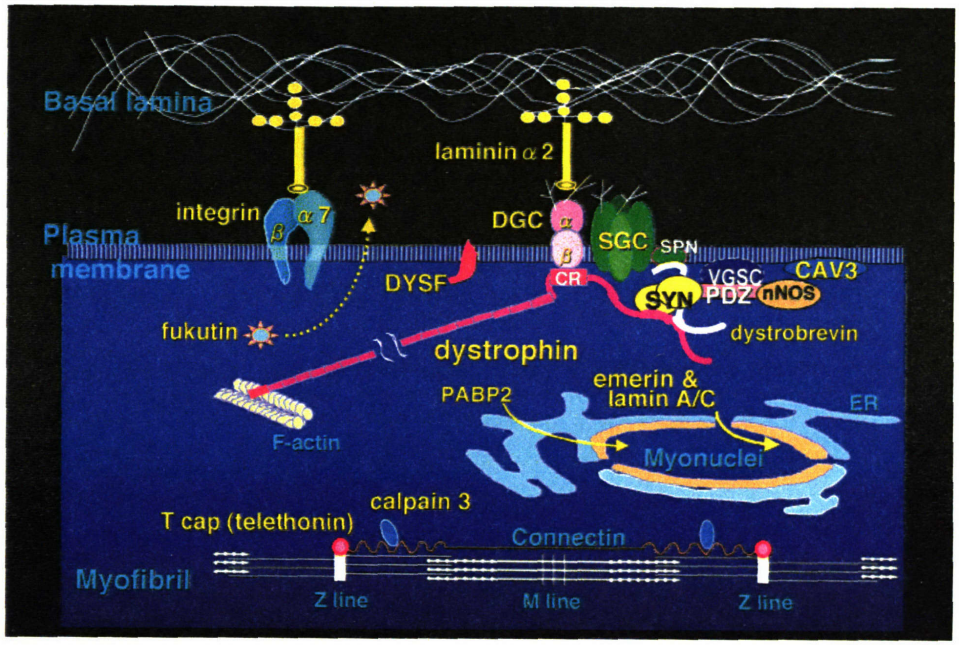

B

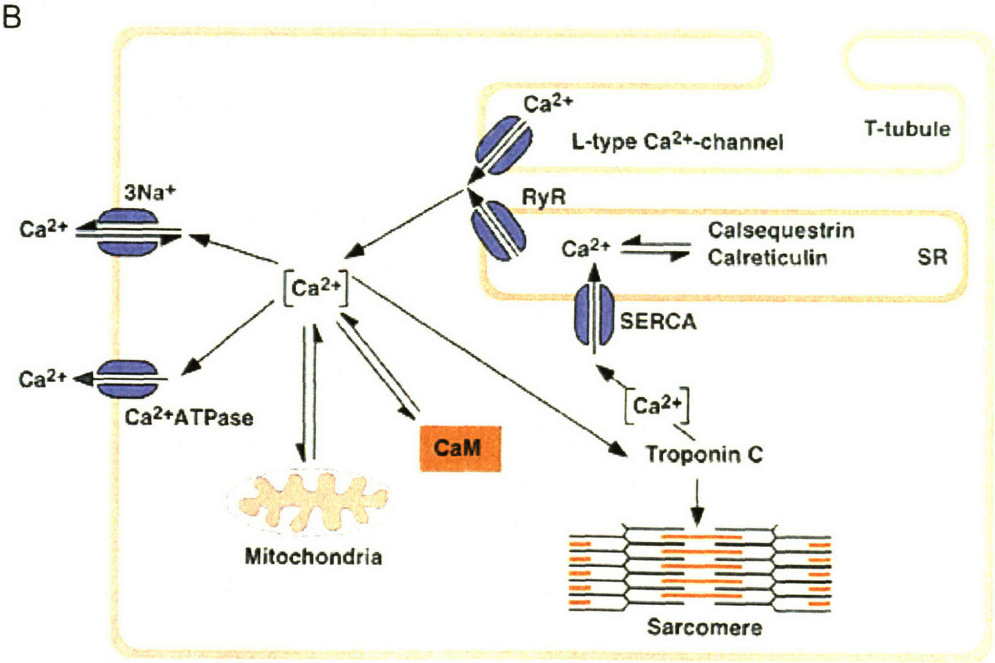

Figure 3: The complexities of muscular dystrophy (A) This figure illustrates only a subset of genes that have been identified which are affected in a number of muscular dystrophies. These components form a large complex of proteins which provide both support for the cell as well as fulcrums for leverage in contraction. (B) A schematic diagram illustrating the major points of control for Ca^{2+} homeostasis in the muscle. These include the sarcolemma, the sarcoplasmic reticulum, the mitochondria, and cytoplasmic buffers. (A) was reproduced from (Arahata, 2000) and (B) was reproduced from (Frey et al., 2000).

extracellular matrix. This connection is mediated by laminin A and C, the gene underlying LGMD1B (Muchir et al., 2000). Another protein thought to play a role in the extracellular matrix is a secreted protein known as fukutin. Deficiencies in this gene have been shown to lead to Fukuyama Congenital muscular dystrophy (Kobayashi et al., 1998). Laminin $\alpha 2$ chain, and an important laminin receptor, integrin $\alpha 7$, are responsible for two forms of congenital muscular dystrophies (Kobayashi et al., 1998; Mayer et al., 1997).

Although many of the muscular dystrophies so far have focused on structural elements extending outward from the cytoskeleton, there are other diseases which affect structural elements from the sarcomere, inward to the nuclei of the muscle. The nuclear membrane seems to be another key structural site within the muscle as several proteins on the nuclear membrane have been implicated in muscular dystrophy. The nuclei require adequate support in order to withstand the constant force generation produced by muscle contraction. The proteins involved in strengthening the nuclear membrane include emerin and lamin A/C. The lamin proteins are intermediate-type filaments found on the nuclear envelope, a component of a network of proteins which stabilize the nuclei under the stress forces of contraction. Mutations in these genes are responsible for two types of Emery-Dreifuss muscular dystrophy (Raffaele Di Barletta et al., 2000).

Calcium as a Potential Mediator of Muscular Dystophy

There are many other forms of muscular dystrophy, and in only a subset of those has there been positive identification of the genetic lesion underlying the disease. The identification of the mutations is only the first step in understanding the diseases of the muscle. Understanding of the mechanistic cascades which follow becomes increasingly important towards developing novel therapeutics and treatments to alleviate the defects. In recent years, data has suggested that Ca^{2+} dysregulation may be central in the pathogenic disease mechanisms and may be a point of access for therapeutic interventions for muscular dystrophies.

The intracellular Ca^{2+} of all cells is tightly regulated, as Ca^{2+} acts as a second messenger for a large and diverse number of signaling mechanisms. In the muscle, it is imperative that Ca^{2+} is controlled, as it functions to regulate the contractile system through troponinC, in addition to mediating signaling events. There are several points of control for Ca^{2+} within the muscle. These include the sarcolemma, intracellular stores, organelle buffers, and cytoplasmic buffers (Figure 3). These mechanisms coordinately regulate the internal Ca^{2+}, and have all been implicated in aspects of disease pathogenesis (Gailly, 2002; Martonosi and Pikula, 2003).

Regulation of Ca^{2+} through the sarcolemma involves the identity and distribution of Ca^{2+}-permeable ion channels. There are several types of ion channels which flux Ca^{2+} through the membrane, including voltage-gated channels and stretch-activated channels. However, in dystrophin-deficient tissue, one major source of Ca^{2+} influx seems to be breaks in sarcolemma, allowing transient large fluxes of Ca^{2+} and other extracellular material into the

cell. In the mouse model of Duchenne's muscular dystrophy (*mdx*), 20% of mutant fibers showed Ca^{2+} influxes up to 10- to 30-fold higher than normal fibers (De Backer et al., 2002). One way in which this Ca^{2+} may affect muscles is by inducing Ca^{2+}-mediated cellular apoptosis through the mitochondria (Duchen, 1999; Sandri et al., 1998).

The mitochondria act as Ca^{2+} buffers for the intracellular environment, performing two essential functions outside of the generation of ATP. The first is in the immediate buffering of fast Ca^{2+} changes, diminishing the spikes of Ca^{2+} in the intracellular environment. In addition, they are also integral to the repletion of Ca^{2+} into the sarcoplasmic reticulum (SR) during the stimulation of calcium-induced Ca^{2+} release (CICR). During large increases in mitochondrial Ca^{2+} concentrations, Ca^{2+} mediated apoptosis may occur, which may contribute to the decreased viability of diseased muscle fibers. In *mdx* mice, Ca^{2+} imaging of the mitochondria has revealed accumulation of Ca^{2+} in the mitochondria at 150%-200% of the normal levels in response to depolarization, indicating that although 90% of fibers have normal intracellular Ca^{2+} levels, mitochondria may be compensating for altered Ca^{2+}, but subsequently become overloaded due to the overall dysregulation (Robert et al., 2001).

The SR is a third point of intracellular Ca^{2+} control, reserving the majority of Ca^{2+} required to stimulate contraction in the muscle. These stores release Ca^{2+} during CICR, stimulated through a complex mechanism involving ion channels that include voltage-gated Ca^{2+} channels in the sarcolemma and ryanodine receptors (RyR) in the SR. Conflicting evidence, however, has made it

unclear whether the SR plays a role in muscle fiber degeneration. Defects in SERCA pump activity have been observed in the *mdx* mouse model, suggesting alterations in Ca^{2+} re-uptake. However, corresponding defects have not been seen in human myotubes (Kargacin and Kargacin, 1996; Takagi et al., 1992; Vandebrouck et al., 1999).

Finally, the cytoplasm controls its own free-Ca^{2+} concentration by use of a number of cytoplasmic Ca^{2+} buffers. In mammals, the major buffer is parvalbumin. These buffers act to keep free Ca^{2+} concentrations low during rest, as well as modulate the relaxation rates of muscles by buffering Ca^{2+} away from the contractile machinery. In diseased states, it is unclear whether these buffers are significantly affected to alter the properties of muscles and contribute to the pathogenesis. Parvalbumin transcription has been shown to be upregulated in dystrophic fibers, suggesting that parvalbumin could play a role in pathogenesis (Gailly et al., 1993). Supporting a modulatory role by parvalbumin, *mdx* mice which also lack the gene encoding parvalbumin, exhibit a modification of the defects from mild dystrophic muscle features to a hypertrophic-like defect (Raymackers et al., 2003; Raymackers et al., 2000).

Data from many labs have suggested that Ca^{2+} homeostasis is altered in mutant muscle fibers in both *mdx* mice and in humans. However, whether this is central in the disease pathogensis, or is a side-effect of a more important cellular response is unknown. Further, if Ca^{2+} homeostasis is altered, the source of this dysregulation has yet to be elucidated. Regardless, changes in the intracellular Ca^{2+} can lead to alterations in Ca^{2+}-dependent signaling and, eventually, affect

transcription. Changing the transcriptional profile of a muscle can drastically alter its functional properties. Therefore, it is necessary to understand the differences in transcriptional output between normal and diseased fibers. Determining whether alterations in gene expression can account for some of the defects associated with muscle disease, or can act to alleviate the defects induced by mutations will help in understanding the pathogenesis of disease.

Changes in the Transcriptional Profile of Diseased Muscle Fibers

One method utilized for studying the changes in gene expression under altered conditions involves microarray analysis. These arrays are either ssDNA oligomers or cDNA spotted onto a solid support, with each spot corresponding to a specific gene within the organism's genome. Using labeled RNA from a specific tissue/organism, one can then assay transcription by measuring the amount of RNA hybridized to a gene of interest by visualizing the intensity of signal provided by the RNA label. Comparing two tissue samples in the expression of any single gene can be done by either comparing the intensity of a specific spot between two samples, or alternatively, labeling the two samples with different flourophores and measuring the ratio between the two flourophores within the same spot on a single array. Using these types of techniques, studies on the expression profiles of several muscular dystrophies have been done.

Expression profiling has yielded some new insights into the pathology of muscle disease. These studies have been done on tissue representing a few of

the known muscular dystrophies, including Duchenne's muscular dystrophy, dyferlinopathies, limb-girdle muscular dystrophy, and Emery-Dreifuss muscular dystrophy (Campanaro et al., 2002; Chamberlain, 2000; Chen et al., 2000; Noguchi et al., 2003; Tsukahara et al., 2002). From these studies, knowledge gained of the transcriptional profiles of diseased tissues has indicated a possibility of common cellular responses to muscle dysfunction.

In Duchenne's muscular dystrophy, expression analysis has been performed on both pooled tissue samples from several patients, as well as individual patients (Chamberlain, 2000; Chen et al., 2000; Noguchi et al., 2003). Common features in the transcriptional profile have been observed between these two experiments. Genes that have been consistently upregulated include cell surface and extracellular matrix proteins. Some of these genes include fibronectins, collagens, and crystallins. In addition, certain types of sarcomere-related genes are upregulated as well. These include myosin light chains, actin, and myosin binding proteins. Several of these upregulated sarcomere-related genes normally have differential expression through development, with high expression during fetal stages and low to undetectable expression in adults. Immune-response related genes also include a large number of upregulated transcripts. These include HLA-DR genes of the major histocompatibility complex (type I and II). This upregulation may reflect activated dendritic cell infiltration into diseased tissue.

Downregulation of genes related to energy and metabolism, especially nuclear-encoded mitochondrial genes, make up the predominant class of

downregulated transcripts. This regulation is thought to be indicative of Ca^{2+} homeostasis problems leading to Ca^{2+} overloading of the mitochondria and Ca^{2+}-mediated apoptosis. However, these observations are correlational at best, and do not indicate a positive causality in the pathogenesis of disease.

Comparing these observations with other types of muscle diseases has proven difficult. In addition to the variability among patients, there is a large variability in experimental methods, microarray design and implementation, and non-standardized annotation. However, some limited comparisons can be made. In particular, when tissue from different muscular dystrophies is assayed within the same experimental protocol, direct comparisons can be made. This type of analysis was done between Duchenne's muscular dystrophy and LGMD2C (Chamberlain, 2000; Chen et al., 2000).

When compared within the same experimental procedure, LGMD2C showed similar changes to those observed in Duchenne's Muscular Dystophy. Extracellular matrix proteins and embryonic sarcomeric proteins were found to be upregulated, whereas those involved in energy and metabolism were downregulated. Transcriptional differences between the two diseases represented only a small number of genes (131 in Duchenne's and 89 in LGMD2C). Additionally, most of these genes were close to the statistical cutoffs used within the experiment, likely representing biological signal noise rather than biological significance. Therefore, the pathogenesis of distinct muscular dystrophies may share common underlying cellular mechanisms that are

activated in response to genetic lesions affecting proteins involved in maintaining structural integrity.

Data obtained with dysferlinopathies (LGMD2B and distal muscular myopathy of Miyoshi) showed some overlap in the transcriptional profile, with the upregulation of developmentally expressed saromeric proteins including developmentally-regulated isoforms of myosin light chain, as well as immune response-related genes. However, unlike the studies in DMD and LGMD2C, there did not seem to be a significant decrease in genes involved with energy and metabolism (Campanaro et al., 2002).

Further, from the profiles obtained in these diseases, all showed a marked regulation of calcium handling proteins, including S100 calcium binding proteins. The alteration in these calcium handling proteins may further support the idea that Ca^{2+} homeostasis is altered in diseased states of the muscle. However, these types of experiments are correlational and difficulties exist in extending hypotheses on causality.

To summarize, muscular dystrophies represent a genetically diverse set of diseases. The common feature of the genetic lesions underlying these diseases is that the mutated genes are all involved in maintaining the structural integrity that the muscle requires to leverage forces, as well as withstand forces exerted onto the muscle during contraction. The primary mutations may lead to overall Ca^{2+} homeostasis alterations in the cytoplasm, which could contribute to Ca^{2+} mediated apoptosis due to Ca^{2+} overload of the mitochondria, as well as lead to downstream changes in the transcriptional profile of the muscle. This alteration

in transcription includes the upregulation of developmentally-regulated sarcomeric proteins, Ca^{2+} handling proteins, and immune response-related proteins and a downregulation of genes involved in energy and metabolism. However, though this transcriptional profile is well documented, it is unknown whether these genes act in a compensatory or contributory manner in pathogenesis. For a specific gene of interest, this distinction may change in a time-dependent manner. Though observations have been made within the cellular responses and transcriptional profiles, determining causality in context of disease pathogenesis remains to be done. One way to begin forming a more thorough picture of muscle disease is to study evolutionarily conserved responses to muscle dysfunction. In muscular dystrophies, although focus has been placed on the skeletal muscle, cardiac muscles also are affected in many cases, as they use share much of the same molecular machinery mediating contraction (Fadic et al., 1996; van der Kooi et al., 1997).

The Genetics of Cardiomyopathy

Heart failure affects up to 4.5 million people in the United States alone, and represents, like muscular dystrophy, a widespread health problem requiring novel therapeutic interventions for those afflicted (Seidman and Seidman, 2001). Within these diseases, the heart is often morphologically remodeled in one of two ways—dilation and hypertrophy. In dilation, the cardiac chamber volumes increase, whereas in hypertrophy, ventricular wall mass increases (Figure 4).

Figure 4

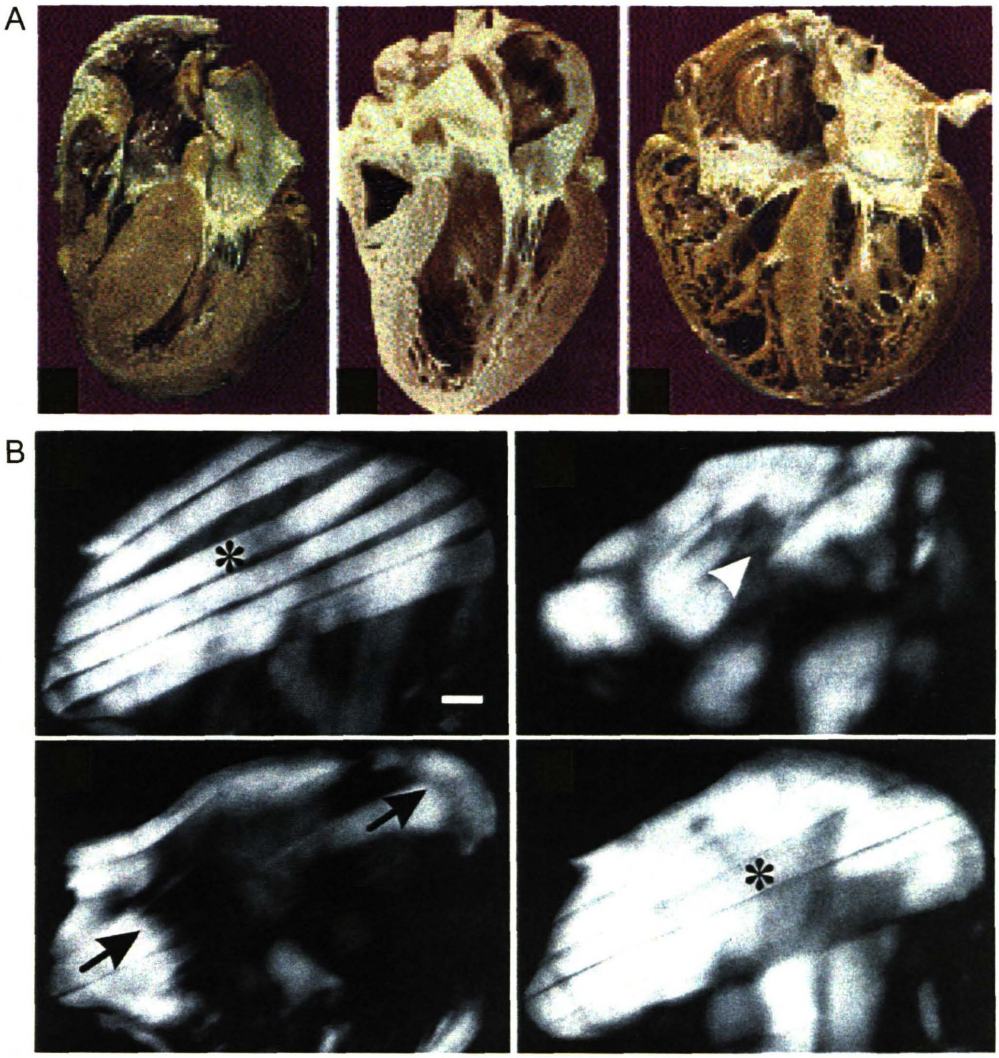

Table I

Hypertrophic Cardiomyopathy	*Drosophila* Gene Homolog	Flightless Mutation
β-cardiac myosin heavy chain	*Myosin heavy chain*	yes
troponin I	*wings up A*	yes
troponin T	*upheld*	yes
α-tropomyosin	*tropomyosin2*	yes
myosin binding protein C	*n/a*	n/a
Essential myosin light chain	*Mlc1*	no
Regulatory myosin light chain	*Mlc2*	yes
Titin	*bent*	yes
	sallimus	no (lethal)

Figure 4: Drawing parallels between hypertrophic cardiomyopathy and *Drosophila* flightless mutations (A) Human hearts showing the effects of cardiomyopathy. (l-r) Hypertrophic cardiomyopathy, Normal, Dilated cardiomyopathy. Note the large ventricular wall thickness in the heart affected by hypertrophic cardiomyopathy and increased chamber volume of the heart affected by dilated cardiomyopathy. (B) The effect of hypercontraction on *Drosophila* flight muscles can be easily visualized using polarized light microsophy. (Clockwise from top left) Normal dorsal longitudinal muscles from a wildtype fly, $wupA^{hdp2}$ pupa at 72h APF, $wupA^{hdp2}$; $Tm2^{D53}$/+, and $wupA^{hdp2}$ post-eclosion. These micrographs illustrate the sensitivity of the flight muscles to mutations in contractile proteins, as well as the strong interactions that have been isolated in genetic screens. (A) was adapted from (Seidman and Seidman, 2001) and (B) from (Naimi et al., 2001).

Table I: A comparison between mammalian cardiac genes implicated in hypertrophic cardiomyopathy and homologous *Drosophila* genes. The third column indicates whether mutations have been isolated in the *Drosophila* homolog that lead to flightless behavior.

These types of changes can occur in response to a variety of stimuli such as mechanical stress, genetic mutations, and aortic valve complications. In addition, there is a subset of heart diseases caused by genetic mutations that do not have external pathologies such as associated muscular dystrophies. These types of diseases are known as primary cardiomyopathies.

Primary cardiomyopathies are a defined set of genetically determined heart diseases which lead almost exclusively to the remodeling of the cardiac structure. Like muscular dystrophies, these diseases have been well defined in the gross anatomical and histological properties, and recently, in the underlying genetic mutations which cause them. In addition, as in the case of muscular dystrophies, although the genetic lesions and transcriptional alterations of the disease are well studied, the cellular processes and molecular cascades responsible for cardiomyopathy are largely unknown. The genetic lesions for hypertrophic cardiomyopathies are better known, with most cases occurring due to mutations in one of ten loci. Dilated cardiomyopthies, however, remain more elusive.

Unlike the muscular dystrophies, primary hypertrophic cardiomyopathies do not affect genes involved in the structural integrity of the heart. Rather, they tend to be mutations in the sarcomere, altering the contractile machinery itself. Of the mutations currently identified, the proteins affected include TnT, titin, myosin binding protein-C, Mhc, actin, Tm, TnI, and the regulatory and essential myosin light chains (Bonne et al., 1995; Geisterfer-Lowrance et al., 1990; Kimura et al., 1997; Mogensen et al., 1999; Poetter et al., 1996; Satoh et al., 1999;

Tanigawa et al., 1990; Thierfelder et al., 1994; Watkins et al., 1995). How these mutations affect the contractile machinery is still under debate. However, most mutations which lead to the disease involve missense mutations and small truncations, suggesting that the mutant proteins do not result in unstable proteins and haploinsufficiency problems. If haploinsufficiency were the problem, the most likely mutations causing hypertrophic cardiomyopathy would involve complete loss-of-function mutations such as deletions and early stop codons. Therefore, these mutations more likely act as dominant effectors of the contractile machinery.

As most of the mutations underlying hypertrophic cardiomyopathy act in a dominant Mendelian fashion, they likely act as activated proteins, negative inhibitors, or carry novel functions due to the mutant residue(s). However, due to the lack of biophysical data on these mutations, it is still unclear as to which of these cases exist for hypertrophic cardiomyopathy. Further studies are required in order to determine whether hypertrophic cardiomyopathies result from general contractile dysfunction or specific vectorial changes (*i.e.* all mutations lead to hypercontraction *versus* hypocontraction). This may become more complex when correlating biophysical data to *in vivo* contexts. For a specific mutation in the mammalian cardiac Mhc, R403Q, data has indicated that it could act as both a dominant negative of contractile function and a dominant activator in a tissue-dependent manner (Cuda et al., 1997; Tyska et al., 2000). Therefore, more data on the nature of all the known mutations in context of cardiac muscle will be required to further our understanding of these diseases.

Calcium as a Potential Mediator of Cardiomyopathy

Like muscular dystrophies, Ca^{2+} has been implicated in being important in the pathogenesis of heart disease. It has been suggested that the alterations in the contractile machinery may lead to an increase of intracellular Ca^{2+} in the myocytes (Bustamante et al., 1991; Marban et al., 1987). Altering the activity of contractile proteins may perturb the balance of the on/off states of the thin filament. Given that the on state requires the binding of Ca^{2+} to the troponin complex, then alteration in the activity of myosin may secondarily cause a buffering of Ca^{2+} in the cytosol through sequestration of Ca^{2+} onto the thin filament. In addition, transcriptional downregulation of SERCA pumps has been observed in cardiomyopathy expression profiles (Hwang et al., 2002). This downregulation may exacerbate abnormal Ca^{2+} handling properties by preventing Ca^{2+} re-uptake into the SR, creating a cyclic progression towards diseased states.

Additional evidence in support of Ca^{2+} being central to the disease process of cardiomyopathy is its responsiveness to calcineurin modulating chemicals. Cardiac myocytes in culture can be induced to undergo hypertrophy by addition of hypertrophic agonists. Some of these include angiotensin II, phenylephrine, norepinephrine, and endothelin-1—activators of Ca^{2+}-dependent signal transduction systems (Karliner et al., 1990; Leite et al., 1994; Molkentin et al., 1998; Sadoshima and Izumo, 1993; Sadoshima et al., 1993). Changes in

Ca^{2+} are thought to transduce signals *via* calcineurin, a calmodulin-dependent phosphatase, inducing hypertrophy. Inhibiting calcineurin activity with characterized immunosuppressant drugs such as cyclosporin A and FK506 can prevent angiotensin II- and phenylephrine-induced hypertrophy in culture (Molkentin et al., 1998; Olson and Molkentin, 1999).

Supporting data in culture studies, transgenic mice were created to express constitutively active calcineurin A in the heart. These mice developed hypertrophic cardiomyopathy which progressed into dilated cardiomyopathy, heart failure, and finally death. Interestingly, hypertrophy in these transgenic mice could be prevented by systematic dosage of cyclosporin A or FK506. Therefore, it seems likely that hypertrophy, and possibly dilated cardiomyopathy, is dependent upon intracellular Ca^{2+} signals that are transduced *via* a calcineurin-dependent pathway (Molkentin et al., 1998; Olson and Molkentin, 1999).

Transcriptional Changes Associated with Cardiomyopathies

The functional effects of hypertrophic-inducing mutations on the transcriptional profile show similarities to those found in muscular dystrophies. Again, the difficulty in drawing conclusions as well making comparisons exists in the large variability in the experimental design and procedures. Even in the case of model systems, there exists a diversity of models utilized to induce

hypertrophic cardiomyopathy in an animal. However, some progress has been made in identifying transcriptional changes in cardiac diseased states.

A number of transcriptional changes occur in response to cardiomyopathy. The most striking of these changes is an upregulation of the fetal cardiac sarcomeric genes with a concomitant downregulation of the adult isoforms and an upregulation of immediate-early genes such as c-fos and c-myc (Chien et al., 1991; Komuro et al., 1991; Sadoshima and Izumo, 1997; Sadoshima et al., 1992). It is still unclear how this dramatic transcriptional change occurs, as many signaling pathways have been implicated in the process. One common feature is that these signaling pathways have been shown to lead to increases in intracellular Ca^{2+}, further supporting a central role of Ca^{2+} in muscle disease pathogenesis. It may be that several signaling pathways, in addition to general Ca^{2+} dysregulation, lead to Ca^{2+}-dependent signaling and a prototypical response in the terminal stages of the hypertrophic process. This response includes the activation of the fetal cardiac genes and immediate-early genes, an event dependent upon several transcription factors, including serum response factor, TEF-1, AP-1, Sp1, and GATA4 (Kariya et al., 1994; Karns et al., 1995; Kovacic-Milivojevic et al., 1996; Liang et al., 2001; Sadoshima and Izumo, 1993). Further, evidence has shown that the process of transcriptional re-programming requires a repression of transcriptional histone deacetylases that act to repress the transcription of fetal cardiac genes in adult tissues (Zhang et al., 2002).

Parallel Comparisons between Skeletal and Cardiac Muscle Diseases

In review of the literature between cardiomyopathies and muscular dystrophies, there are strong parallels that seem to exist between these diseases. Indeed, some animal models of dystrophin deficiency display hypertrophy of the skeletal muscle rather than degeneration as the primary defect, as in the case of rats and mice (Hoffman and Dressman, 2001). Thus, it seems that the underlying molecular mechanisms are shared between these types of diseases, and modulation of this unknown common pathway could determine the outcomes of hypertrophy or degeneration.

Muscular dystrophies are caused by mutations in genes that function in the structural support of the muscle, whereas cardiomyopathies are caused by mutations in the contractile machinery proteins. However, many muscular dystrophy mutations have associated heart defects. It may be that the absence of contractile mutations in muscular dystrophy may reflect inviability, rather than a fundamental difference between the two diseases. Despite the differences in genetic basis, both diseases have implicated Ca^{2+} as a central mediator of disease pathogenesis. Further, Ca^{2+}-dependent signaling may result in the activation of transcripts which are normally expressed early in development and repressed in adult tissue.

The parallels drawn between muscular dystrophy and cardiomyopathy remain tenuous until more experimentation is done. Several issues exist, some of which have been touched upon, in strengthening a comprehensive study of muscle disease. Foremost is the diversity of diseases which exist in human and

mammalian models. There are many ways in which these diseases occur in humans, as well as many ways to induce similar phenotypes in higher vertebrates such as mice. Elucidation of the underlying cellular mechanisms remains difficult in such diversity. Further, characterization of the diseases in mammalian models lacks a standardization of protocol, especially in the assessment of alterations in the transcriptional profiles. Using different types of tissue/models in different stages of pathogenesis, different microarrays, and lab-specific annotation systems has led to difficulties in understanding commonalities between multiple experiments. Even if standardization could occur in assaying transcriptional profiles, understanding the functional consequences of these alterations becomes a problem due to incapacity for human experimentation and the slow progression in murine molecular genetics. It takes several months to years to create transgenic mice with single mutations, preventing high-throughput follow up of a microarray experiment. Although we may be able to determine how the transcriptional profile is altered in mutant muscle tissue, whether these changes are compensatory or contributory to disease pathogenesis is an unanswered question. Despite these difficulties, there remains an apparent parallel between different model systems of muscle disease in mammals, suggesting that the pathways underlying these diseases have been conserved throughout evolution. Therefore, invertebrate model systems with a diverse repertoire of genetic tools are likely to be important for modeling human myopathies.

Lower Invertebrate Model Systems for the Study of Muscle Disease

For high-throughput genetic and cellular analysis of muscle dysfunction, there are two well characterized model systems—*C. elegans* and *Drosophila*. These invertebrate model systems offer a large breadth of genetic tools in order to manipulate the organism. In addition, completed genome sequencing facilitates the identification of novel genes by acting as a tool in both forward and reverse genetic analyses. Their small size and short generation times also lend these organisms to large-scale screening and behavioral genetics.

C. elegans *as a Model System for Muscle Disease*

Invertebrate models offer the ability for high-throughput analysis of muscle structure and function and provide a platform for identifying conserved pathways which may be activated in many forms of muscle dysfunction. In *C. elegans,* many important genetic parallels have been found in muscular dystrophies. Although the body wall muscles of the nematode differ from mammals in that they do not form syncitia and are completely post-mitotic (no satellite cell equivalents), the underlying molecules and mechanisms are conserved. The *C. elegans* dystrophin homolog, *dys-1*, when mutated, causes a mild dystrophic defect. This result is similar to the murine *mdx* model, where mutations in the dystrophin locus result in a mild dystrophic defect as well (Bessou et al., 1998). In support of evolutionarily conserved mechanisms underlying muscle function,

double mutants in both mice and worms involving dystrophin and MyoD (*hlh-1*) show severe myopathy and degeneration, though debate remains as to whether the mechanism of this synergy is similar (Gieseler et al., 2000; Megeney et al., 1996). In addition, genetic analysis has supported the role of Ca^{2+} being an integral part of this process, as RNAi knockdown of *egl-19*, the major subunit of voltage-gated calcium channels in the body wall muscles, can partially suppress the *dys-1;hlh-1* degeneration, while gain-of-function mutations in *egl-19* act as enhancers of *dys-1* (Mariol and Segalat, 2001).

C. elegans as a model system for cardiomyopathies is less characterized. Although the genetic power of the organism has identified many of the same players and interactions in muscle contraction, cellular consequences and transcriptional profile alterations are less defined (Gengyo-Ando and Kagawa, 1991; Greenwald and Horvitz, 1982; Moerman et al., 1982; Park and Horvitz, 1986). In addition, the role of calcium is yet to be fully explored. Data in *C. elegans* has revealed a physical interaction between IP_3 receptors and myosin heavy chain. Disruption of this interaction by overexpression of interfering peptides results in pharyngeal pumping defects without effect on defecation, both of which are IP_3-dependent behaviors. This suggests that myosin heavy chain may also contribute to the specificity of IP_3 receptor signaling, which has been shown to localize and regulate Ca^{2+} signals in the cell. This interaction may provide clues to hypertrophic cardiomyopathies and the alterations in Ca^{2+} homeostasis (Walker et al., 2002a; Walker et al., 2002b).

Drosophila *as Model System for Muscle Disease*

Using *Drosophila* as a model system for the study of muscle diseases, much like *C. elegans*, is still in the early stages of establishment. Complementary to the *C. elegans* model system, the work established on *Drosophila* musculature lends itself more readily to cardiomyopathies rather than muscular dystrophy.

The *Drosophila* muscles for flight include six indirect flight muscles (IFM) in the adult thorax. Structurally, these muscles resemble mammalian striated skeletal muscle. In addition, the molecular components underlying contraction, as well as the regulation of the contractile machinery are well conserved from flies to humans. However, unlike skeletal muscle, the IFM share similarity to vertebrate cardiac muscles in that they are stretch-activated, requiring mechanical tension for full activation (Peckham et al., 1990). As a model system, these muscles provide a prototypical muscle that can be used for studying the common features between skeletal and cardiac muscles of vertebrates.

Using traditional forward genetic screens, mutations in muscle function were identified through use of a readily assayable behavior, flight. Flight lends itself well as a behavioral tool, as the flightless mutants are easily identifiable in genetic screens. The simplicity of screens searching for flightless behavior allows for a high-throughput identification of mutations which affect genes involved muscle function using forward-genetic techniques. These types of

screens provide a non-biased way to identify genes with biological relevance to an *in vivo* complex process.

Flightless behavior in *Drosophila* can be caused by several defects. Many of the genes in the *Drosophila* flight muscles are sensitive to dosage. Haploinsufficiency can account for several mutations which display flightless defects. Loss-of-function mutations in *Mhc*, *dMLC2*, *Tm2*, and *act88F* lead to flightless behavior due to the sensitivity of muscle function and the amounts of protein encoded by these genes (Bernstein et al., 1993). Further, four copies of *Mhc* cause IFM defects, whereas four copies of *act88F* have little effect (Cripps et al., 1994b; Homyk and Emerson, 1988). Therefore, not only are the IFM sensitive to dosage, but the dosage requirement for each gene is specific.

Another form of flightlessness can arise from hypercontraction of the muscle. Hypercontraction of the muscle is defined as muscles which show proper development of the sarcomere and its support structures, but show use-dependent degradation post-development. These types of mutations are of great interest as they may reflect the diseased states of cardiomyopathies and muscular dystrophies. Rather than representing a developmental or gene dosage defect, these mutants have otherwise normal musculature, but once muscle activity occurs, the muscles quickly degrade.

Many of the hypercontraction mutants were isolated in the original screens for flightless mutants (Figure 4, Table I). The genes which have shown this type of defect include *Mhc*, *act88F*, *wings up A* (troponin I), and *upheld* (troponin T) (Beall and Fyrberg, 1991; Cripps et al., 1994a; Deak et al., 1982; Ferrus et al.,

2000; Mogami and Hotta, 1981; Vigoreaux, 2001). Most of these mutations have a secondary defect of wing positioning, with wings held up in a vertical position. This defect allowed for simple identification of modifiers of the improper wing positions. From these secondary screens, two classes of mutations were mainly isolated. The first were intragenic suppressors, allowing detailed structure/function analysis of these proteins in an *in vivo* context. The second, extragenic suppressors, was useful in dissecting the functional relationships between genes of the sarcomere.

When identifying suppressors for *wings up* $A^{heldup2}$ ($wupA^{hdp2}$), two important functional relationships were identified in an *in vivo* context. The first is an allele specific suppression of TnI induced hypercontraction by Mhc (Kronert et al., 1999). The suppressor alleles of Mhc clustered around the ATP binding/hydrolysis site of the Mhc globular head. The study suggested that a physical link, direct or indirect, between Mhc and TnI may exist, and Mhc could be a source of regulation on the activity of TnI. However, this data is in conflict with another study suggesting that instead of Mhc regulating thin filament dynamics through direct interactions, suppression of hypercontraction by mutations in *Mhc* occur by decreasing force production in the muscle, thereby decreasing forces produced in the altered regulation of troponinI and troponinT mutants (Nongthomba et al., 2003). Regardless of the mechanism, a clear functional relationship is established between Mhc and the thin filament regulatory system.

A second important suppressor of abnormal wing positioning identified was an allele of *Tm2, Tm2*^{D53} (Naimi et al., 2001). The significance of this finding was that there exists no direct interaction between Tm2 and TnI in models of thin filament regulation in muscle contraction. It is likely that the mode of suppression by this allele abrogates the altered regulation by mutations in TnI by changing the motility of Tm2 on the actin filament. Thus, although *wupA*^{hdp2} acts to derepress the thin filament, this derepression does not occur due to inability of *Tm2*^{D53} to undergo proper movement along the thin filament. Genetic interactions such as these give functional insight into the roles mediate by these genes in the muscle.

Using Drosophila *to Study Mutations in* Mhc *and Comparisons to Hypertrophic Cardiomyopathy*

In comparison to hypertrophic cardiomyopathies, the mutant alleles identified in *Drosophila* screens provide a genetic model system to understand the defects associated with contractile disruption. In particular, many of the mutations isolated in *Drosophila* are clustered near mutations known to cause primary hypertrophic cardiomyopathy. In fact, β-cardiac Mhc mutations account for 10-30% of cases of hypertrophic cardiomyopathy, with over 29 different alleles representing this subpopulation (Rayment et al., 1995). Given that nearly 100 mutations exist for the *Drosophila Mhc* locus, detailed structure/function analysis can be done to determine the effects of different types of mutations on the overall physiology of the muscle.

In primary hypertrophic cardiomyopathies, over 29 different mutations can account for those in which the β-cardiac Mhc gene is altered. These mutations are distributed throughout the protein in a non-random fashion, clustering in specific regions within the protein (Figure 5). However, whether the disease is due to similar vectorial changes in the contractile activity (*i.e.* increased contraction or decreased contraction), or whether any alteration in the biophysical properties can lead to hypertrophic cardiomyopathy is still under debate. Therefore, understanding the alterations of a mutation in a defined and reproducible *in vivo* context is important in understanding the pathology of cardiomyopathies.

The *Drosophila Mhc* locus was originally identified using two independent lines of experimentation. The molecular identification occurred through use of cross-hybridization techniques under non-stringent conditions using probes generated from *C. elegans* Mhc sequences (Bernstein et al., 1983; Rozek and Davidson, 1983). Unlike most animals, the *Drosophila* genome contained only one muscle specific *Mhc* locus, rather than different isoforms being encoded in separate loci. *C. elegans* contains 4 muscle-specific isoforms of Mhc, encoded by *unc-54, myo-1, myo-2, and myo-3* ((Ardizzi and Epstein, 1987). Further characterization of the *Drosohila Mhc* gene has revealed a complex locus spanning 20kb of DNA containing 19 exons (Collier et al., 1990; George et al., 1989; Hess and Bernstein, 1991; Wassenberg et al., 1987). These exons include seven alternative exons, 13 constitutive exons, and two alternative start sites. Theoretically, the locus could encode up to 484 molecularly distinct

Figure 5

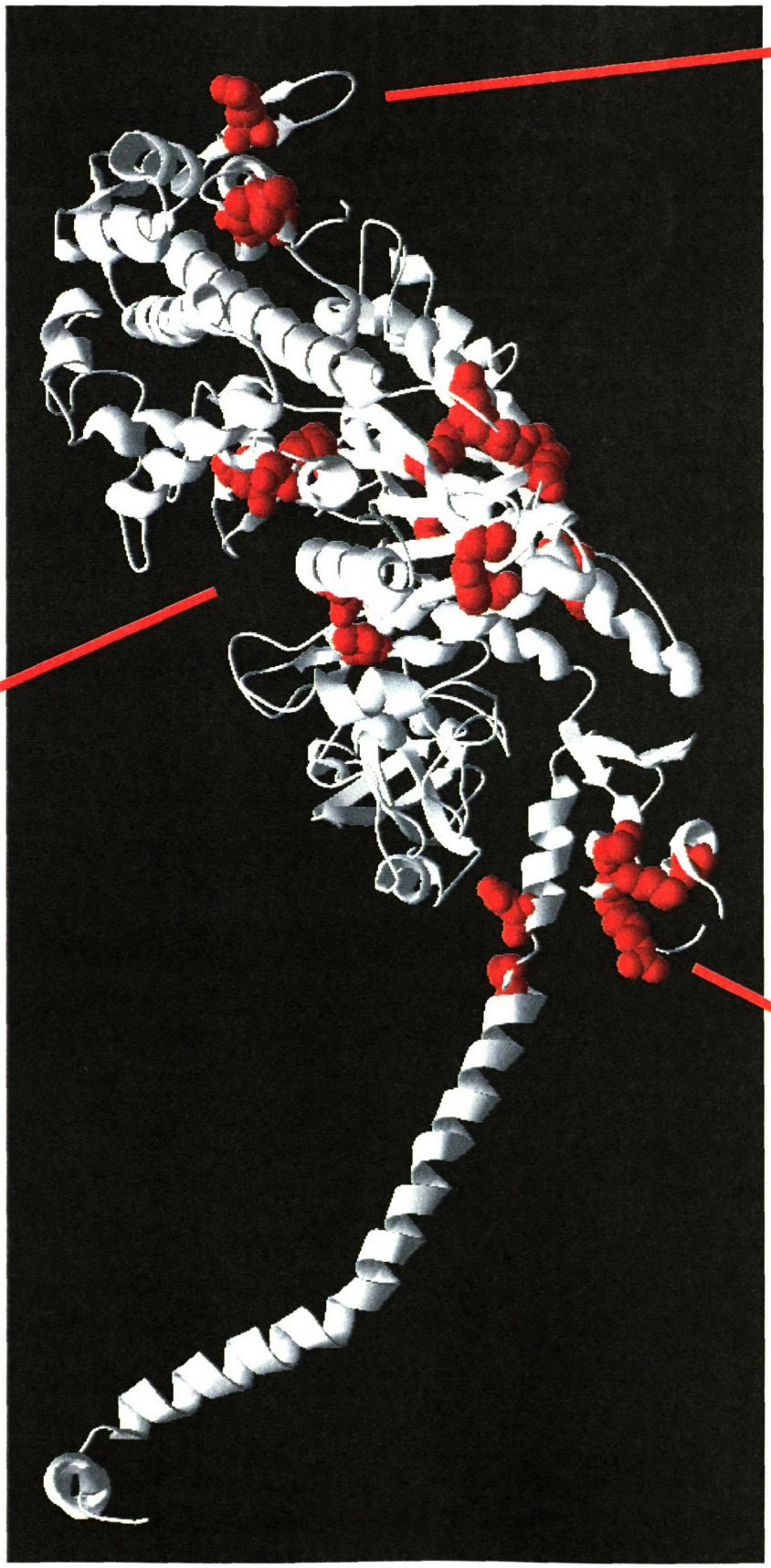

Figure 5: Mutations identified in β-cardiac Mhc that cause hypertrophic cardiomyopathy Mutations that have been identified in β-cardiac Mhc which cause hypertrophic cardiomyopathy are mapped onto equivalent residues in the chicken Mhc crystal structure based upon BLAST analysis. Note the clustering of the mutations in specific regions of the protein. Data from (Rayment et al., 1995).

transcripts, although only 14 of these have been further identified to be expressed. Studies on the alternative exons suggest that alternative splice forms have differential biophysical activity, and thus act to modulate the overall output of the muscles in which these splice forms are expressed (Collier et al., 1990; George et al., 1989; Hess and Bernstein, 1991; Wassenberg et al., 1987). The alternative start site encodes only the rod domain of the Mhc molecule, utilized in specific muscles in *Drosophila* to act as spacers, limiting the number of available active head domains, therefore decreasing overall power output of the muscle (Standiford et al., 1997).

In parallel studies, *Mhc* was identified in forward genetic screens to isolate flightless mutations. Interestingly, both loss-of-function and gain-of-function mutations in *Mhc* alter the flight ability of the fruit fly. Loss-of-function mutations disrupt the gene dosage sensitivity of the IFM, whereas gain-of-function mutations alter the kinetics of contraction, creating excess force on the IFM, leading to eventual degradation of the muscle fibers (Homyk and Emerson, 1988; Kronert et al., 1995). Further, *Mhc* alleles were isolated in modifier screens of hypercontraction defects found in alleles of *wupA* which affect contractile activity. These alleles have led to insights in the functional and structural connectivity between different proteins of the sarcomere (Kronert et al., 1999; Nongthomba et al., 2003).

Here, we describe the analysis of hypercontraction mutations in *Mhc*, and the effects they have on the physiology of the muscle in *Drosophila*. We extend beyond the biophysical consequences of these mutations and investigate the

cellular responses which occur. In addition, we show parallels between the *Drosophila* model system and vertebrate model systems in order to establish *Drosophila* as a model for hypertrophic cardiomyopathy. Not only has this system provided a genetic model in which to identify the key players of muscle function, but we demonstrate that the cellular responses of muscle dysfunction may be conserved as well. Further, these responses may utilize a conserved Ca^{2+}-dependent signaling mechanism that functions other cellular contexts, such as memory formation and stabilization in neurons. In this system, parallel studies may be done in order to understand the role of Ca^{2+}-dependent signaling in the modification and stabilization of the actin cytoskeleton in response to external signals, whether those signals originate from synaptic transmission or mechanical stress induced by contractile mutations.

References

Arahata, K. 2000. Muscular dystrophy. *Neuropathology*. 20 Suppl:S34-41.

Ardizzi, J.P., and H.F. Epstein. 1987. Immunochemical localization of myosin heavy chain isoforms and paramyosin in developmentally and structurally diverse muscle cell types of the nematode Caenorhabditis elegans. *J Cell Biol*. 105:2763-70.

Beall, C.J., and E. Fyrberg. 1991. Muscle abnormalities in Drosophila melanogaster heldup mutants are caused by missing or aberrant troponin-I isoforms. *J Cell Biol*. 114:941-51.

Bernstein, S.I., K. Mogami, J.J. Donady, and C.P. Emerson, Jr. 1983. Drosophila muscle myosin heavy chain encoded by a single gene in a cluster of muscle mutations. *Nature*. 302:393-7.

Bernstein, S.I., P.T. O'Donnell, and R.M. Cripps. 1993. Molecular genetic analysis of muscle development, structure, and function in Drosophila. *Int Rev Cytol*. 143:63-152.

Bessou, C., J.B. Giugia, C.J. Franks, L. Holden-Dye, and L. Segalat. 1998. Mutations in the Caenorhabditis elegans dystrophin-like gene dys-1 lead to hyperactivity and suggest a link with cholinergic transmission. *Neurogenetics*. 2:61-72.

Bonne, G., L. Carrier, J. Bercovici, C. Cruaud, P. Richard, B. Hainque, M. Gautel, S. Labeit, M. James, J. Beckmann, and et al. 1995. Cardiac myosin binding protein-C gene splice acceptor site mutation is associated with familial hypertrophic cardiomyopathy. *Nat Genet*. 11:438-40.

Bonnemann, C.G., R. Modi, S. Noguchi, Y. Mizuno, M. Yoshida, E. Gussoni, E.M. McNally, D.J. Duggan, C. Angelini, and E.P. Hoffman. 1995. Beta-sarcoglycan (A3b) mutations cause autosomal recessive muscular dystrophy with loss of the sarcoglycan complex. *Nat Genet*. 11:266-73.

Bustamante, J.O., A. Ruknudin, and F. Sachs. 1991. Stretch-activated channels in heart cells: relevance to cardiac hypertrophy. *J Cardiovasc Pharmacol*. 17 Suppl 2:S110-3.

Campanaro, S., C. Romualdi, M. Fanin, B. Celegato, B. Pacchioni, S. Trevisan, P. Laveder, C. De Pitta, E. Pegoraro, Y.K. Hayashi, G. Valle, C. Angelini, and G. Lanfranchi. 2002. Gene expression profiling in dysferlinopathies using a dedicated muscle microarray. *Hum Mol Genet*. 11:3283-98.

Chamberlain, J.S. 2000. Muscular dystrophy meets the gene chip. New insights into disease pathogenesis. *J Cell Biol*. 151:F43-6.

Chen, Y.W., P. Zhao, R. Borup, and E.P. Hoffman. 2000. Expression profiling in the muscular dystrophies: identification of novel aspects of molecular pathophysiology. *J Cell Biol*. 151:1321-36.

Chien, K.R., K.U. Knowlton, H. Zhu, and S. Chien. 1991. Regulation of cardiac gene expression during myocardial growth and hypertrophy: molecular studies of an adaptive physiologic response. *Faseb J*. 5:3037-46.

Collier, V.L., W.A. Kronert, P.T. O'Donnell, K.A. Edwards, and S.I. Bernstein. 1990. Alternative myosin hinge regions are utilized in a tissue-specific fashion that correlates with muscle contraction speed. *Genes Dev*. 4:885-95.

Cripps, R.M., E. Ball, M. Stark, A. Lawn, and J.C. Sparrow. 1994a. Recovery of dominant, autosomal flightless mutants of Drosophila melanogaster and identification of a new gene required for normal muscle structure and function. *Genetics*. 137:151-64.

Cripps, R.M., K.D. Becker, M. Mardahl, W.A. Kronert, D. Hodges, and S.I. Bernstein. 1994b. Transformation of Drosophila melanogaster with the wild-type myosin heavy-chain gene: rescue of mutant phenotypes and analysis of defects caused by overexpression. *J Cell Biol*. 126:689-99.

Cuda, G., L. Fananapazir, N.D. Epstein, and J.R. Sellers. 1997. The in vitro motility activity of beta-cardiac myosin depends on the nature of the beta-myosin heavy chain gene mutation in hypertrophic cardiomyopathy. *J Muscle Res Cell Motil*. 18:275-83.

De Backer, F., C. Vandebrouck, P. Gailly, and J.M. Gillis. 2002. Long-term study of Ca(2+) homeostasis and of survival in collagenase-isolated muscle fibres from normal and mdx mice. *J Physiol*. 542:855-65.

Deak, II, P.R. Bellamy, M. Bienz, Y. Dubuis, E. Fenner, M. Gollin, A. Rahmi, T. Ramp, C.A. Reinhardt, and B. Cotton. 1982. Mutations affecting the indirect flight muscles of Drosophila melanogaster. *J Embryol Exp Morphol.* 69:61-81.

Duchen, M.R. 1999. Contributions of mitochondria to animal physiology: from homeostatic sensor to calcium signalling and cell death. *J Physiol.* 516 (Pt 1):1-17.

Fadic, R., Y. Sunada, A.J. Waclawik, S. Buck, P.J. Lewandoski, K.P. Campbell, and B.P. Lotz. 1996. Brief report: deficiency of a dystrophin-associated glycoprotein (adhalin) in a patient with muscular dystrophy and cardiomyopathy. *N Engl J Med.* 334:362-6.

Ferrus, A., A. Acebes, M.C. Marin, and A. Hernandez-Hernandez. 2000. A genetic approach to detect muscle protein interactions in vivo. *Trends Cardiovasc Med.* 10:293-8.

Frey, N., T.A. McKinsey, and E.N. Olson. 2000. Decoding calcium signals involved in cardiac growth and function. *Nat Med.* 6:1221-7.

Gailly, P. 2002. New aspects of calcium signaling in skeletal muscle cells: implications in Duchenne muscular dystrophy. *Biochim Biophys Acta.* 1600:38-44.

Gailly, P., E. Hermans, J.N. Octave, and J.M. Gillis. 1993. Specific increase of genetic expression of parvalbumin in fast skeletal muscles of mdx mice. *FEBS Lett.* 326:272-4.

Geisterfer-Lowrance, A.A., S. Kass, G. Tanigawa, H.P. Vosberg, W. McKenna, C.E. Seidman, and J.G. Seidman. 1990. A molecular basis for familial hypertrophic cardiomyopathy: a beta cardiac myosin heavy chain gene missense mutation. *Cell.* 62:999-1006.

Gengyo-Ando, K., and H. Kagawa. 1991. Single charge change on the helical surface of the paramyosin rod dramatically disrupts thick filament assembly in Caenorhabditis elegans. *J Mol Biol.* 219:429-41.

George, E.L., M.B. Ober, and C.P. Emerson, Jr. 1989. Functional domains of the Drosophila melanogaster muscle myosin heavy-chain gene are encoded by alternatively spliced exons. *Mol Cell Biol*. 9:2957-74.

Gieseler, K., K. Grisoni, and L. Segalat. 2000. Genetic suppression of phenotypes arising from mutations in dystrophin-related genes in Caenorhabditis elegans. *Curr Biol*. 10:1092-7.

Greenwald, I.S., and H.R. Horvitz. 1982. Dominant suppressors of a muscle mutant define an essential gene of Caenorhabditis elegans. *Genetics*. 101:211-25.

Hess, N.K., and S.I. Bernstein. 1991. Developmentally regulated alternative splicing of Drosophila myosin heavy chain transcripts: in vivo analysis of an unusual 3' splice site. *Dev Biol*. 146:339-44.

Hoffman, E.P., R.H. Brown, Jr., and L.M. Kunkel. 1987a. Dystrophin: the protein product of the Duchenne muscular dystrophy locus. *Cell*. 51:919-28.

Hoffman, E.P., and D. Dressman. 2001. Molecular pathophysiology and targeted therapeutics for muscular dystrophy. *Trends Pharmacol Sci*. 22:465-70.

Hoffman, E.P., C.M. Knudson, K.P. Campbell, and L.M. Kunkel. 1987b. Subcellular fractionation of dystrophin to the triads of skeletal muscle. *Nature*. 330:754-8.

Homyk, T., Jr., and C.P. Emerson, Jr. 1988. Functional interactions between unlinked muscle genes within haploinsufficient regions of the Drosophila genome. *Genetics*. 119:105-21.

Hwang, J.J., P.D. Allen, G.C. Tseng, C.W. Lam, L. Fananapazir, V.J. Dzau, and C.C. Liew. 2002. Microarray gene expression profiles in dilated and hypertrophic cardiomyopathic end-stage heart failure. *Physiol Genomics*. 10:31-44.

Kargacin, M.E., and G.J. Kargacin. 1996. The sarcoplasmic reticulum calcium pump is functionally altered in dystrophic muscle. *Biochim Biophys Acta*. 1290:4-8.

Kariya, K., L.R. Karns, and P.C. Simpson. 1994. An enhancer core element mediates stimulation of the rat beta-myosin heavy chain promoter by an alpha 1-adrenergic agonist and activated beta-protein kinase C in hypertrophy of cardiac myocytes. *J Biol Chem*. 269:3775-82.

Karliner, J.S., T. Kagiya, and P.C. Simpson. 1990. Effects of pertussis toxin on alpha 1-agonist-mediated phosphatidylinositide turnover and myocardial cell hypertrophy in neonatal rat ventricular myocytes. *Experientia*. 46:81-4.

Karns, L.R., K. Kariya, and P.C. Simpson. 1995. M-CAT, CArG, and Sp1 elements are required for alpha 1-adrenergic induction of the skeletal alpha-actin promoter during cardiac myocyte hypertrophy. Transcriptional enhancer factor-1 and protein kinase C as conserved transducers of the fetal program in cardiac growth. *J Biol Chem*. 270:410-7.

Kimura, A., H. Harada, J.E. Park, H. Nishi, M. Satoh, M. Takahashi, S. Hiroi, T. Sasaoka, N. Ohbuchi, T. Nakamura, T. Koyanagi, T.H. Hwang, J.A. Choo, K.S. Chung, A. Hasegawa, R. Nagai, O. Okazaki, H. Nakamura, M. Matsuzaki, T. Sakamoto, H. Toshima, Y. Koga, T. Imaizumi, and T. Sasazuki. 1997. Mutations in the cardiac troponin I gene associated with hypertrophic cardiomyopathy. *Nat Genet*. 16:379-82.

Kobayashi, K., Y. Nakahori, M. Miyake, K. Matsumura, E. Kondo-Iida, Y. Nomura, M. Segawa, M. Yoshioka, K. Saito, M. Osawa, K. Hamano, Y. Sakakihara, I. Nonaka, Y. Nakagome, I. Kanazawa, Y. Nakamura, K. Tokunaga, and T. Toda. 1998. An ancient retrotransposal insertion causes Fukuyama-type congenital muscular dystrophy. *Nature*. 394:388-92.

Koenig, M., E.P. Hoffman, C.J. Bertelson, A.P. Monaco, C. Feener, and L.M. Kunkel. 1987. Complete cloning of the Duchenne muscular dystrophy (DMD) cDNA and preliminary genomic organization of the DMD gene in normal and affected individuals. *Cell*. 50:509-17.

Komuro, I., Y. Katoh, T. Kaida, Y. Shibazaki, M. Kurabayashi, E. Hoh, F. Takaku, and Y. Yazaki. 1991. Mechanical loading stimulates cell hypertrophy and specific gene expression in cultured rat cardiac myocytes. Possible role of protein kinase C activation. *J Biol Chem*. 266:1265-8.

Kovacic-Milivojevic, B., V.S. Wong, and D.G. Gardner. 1996. Selective regulation of the atrial natriuretic peptide gene by individual components of the activator protein-1 complex. *Endocrinology*. 137:1108-17.

Kronert, W.A., A. Acebes, A. Ferrus, and S.I. Bernstein. 1999. Specific myosin heavy chain mutations suppress troponin I defects in Drosophila muscles. *J Cell Biol.* 144:989-1000.

Kronert, W.A., P.T. O'Donnell, A. Fieck, A. Lawn, J.O. Vigoreaux, J.C. Sparrow, and S.I. Bernstein. 1995. Defects in the Drosophila myosin rod permit sarcomere assembly but cause flight muscle degeneration. *J Mol Biol.* 249:111-25.

Lehrer, S.S., and M.A. Geeves. 1998. The muscle thin filament as a classical cooperative/allosteric regulatory system. *J Mol Biol.* 277:1081-9.

Leite, M.F., E. Page, and S.K. Ambler. 1994. Regulation of ANP secretion by endothelin-1 in cultured atrial myocytes: desensitization and receptor subtype. *Am J Physiol.* 267:H2193-203.

Liang, Q., L.J. De Windt, S.A. Witt, T.R. Kimball, B.E. Markham, and J.D. Molkentin. 2001. The transcription factors GATA4 and GATA6 regulate cardiomyocyte hypertrophy in vitro and in vivo. *J Biol Chem.* 276:30245-53.

Marban, E., M. Kitakaze, H. Kusuoka, J.K. Porterfield, D.T. Yue, and V.P. Chacko. 1987. Intracellular free calcium concentration measured with 19F NMR spectroscopy in intact ferret hearts. *Proc Natl Acad Sci U S A.* 84:6005-9.

Mariol, M.C., and L. Segalat. 2001. Muscular degeneration in the absence of dystrophin is a calcium-dependent process. *Curr Biol.* 11:1691-4.

Martonosi, A.N., and S. Pikula. 2003. The network of calcium regulation in muscle. *Acta Biochim Pol.* 50:1-30.

Matsumura, K., F.M. Tome, H. Collin, K. Azibi, M. Chaouch, J.C. Kaplan, M. Fardeau, and K.P. Campbell. 1992. Deficiency of the 50K dystrophin-associated glycoprotein in severe childhood autosomal recessive muscular dystrophy. *Nature.* 359:320-2.

Mayer, U., G. Saher, R. Fassler, A. Bornemann, F. Echtermeyer, H. von der Mark, N. Miosge, E. Poschl, and K. von der Mark. 1997. Absence of

integrin alpha 7 causes a novel form of muscular dystrophy. *Nat Genet.* 17:318-23.

McNally, E.M., C.T. Ly, H. Rosenmann, S. Mitrani Rosenbaum, W. Jiang, L.V. Anderson, D. Soffer, and Z. Argov. 2000. Splicing mutation in dysferlin produces limb-girdle muscular dystrophy with inflammation. *Am J Med Genet.* 91:305-12.

Megeney, L.A., B. Kablar, K. Garrett, J.E. Anderson, and M.A. Rudnicki. 1996. MyoD is required for myogenic stem cell function in adult skeletal muscle. *Genes Dev.* 10:1173-83.

Minetti, C., F. Sotgia, C. Bruno, P. Scartezzini, P. Broda, M. Bado, E. Masetti, M. Mazzocco, A. Egeo, M.A. Donati, D. Volonte, F. Galbiati, G. Cordone, F.D. Bricarelli, M.P. Lisanti, and F. Zara. 1998. Mutations in the caveolin-3 gene cause autosomal dominant limb-girdle muscular dystrophy. *Nat Genet.* 18:365-8.

Moerman, D.G., S. Plurad, R.H. Waterston, and D.L. Baillie. 1982. Mutations in the unc-54 myosin heavy chain gene of Caenorhabditis elegans that alter contractility but not muscle structure. *Cell.* 29:773-81.

Mogami, K., and Y. Hotta. 1981. Isolation of Drosophila flightless mutants which affect myofibrillar proteins of indirect flight muscle. *Mol Gen Genet.* 183:409-17.

Mogensen, J., I.C. Klausen, A.K. Pedersen, H. Egeblad, P. Bross, T.A. Kruse, N. Gregersen, P.S. Hansen, U. Baandrup, and A.D. Borglum. 1999. Alpha-cardiac actin is a novel disease gene in familial hypertrophic cardiomyopathy. *J Clin Invest.* 103:R39-43.

Molkentin, J.D., J.R. Lu, C.L. Antos, B. Markham, J. Richardson, J. Robbins, S.R. Grant, and E.N. Olson. 1998. A calcineurin-dependent transcriptional pathway for cardiac hypertrophy. *Cell.* 93:215-28.

Monaco, A.P., C.J. Bertelson, W. Middlesworth, C.A. Colletti, J. Aldridge, K.H. Fischbeck, R. Bartlett, M.A. Pericak-Vance, A.D. Roses, and L.M. Kunkel. 1985. Detection of deletions spanning the Duchenne muscular dystrophy locus using a tightly linked DNA segment. *Nature.* 316:842-5.

Monaco, A.P., R.L. Neve, C. Colletti-Feener, C.J. Bertelson, D.M. Kurnit, and L.M. Kunkel. 1986. Isolation of candidate cDNAs for portions of the Duchenne muscular dystrophy gene. *Nature.* 323:646-50.

Montana, E.S., and J.T. Littleton. 2004. Characterization of a hypercontraction-induced myopathy in Drosophila caused by mutations in Mhc. *J Cell Biol.* 164:1045-54.

Muchir, A., G. Bonne, A.J. van der Kooi, M. van Meegen, F. Baas, P.A. Bolhuis, M. de Visser, and K. Schwartz. 2000. Identification of mutations in the gene encoding lamins A/C in autosomal dominant limb girdle muscular dystrophy with atrioventricular conduction disturbances (LGMD1B). *Hum Mol Genet.* 9:1453-9.

Naimi, B., A. Harrison, M. Cummins, U. Nongthomba, S. Clark, I. Canal, A. Ferrus, and J.C. Sparrow. 2001. A tropomyosin-2 mutation suppresses a troponin I myopathy in Drosophila. *Mol Biol Cell.* 12:1529-39.

Nigro, V., E. de Sa Moreira, G. Piluso, M. Vainzof, A. Belsito, L. Politano, A.A. Puca, M.R. Passos-Bueno, and M. Zatz. 1996. Autosomal recessive limb-girdle muscular dystrophy, LGMD2F, is caused by a mutation in the delta-sarcoglycan gene. *Nat Genet.* 14:195-8.

Noguchi, S., T. Tsukahara, M. Fujita, R. Kurokawa, M. Tachikawa, T. Toda, A. Tsujimoto, K. Arahata, and I. Nishino. 2003. cDNA microarray analysis of individual Duchenne muscular dystrophy patients. *Hum Mol Genet.* 12:595-600.

Nongthomba, U., M. Cummins, S. Clark, J.O. Vigoreaux, and J.C. Sparrow. 2003. Suppression of Muscle Hypercontraction by Mutations in the Myosin Heavy Chain Gene of Drosophila melanogaster. *Genetics.* 164:209-22.

Olson, E.N., and J.D. Molkentin. 1999. Prevention of cardiac hypertrophy by calcineurin inhibition: hope or hype? *Circ Res.* 84:623-32.

Park, E.C., and H.R. Horvitz. 1986. Mutations with dominant effects on the behavior and morphology of the nematode Caenorhabditis elegans. *Genetics.* 113:821-52.

Peckham, M., J.E. Molloy, J.C. Sparrow, and D.C. White. 1990. Physiological properties of the dorsal longitudinal flight muscle and the tergal depressor of the trochanter muscle of Drosophila melanogaster. *J Muscle Res Cell Motil.* 11:203-15.

Poetter, K., H. Jiang, S. Hassanzadeh, S.R. Master, A. Chang, M.C. Dalakas, I. Rayment, J.R. Sellers, L. Fananapazir, and N.D. Epstein. 1996. Mutations in either the essential or regulatory light chains of myosin are associated with a rare myopathy in human heart and skeletal muscle. *Nat Genet.* 13:63-9.

Raffaele Di Barletta, M., E. Ricci, G. Galluzzi, P. Tonali, M. Mora, L. Morandi, A. Romorini, T. Voit, K.H. Orstavik, L. Merlini, C. Trevisan, V. Biancalana, I. Housmanowa-Petrusewicz, S. Bione, R. Ricotti, K. Schwartz, G. Bonne, and D. Toniolo. 2000. Different mutations in the LMNA gene cause autosomal dominant and autosomal recessive Emery-Dreifuss muscular dystrophy. *Am J Hum Genet.* 66:1407-12.

Ray, P.N., B. Belfall, C. Duff, C. Logan, V. Kean, M.W. Thompson, J.E. Sylvester, J.L. Gorski, R.D. Schmickel, and R.G. Worton. 1985. Cloning of the breakpoint of an X;21 translocation associated with Duchenne muscular dystrophy. *Nature.* 318:672-5.

Raymackers, J.M., H. Debaix, M. Colson-Van Schoor, F. De Backer, N. Tajeddine, B. Schwaller, P. Gailly, and J.M. Gillis. 2003. Consequence of parvalbumin deficiency in the mdx mouse: histological, biochemical and mechanical phenotype of a new double mutant. *Neuromuscul Disord.* 13:376-87.

Raymackers, J.M., P. Gailly, M.C. Schoor, D. Pette, B. Schwaller, W. Hunziker, M.R. Celio, and J.M. Gillis. 2000. Tetanus relaxation of fast skeletal muscles of the mouse made parvalbumin deficient by gene inactivation. *J Physiol.* 527 Pt 2:355-64.

Rayment, I., H.M. Holden, J.R. Sellers, L. Fananapazir, and N.D. Epstein. 1995. Structural interpretation of the mutations in the beta-cardiac myosin that have been implicated in familial hypertrophic cardiomyopathy. *Proc Natl Acad Sci U S A.* 92:3864-8.

Roberds, S.L., F. Leturcq, V. Allamand, F. Piccolo, M. Jeanpierre, R.D. Anderson, L.E. Lim, J.C. Lee, F.M. Tome, N.B. Romero, and et al. 1994.

Missense mutations in the adhalin gene linked to autosomal recessive muscular dystrophy. *Cell.* 78:625-33.

Robert, V., M.L. Massimino, V. Tosello, R. Marsault, M. Cantini, V. Sorrentino, and T. Pozzan. 2001. Alteration in calcium handling at the subcellular level in mdx myotubes. *J Biol Chem.* 276:4647-51.

Rozek, C.E., and N. Davidson. 1983. Drosophila has one myosin heavy-chain gene with three developmentally regulated transcripts. *Cell.* 32:23-34.

Sadoshima, J., and S. Izumo. 1993. Signal transduction pathways of angiotensin II--induced c-fos gene expression in cardiac myocytes in vitro. Roles of phospholipid-derived second messengers. *Circ Res.* 73:424-38.

Sadoshima, J., and S. Izumo. 1997. The cellular and molecular response of cardiac myocytes to mechanical stress. *Annu Rev Physiol.* 59:551-71.

Sadoshima, J., L. Jahn, T. Takahashi, T.J. Kulik, and S. Izumo. 1992. Molecular characterization of the stretch-induced adaptation of cultured cardiac cells. An in vitro model of load-induced cardiac hypertrophy. *J Biol Chem.* 267:10551-60.

Sadoshima, J., Y. Xu, H.S. Slayter, and S. Izumo. 1993. Autocrine release of angiotensin II mediates stretch-induced hypertrophy of cardiac myocytes in vitro. *Cell.* 75:977-84.

Sandri, M., C. Minetti, M. Pedemonte, and U. Carraro. 1998. Apoptotic myonuclei in human Duchenne muscular dystrophy. *Lab Invest.* 78:1005-16.

Satoh, M., M. Takahashi, T. Sakamoto, M. Hiroe, F. Marumo, and A. Kimura. 1999. Structural analysis of the titin gene in hypertrophic cardiomyopathy: identification of a novel disease gene. *Biochem Biophys Res Commun.* 262:411-7.

Seidman, J.G., and C. Seidman. 2001. The genetic basis for cardiomyopathy: from mutation identification to mechanistic paradigms. *Cell.* 104:557-67.

Standiford, D.M., M.B. Davis, K. Miedema, C. Franzini-Armstrong, and C.P. Emerson, Jr. 1997. Myosin rod protein: a novel thick filament component of Drosophila muscle. *J Mol Biol.* 265:40-55.

Takagi, A., S. Kojima, M. Ida, and M. Araki. 1992. Increased leakage of calcium ion from the sarcoplasmic reticulum of the mdx mouse. *J Neurol Sci.* 110:160-4.

Tanigawa, G., J.A. Jarcho, S. Kass, S.D. Solomon, H.P. Vosberg, J.G. Seidman, and C.E. Seidman. 1990. A molecular basis for familial hypertrophic cardiomyopathy: an alpha/beta cardiac myosin heavy chain hybrid gene. *Cell.* 62:991-8.

Thierfelder, L., H. Watkins, C. MacRae, R. Lamas, W. McKenna, H.P. Vosberg, J.G. Seidman, and C.E. Seidman. 1994. Alpha-tropomyosin and cardiac troponin T mutations cause familial hypertrophic cardiomyopathy: a disease of the sarcomere. *Cell.* 77:701-12.

Tsukahara, T., S. Tsujino, and K. Arahata. 2002. CDNA microarray analysis of gene expression in fibroblasts of patients with X-linked Emery-Dreifuss muscular dystrophy. *Muscle Nerve.* 25:898-901.

Tyska, M.J., E. Hayes, M. Giewat, C.E. Seidman, J.G. Seidman, and D.M. Warshaw. 2000. Single-molecule mechanics of R403Q cardiac myosin isolated from the mouse model of familial hypertrophic cardiomyopathy. *Circ Res.* 86:737-44.

van der Kooi, A.J., M. van Meegen, T.M. Ledderhof, E.M. McNally, M. de Visser, and P.A. Bolhuis. 1997. Genetic localization of a newly recognized autosomal dominant limb-girdle muscular dystrophy with cardiac involvement (LGMD1B) to chromosome 1q11-21. *Am J Hum Genet.* 60:891-5.

Vandebrouck, C., N. Imbert, G. Duport, C. Cognard, and G. Raymond. 1999. The effect of methylprednisolone on intracellular calcium of normal and dystrophic human skeletal muscle cells. *Neurosci Lett.* 269:110-4.

Vigoreaux, J.O. 2001. Genetics of the Drosophila flight muscle myofibril: a window into the biology of complex systems. *Bioessays.* 23:1047-63.

Walker, D.S., N.J. Gower, S. Ly, G.L. Bradley, and H.A. Baylis. 2002a. Regulated disruption of inositol 1,4,5-trisphosphate signaling in Caenorhabditis elegans reveals new functions in feeding and embryogenesis. *Mol Biol Cell*. 13:1329-37.

Walker, D.S., S. Ly, K.C. Lockwood, and H.A. Baylis. 2002b. A direct interaction between IP(3) receptors and myosin II regulates IP(3) signaling in C. elegans. *Curr Biol*. 12:951-6.

Wassenberg, D.R., 2nd, W.A. Kronert, P.T. O'Donnell, and S.I. Bernstein. 1987. Analysis of the 5' end of the Drosophila muscle myosin heavy chain gene. Alternatively spliced transcripts initiate at a single site and intron locations are conserved compared to myosin genes of other organisms. *J Biol Chem*. 262:10741-7.

Watkins, H., D. Conner, L. Thierfelder, J.A. Jarcho, C. MacRae, W.J. McKenna, B.J. Maron, J.G. Seidman, and C.E. Seidman. 1995. Mutations in the cardiac myosin binding protein-C gene on chromosome 11 cause familial hypertrophic cardiomyopathy. *Nat Genet*. 11:434-7.

Zhang, C.L., T.A. McKinsey, S. Chang, C.L. Antos, J.A. Hill, and E.N. Olson. 2002. Class II histone deacetylases act as signal-responsive repressors of cardiac hypertrophy. *Cell*. 110:479-88.

Characterization of a hypercontraction-induced myopathy in *Drosophila* caused by mutations in *Mhc*

Enrico S. Montana[1] & J. Troy Littleton[1,2]

[1]Department of Biology, [1]Picower Center for Learning and Memory, [2]Department of Brain and Cognitive Sciences, Massachusetts Institute of Technology, Cambridge, MA 02139

This work began with a screen for temperature-sensitive behavioral mutants performed by Troy Littleton as a postdoctoral fellow in the lab of Barry Ganetzky. From the original screen, he isolated Mhc^{S1}, $Swing^{X118}$, and $Breakdance^{J29}$. He further performed rough recombination mapping of the dominant mutations and isolated potential gamma-ray revertants of each of the mutants. Finer mapping and the rest of the experiments were done by me under the guidance of Troy. This work has been published in *J. Cell Biology* **164**: 1045-1054.

Abstract

The *Myosin heavy chain* (*Mhc*) locus encodes the muscle-specific motor mediating contraction in *Drosophila*. In a screen for temperature-sensitive behavioral mutants, we have identified two dominant *Mhc* alleles that lead to a hypercontraction-induced myopathy. These mutants are caused by single point mutations in the ATP binding/hydrolysis domain of Mhc and lead to degeneration of the flight muscles. Electrophysiological analysis in the adult giant fiber flight circuit demonstrates temperature-dependent seizure activity that requires neuronal input, as genetic blockage of neuronal activity suppresses the electrophysiological seizure defects. Intracellular recordings at the third instar neuromuscular junction show spontaneous muscle movements in the absence of neuronal stimulation and extracellular Ca^{2+}, suggesting a dysregulation of intracellular calcium homeostasis within the muscle or an alteration of the Ca^{2+}-dependence of contraction. Characterization of these new *Mhc* alleles suggests that hypercontraction occurs *via* a mechanism which is molecularly distinct from mutants previously identified in troponin I and troponin T.

Introduction

Muscle contraction is a highly complex and coordinated process, involving a molecular machine tightly regulated to provide ATP-dependent motion in response to neuronal stimulation. Activation of the muscle from the innervating neuron results in a postsynaptic action potential which stimulates release of Ca^{2+} from internal stores. Ca^{2+} binds to regulatory proteins on the thin filament of the muscle. This leads to coordinated conformational changes in a large number of proteins, allowing myosin to shorten the length of the sarcomere in an ATP-dependent process. In addition to proteins required during contraction, numerous secondary proteins are required for its continued maintenance, structural support, and force transduction (Huxley, 2000; Lamb, 2000; Poage and Meriney, 2002; Pollard, 2000; Ruff, 2003). Characterization of this complex system may lead to molecular understanding of human diseases such as cardiomyopathies, which arise from perturbations in several known cardiac muscle proteins (Seidman and Seidman, 2001).

The genetic tractability of *Drosophila* has made it an ideal system to characterize mutations affecting neuromuscular function. Many of these mutants have been identified by screening for temperature-sensitive (TS) behavioral defects, allowing the identification of gene products important for neuromuscular function (Ganetzky and Wu, 1983; Littleton et al., 1998). Additionally, the *Drosophila* flight system has provided an efficient genetic model for hypertrophic cardiomyopathies. Mutated genes leading to flightless behavior in *Drosophila*

are also disrupted in many forms of primary hypertrophic cardiomyopathies, including *Myosin heavy chain* (*Mhc), Tropomyosin2* (*Tm2), wings up A (wupA*—troponin I), *actin88F* (*act88F*), and *upheld* (*up*—troponin T). Mutations in these genes also show extensive genetic interactions, providing key insights into the regulatory pathways underlying muscle function (Ferrus et al., 2000; Vigoreaux, 2001).

Flightless behavior in *Drosophila* can arise from mutations which lead to muscle hypercontraction. Hypercontraction of the *Drosophila* indirect flight muscles (IFM) occurs due to specific mutations of the contractile machinery which lead to either decreased structural integrity of the sarcomere, or dysregulation of the contractile process *in vivo*. These mutations result in a degeneration of the IFM of adult flies following muscle differentiation and development (Beall and Fyrberg, 1991; Deak et al., 1982; Fekete and Szidonya, 1979; Homyk and Emerson, 1988). Hypercontraction mutants can be genetically suppressed by specific mutant alleles of *Mhc*. The mechanism of suppression has been suggested to be a potential Mhc-Troponin I direct interaction (Kronert et al., 1999). However, additional data suggests that an overall decrease in actomyosin force is sufficient to explain suppression of hypercontraction by mutant Mhc (Nongthomba et al., 2003). The identification of *Mhc* alleles that directly cause hypercontraction and enhance the hypercontraction defects of other mutants may facilitate defining the role of myosin in the regulation of contraction.

To further understand the molecular and cellular processes underlying neuromuscular function, we performed a screen for *Drosophila* TS behavioral mutants. One complementation group isolated in our screens, *Samba*, disrupts the *Mhc* locus, leading to hypercontraction and muscle degeneration. Characterization of the *Samba* mutants has revealed potential molecular mechanisms which lead to muscle degeneration through hypercontraction *via* distinct mechanisms from previously characterized hypercontraction mutants. In addition, these mutants give insight into the role of Mhc in the regulation of the contractile process in addition to its role in the ATP-dependent motor function.

Results

Isolation and characterization of the Samba mutants, Mhc^{S1} and Mhc^{S2}

The *Samba* (*$Samba^{1}$* and *$Samba^{2}$*) mutants were isolated in an ethylmethane sulfonate mutagenesis, screening for X-linked and autosomal dominant TS behavioral mutants. *Samba* adults exhibit dominant TS behavioral defects that include a rapid onset of seizure-like behavior and TS loss of mesothoracic leg function. This behavior is readily evident in all flies by one minute of exposure to 38°C (Figure 1A). *Samba* mutants also display defects at permissive temperatures. *Samba/+* flies are flightless, with thoracic indentations similar to those found in *ether-ago-go^{1}*, *$Shaker^{133}$* (*eag^{1}*, *Sh^{133}*) mutant flies (Figure 1B). Thoracic indentations in *eag^{1}*, *Sh^{133}* flies occur through hypercontraction of the indirect flight muscles (IFM) thought to be induced by excessive neurotransmitter release in the presynaptic neuron, which is caused by loss of voltage-gated potassium channels and subsequent reduction in repolarization (Ganetzky and Wu, 1983; Wu et al., 1983). Although homozygous *Samba* mutants are lethal, rare *$Samba^{1}$* escapers with femur hypercontration defects can be found.

In addition to *Samba*, two other complementation groups, *Swing* (*Swg^{X118}*) and *Breakdance* (*$Brkd^{J29}$*), were isolated in our screens that exhibited similar dominant TS behavioral defects and showed genetic interactions with *Samba*. Double heterozygotes of *Swg^{X118}* and *$Samba^{1}$* or *$Samba^{2}$* and double

Figure 1

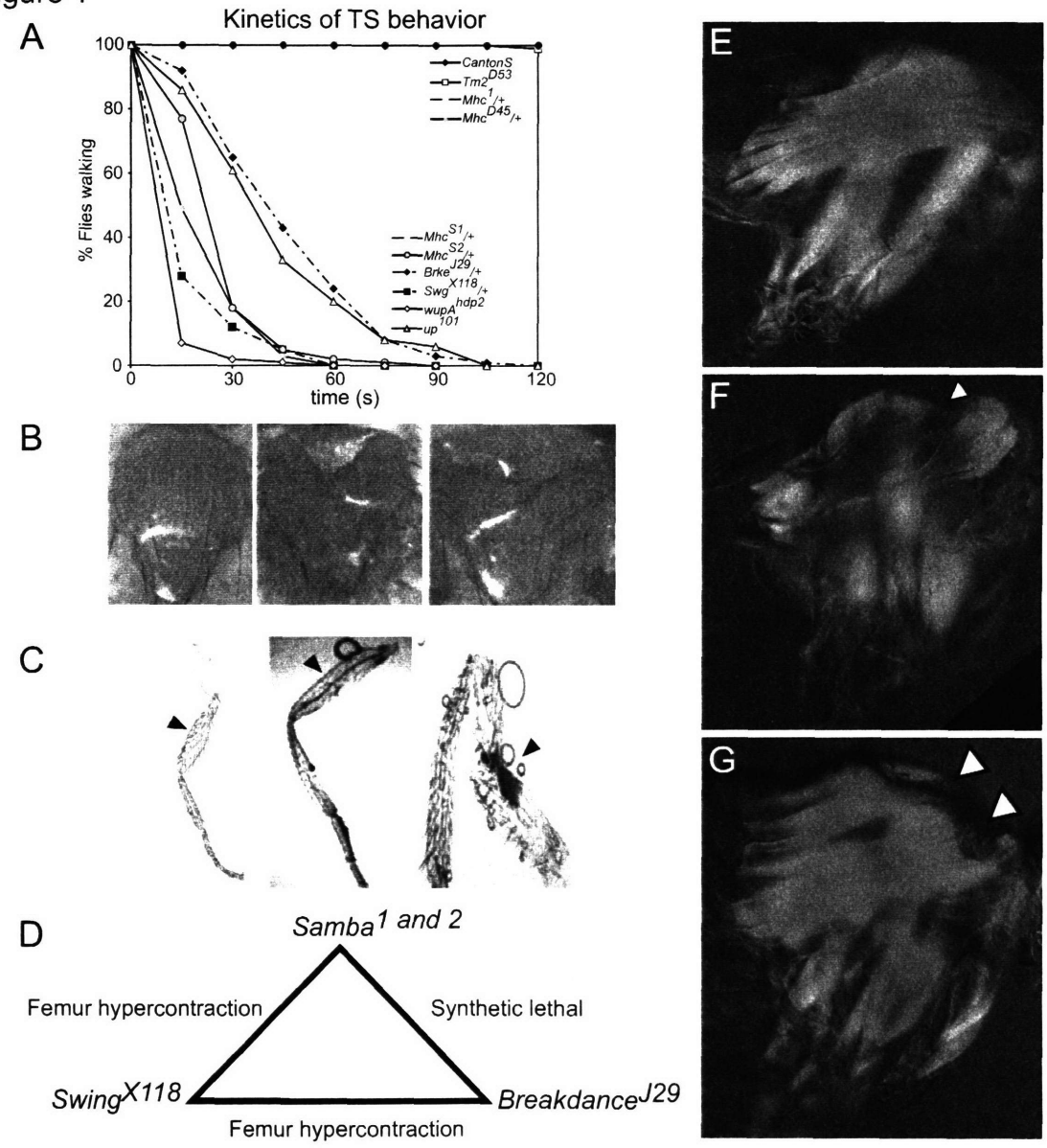

Figure 1: Characterization of the *Samba* mutants, Mhc^{S1} and Mhc^{S2}. (A) Temperature-sensitivity curves of several mutant strains that affect muscle function. TS behavioral defects are found only in hypercontraction mutants. (B) Thoraces of *CantonS* (left), eag^{1}, Sh^{133}/Y (center), and $Samba^{1}/+$ (right) adult male flies. (C) Schematic of a normal fly leg (left), a leg dissected from *CantonS* (center), and a leg showing femur hypercontraction from a $Swg^{X118}/+;Bkde^{J29}/+$ double heterozygote (right). Arrows indicate femoral segment. (D) Schematic depicting the genetic interactions of the *Samba* locus. (E-G) Polarized light micrographs showing hypercontraction of the IFM are shown in sagittal views of the thorax from adult flies of *CantonS* (E), $Samba^{1}/+$, (F)and $Samba^{1}/+;Tm2^{D53}$ (G). Partial suppression is observed in $Samba^{1}/+;Tm2^{D53}$, as IFM are found less degraded despite the presence of thoracic indentations (arrows).

heterozygotes of *Swg*^{X118} and *Brkd*^{J29} are semi-lethal with escapers having hypercontracted femurs (Figure 1C). Double heterozygotes of *Samba*^{1} or *Samba*^{2} and *Brkd*^{J29} are synthetic lethal (Figure 1D). These genetic interactions and similarities to *eag*^{1}, *Sh*^{133} double mutants suggest that *Samba, Swing,* and *Breakdance* define a genetic pathway required in the regulation of membrane excitability, and when disrupted, lead to abnormal muscle hypercontraction.

Segregation analysis of *Samba* revealed an autosomal dominant mutation on the second chromosome, refined to 2-52 cM by recombination mapping. Deficiency mapping by lethality narrowed the cytological interval between 36A8 and 36C4 on the left arm of chromosome 2. To help identify the *Samba* locus, we screened for revertants of TS seizure behavior in a γ-irradiation reversion screen in order to isolate potential loss of function mutations in the *Samba* locus. Three revertants were identified by loss of TS behavioral defects. These revertants were embryonic lethal with normal morphological development, but showed complete loss of muscle wave propagation in late stage embryos (data not shown). Non-complementation to *Mhc*^{1} by both the TS mutants and the three revertants identified the *Samba* mutations as new alleles of the *Myosin Heavy Chain* (*Mhc*) locus (Mogami and Hotta, 1981). We designated the *Samba*^{1} and *Samba*^{2} alleles *Mhc*^{S1} and *Mhc*^{S2}, respectively, and the revertants *Mhc*^{rv1}, *Mhc*^{rv2}, and *Mhc*^{rv3}.

The *Mhc* locus is complex, encoding all muscle-specific isoforms through the use of extensive alternative splice patterns (Bernstein et al., 1983; Rozek and Davidson, 1983). The locus contains 19 coding exons, 5 of which are

alternatively spliced, and one that is either included or excluded (Collier et al., 1990; George et al., 1989; Hess and Bernstein, 1991; Wassenberg et al., 1987; Zhang and Bernstein, 2001). A previously isolated allele, Mhc^5 (G200D), causes similar hypercontraction defects to the *Samba* mutants. Mhc^5 introduces a point mutation in exon 4 of the *Mhc* locus, disrupting the ATPase domain of Mhc (Homyk and Emerson, 1988). Due to the phenotypic similarities with Mhc^5, exon 4 of these new alleles was sequenced. Both Mhc^{S1} and Mhc^{S2} were found to be point mutations (V235E and E187K, respectively) mapping to the ATP binding and hydrolysis site of the protein (Figure 2A-E).

Seizure activity in Samba flies is dependent upon neuronal activity

Extracellular dorsal longitudinal muscle (DLM) recordings were utilized in order to characterize the behavioral seizures at restrictive temperatures (Engel and Wu, 1992). Electrical activity was observed in adult flies at room temperature, shifted to 38°C, and returned to room temperature. Correlating with the behavioral defects, abnormal spiking activity in the DLMs was recorded at restrictive temperatures that was not observed at permissive temperatures, nor in *CantonS* at 38°C (Figure 3A, 3B, 3D, 3F). Similar seizure activity was observed in Swg^{X118} and $Brkd^{J29}$ (Figure 3H, 3J). This abnormal activity could be either muscle autonomous or dependent upon synaptic input. To address these possibilities, we utilized a mutation in the voltage-gated Na^+ channel, *paralytic* ($para^{ts1}$), which is required for action potential propagation in the motor neuron

Figure 2

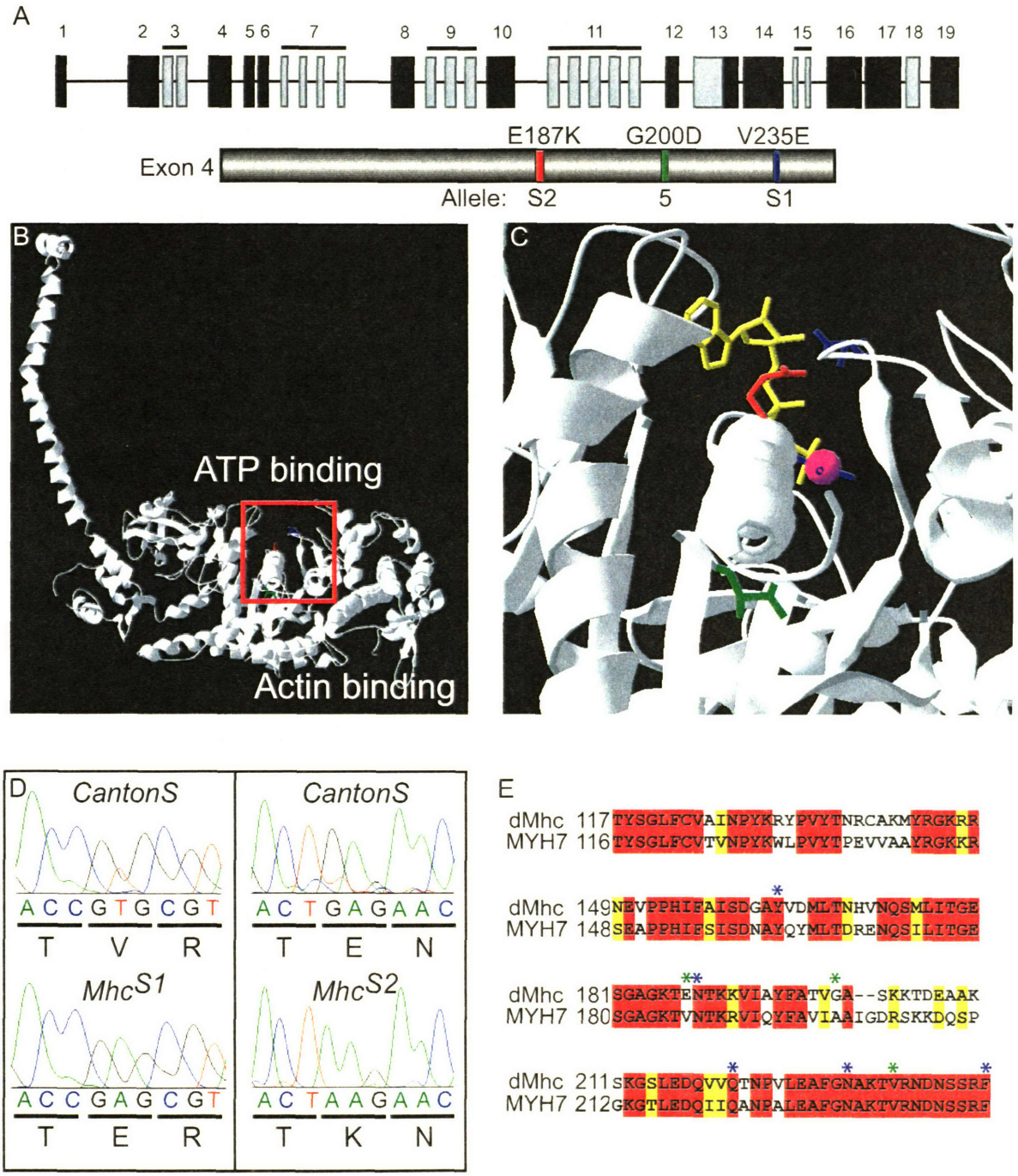

Figure 2: Localization of the *Mhc^{S1}* and *Mhc^{S2}* mutations onto the crystal structure. (A) Schematic of the *Mhc* locus. Constitutive exons are depicted in black, and alternative exons in gray. Exon 4 has been expanded to show the relative positions of the point mutations in *Mhc^{5}*, *Mhc^{S1}*, and *Mhc^{S2}*. (B) A view of the crystal structure of chicken Mhc depicting the mutations *Mhc^{5}* (green), *Mhc^{S1}* (blue), and *Mhc^{S2}* (red). (C) The region corresponding to the red box has been expanded from a crystal structure from the motor domain of *Dictyostelium* Mhc showing the mutation positions in relation to the ATP analog (yellow) and bound Mg^{2+} (magenta). (D) Sequence data showing the base pair changes in *Mhc^{S1}* and *Mhc^{S2}* and the corresponding amino acid point mutations. (E) An alignment of exon 4 of *Drosophila* Mhc with β-cardiac myosin heavy chain (MYH7) from humans. Red corresponds to identical amino acids, and yellow identifies similar amino acids. Positions of *Drosophila* mutations are indicated in green relative to amino acids that are mutated in several primary hypertrophic cardiomyopathies, shown in blue.

(Suzuki et al., 1971). This mutation specifically abolishes neuronal action potentials at elevated temperatures, as *para* expression is not detected in muscles (Hong and Ganetzky, 1994). In $para^{ts1}/Y;Mhc^{X}/+$ (X indicating 5, S1 or S2) flies, we observed a suppression of the seizure activity at 38°C (Figure 3C, 3E, 3G). Similarly, suppression of activity was observed with $para^{ts1}/Y;Swg^{X118}/+$ and $para^{ts1}/Y;Brkd^{J29}/+$ (Figure 3I, 3K). These data suggest that mutant muscles are hyperexcitable at restrictive temperatures. This hyperexcitable state, however, cannot lead to autonomous muscle firing, but must be triggered by an initial input by the innervating motor neuron.

Samba mutations lead to hypercontraction

To further define how the *Samba* mutants affect Mhc function, we analyzed genetic interactions with known muscle mutants that increase or decrease the contractile state of the muscle. We characterized genetic interactions with mutations in Troponin I, Troponin T, and Tropomyosin 2. Troponin I is encoded by the *wings up A* locus. A mutation in troponin I, $heldup^{2}$ ($wupA^{hdp2}$), has been previously identified as a hypercontraction mutation (Beall and Fyrberg, 1991; Deak et al., 1982). A mutation in Troponin T, $upheld^{101}$ (up^{101}), is similar to $wupA^{hdp2}$, also causing hypercontraction (Fekete and Szidonya, 1979; Homyk et al., 1980). Hemizygous flies for either $wupA^{hdp2}$ or up^{101} and heterozygous for Mhc^{S1} or Mhc^{S2} are synthetic lethal, whereas double heterozygous females have femur hypercontraction defects (data not shown). A

Figure 3

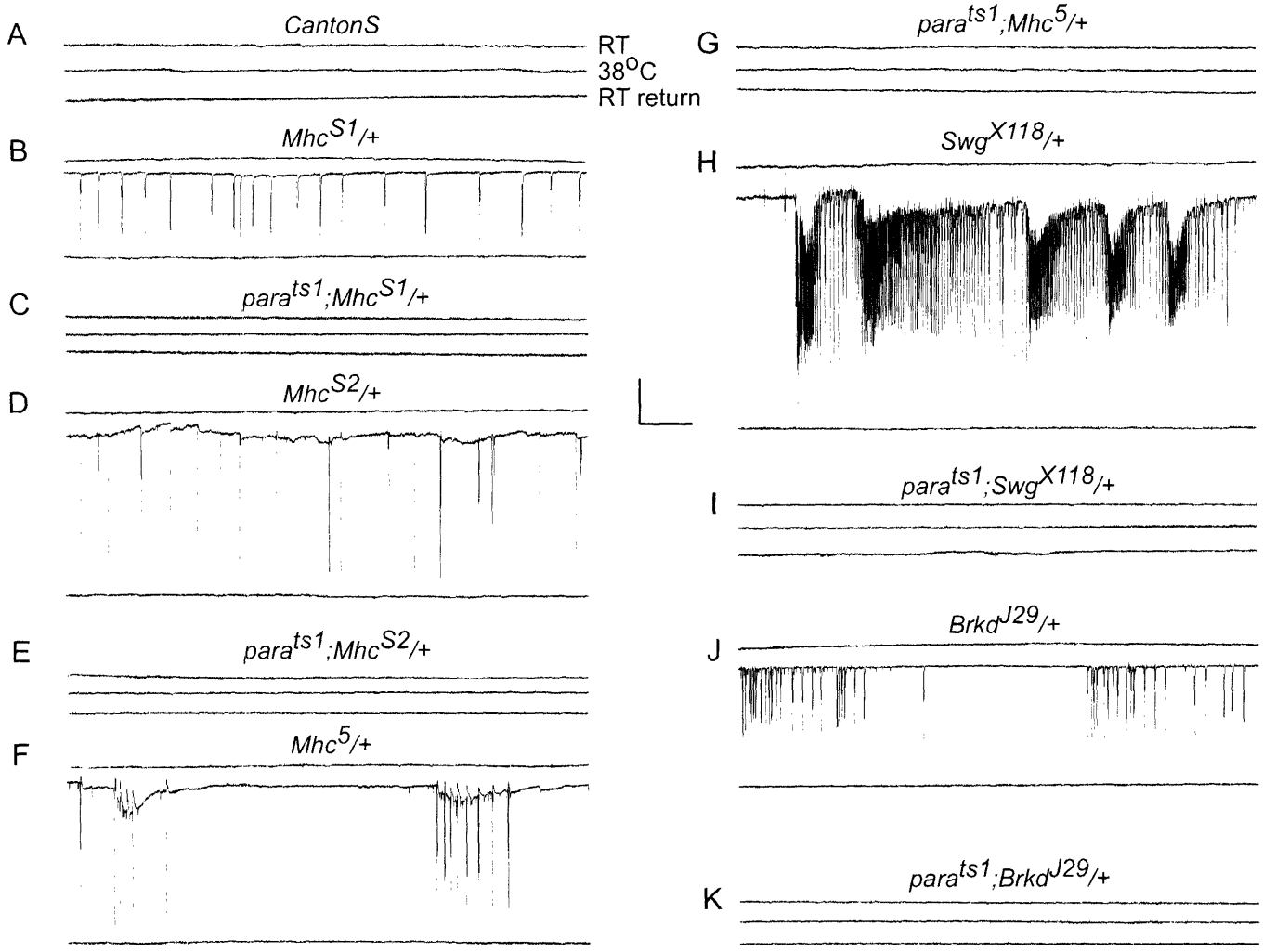

Figure 3: Extracellular DLM recordings reveal abnormal activity at restrictive temperatures which is dependent upon neuronal activity. Recordings were done on male flies of genotypes (A) *CantonS,* (B) Mhc^{S1}/+, (C) $para^{TS1}$;Mhc^{S1}/+, (D) Mhc^{S2}/+, (E) $para^{TS1}$;Mhc^{S2}/+, (F) Mhc^{5}/+, (G) $para^{TS1}$;Mhc^{5}/+, (H) Swg^{X118}/+, (I) $para^{TS1}$;Swg^{X118}/+, (J) $Bkde^{J29}$/+, and (K) $para^{TS1}$;$Bkde^{J29}$/+. Representative traces are shown from a single male fly of the indicated genotype at room temperature, 38°C, and subsequent recovery to room temperature. Scale bar indicates 500 ms, 10mV.

mutation in *Tropomyosin 2* ($Tm2^{D53}$) suppresses the hypercontraction of both up^{101} and $wupA^{hdp2}$ (Naimi et al., 2001). Similarly, $Tm2^{D53}$ suppresses the recessive lethality of Mhc^{S1}, increasing viability of the homozygotes from 2.38% to 80.92% (Mhc^{S1} n=435, $Mhc^{S1};Tm2^{D53}$ n=505). These results indicate that the *Samba* alleles of *Mhc* cause hypercontraction defects similar to $wupA^{hdp2}$ and up^{101}. Interestingly, both up^{101} and $wupA^{hdp2}$ exhibit abnormal TS behavior similar to Mhc^{S1} and Mhc^{S2}, suggesting that the behavioral defects are most likely a TS susceptibility resulting from an altered state of the muscle secondary to hypercontraction, as opposed to a specific TS dysfunction of the Mhc protein (Figure 1A). In contrast to the TS seizure behavior in hypercontraction mutants, $Tm2^{D53}$ flies do not show abnormal behavior at 38°C, nor do heterozygotes of the *Mhc* null (Mhc^{1}/+) and heterozygotes of a hypercontraction suppressor mutant (Mhc^{D45}/+) (Figure 1A).

To confirm that the *Samba* phenotype results from hypercontraction, we analyzed the structure of the IFM in Mhc^{S1}/+ flies. The ordered array of filaments in muscles leads to birefringent properties, allowing muscle visualization under polarized light microscopy. In previously characterized hypercontraction mutants, the IFM exhibit one of two defects. Some show loss of birefringence in the middle of the muscles due to breakage or degradation, with the bulk of the muscle fiber at either one or both of the attachment sites. Others show separation from the attachment sites, with birefringence found only in the middle of the fiber (Nongthomba et al., 2003). Mhc^{S1}/+ flies exhibited the former defect, showing birefringence at the attachment sites, with loss of birefringence in the

middle of the IFM. This defect was partially suppressed in the background of $Tm2^{D53}$, as the IFM of double mutants displayed less degradation despite the presence of indented thoraces compared to similarly aged *Samba* flies (Figure 1E-G). These data confirm that the *Samba* mutants lead to hypercontraction defects in the muscle.

Samba mutant muscles do not alter synaptic function but move independently of neuronal input

Hypercontraction in *Drosophila* muscles induced by the *Samba* mutants leads to progressive degradation of fibers, similar to degeneration observed in muscular dystrophies. In some animal models of muscular dystrophy, loss of acetylcholine receptor clustering results in the functional denervation of diseased fibers (Rafael et al., 2000). Because Mhc^{S1} and Mhc^{S2} were isolated by TS behavioral defects and abnormal extracellular DLM activity, we hypothesized that these mutations may cause functional or structural changes at the NMJ.

Bouton number at the NMJ is tightly regulated and is sensitive to disruptions in both presynaptic and postsynaptic function. Though poorly understood, postsynaptic defects can alter presynaptic structural and functional properties through homeostatic regulatory pathways (Davis et al., 1998; Petersen et al., 1997). To analyze the morphology of the NMJ in *Samba* mutants, we stained third instar larvae with α-synaptotagmin I antisera, a marker for presynaptic terminals, and analyzed muscle fibers 6 and 7 (*CantonS* n=18

larvae, 97 muscles; Mhc^{S1}/+ n=27, 157). Type I innervation from glutamatergic motor neurons was not altered in Mhc^{S1}/+ animals, suggesting little effect of dysfunctional muscles on excitatory innervation (Figure 4J). The number of muscles showing ectopic innervation, however, was found to be more frequent than wildtype, increasing from 4.1% in control animals to 15.9% in Mhc^{S1}/+ animals (Figure 4A-F, 4K). These were determined to be Type II synapses due to their morphology and the absence of postsynaptic DLG staining (Figure 4G-4I). Type II synapses are neuromodulatory, influencing the state of excitation in body wall muscles through release of octopamine (Gramates and Budnik, 1999). Increases in type II innervation have also been reported in mutants such as *tipE* and *nap*, which reduce nerve excitability (Jarecki and Keshishian, 1995). The increase in Type II innervation suggests that alterations in muscle function can lead to altered neuromodulation. Similar data was obtained with Mhc^{S2}/+ larvae (data not shown).

To determine whether the altered innervation pattern correlated with abnormal synaptic transmission, we characterized miniature excitatory junctional potential amplitude (mEJP), excitatory junctional potential amplitude (EJP), and mEJP frequency from the muscle 6 NMJ in 0.4 mM Ca^{2+} using intracellular recording techniques (Figure 5A, Table I). Wildtype fibers were found to have a mEJP of 0.95 ± 0.04 mV and EJP of 39.6 ± 1.9 mV (n=8, 23). In mutant fibers, these values were 0.79 ± 0.02 mV and 34.2 ± 1.7 mV, respectively (n=11, 29). Although these differences are statistically significant and may reflect subtle changes in synaptic function, the change in release is small and the differences

Figure 4

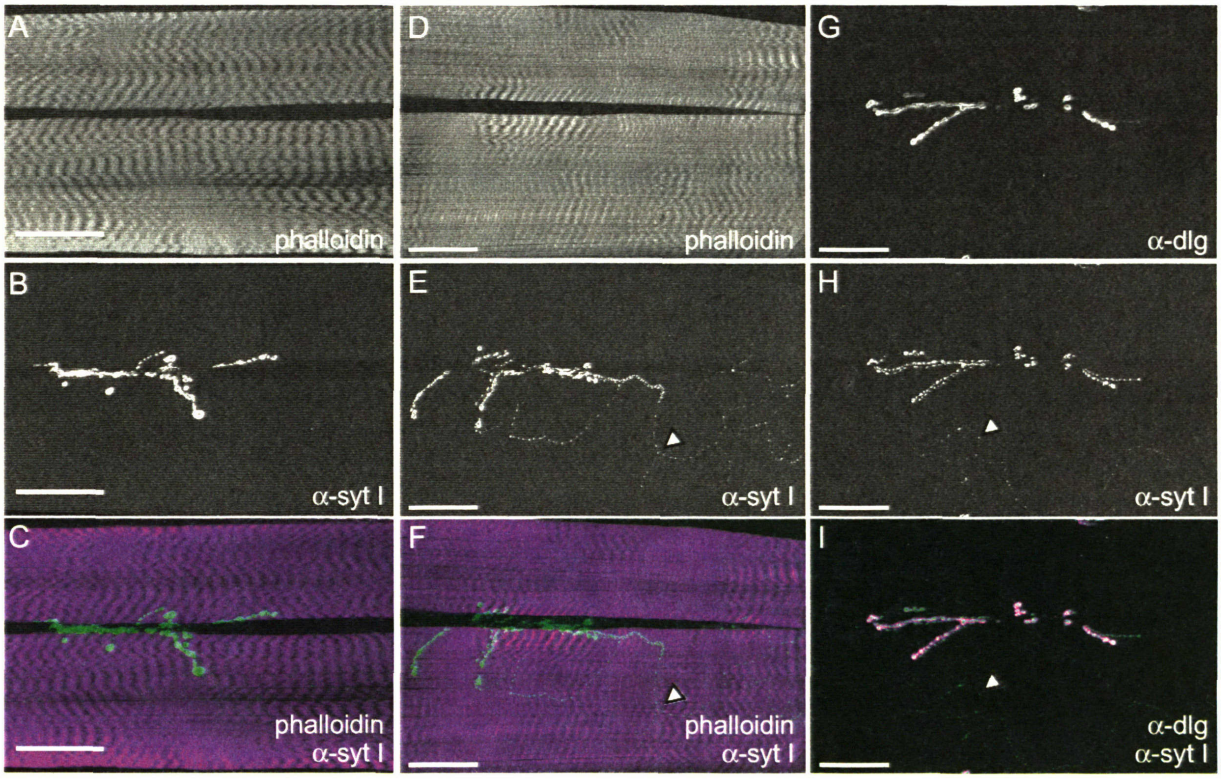

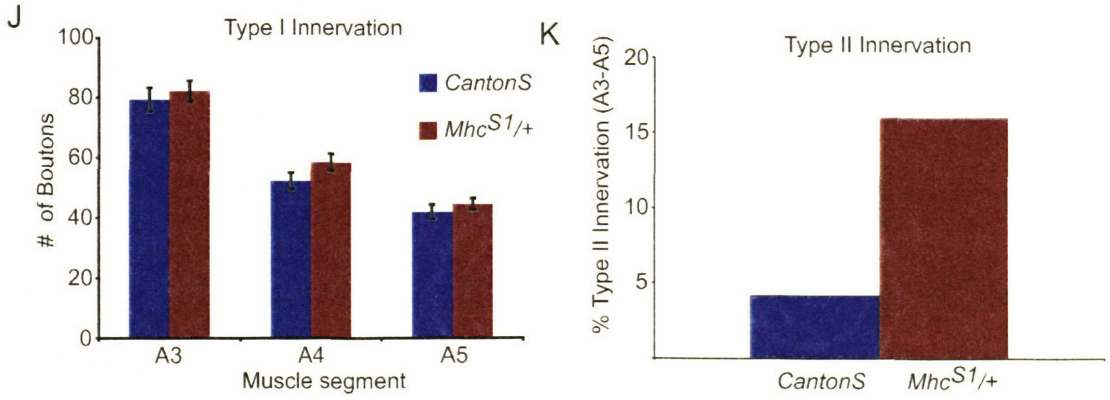

Figure 4: Structural properties of the neuromuscular junction in *Mhc^{S1}/+* mutants. Third instar larvae neuromuscular junctions from (A-C) *CantonS* and (D-I) *Mhc^{S1}/+* labeled with the indicated markers. Arrows indicate an axonal branch containing Type II synapses as evidenced by the absence of postsynaptic DLG staining. Scale bar represents 50μm. (J) Excitatory Type I glutamatergic innervation on muscles 6/7 does not change in mutant muscles despite altered muscular function. (K) Ectopic Type II innervation increases in mutant muscles.

more likely reflect the complication caused by an apparent oscillation of the resting membrane potential due to spontaneous muscle movement in *Samba* mutants (Figure 5B). Movements such as these can lead to apparent voltage changes due to electrode motion. Spontaneous muscle movements did not resemble action potential-induced contraction events. Instead, a slow, cyclic activity that did not utlilize the full contractile potential of the muscle cell was continuously observed in the *Samba* mutants. Because contraction usually depends upon Ca^{2+} influx through L-type calcium channels in the sarcolemma, we hypothesized that alterations of Ca^{2+} influx through these channels may be responsible for the spontaneous contractions in *Samba* mutants. To test this, we recorded from mutant muscles in Ca^{2+}-free saline. Spontaneous contractions were still observed in Ca^{2+}-free saline similar to those in high extracellular Ca^{2+} (Figure 5B). An alternative possibility is that spontaneous contractions may reflect altered signaling from the innervating neuron. Although these recordings are normally done in preparations in which the axon has been severed from the cell body, we further tested this possibility in brain-intact preparations in the presence or absence of 3μM TTX. Spontaneous movements were seen regardless of neuronal activity (Figure 5B). These results indicate that hypercontraction in *Samba* mutants is not due to an increase in neuronal activity or neurotransmitter release, nor to multiple release events per axonal action potential, but can be explained by autonomous movement in the absence of neuronal input. This movement is not dependent upon extracellular Ca^{2+},

Figure 5

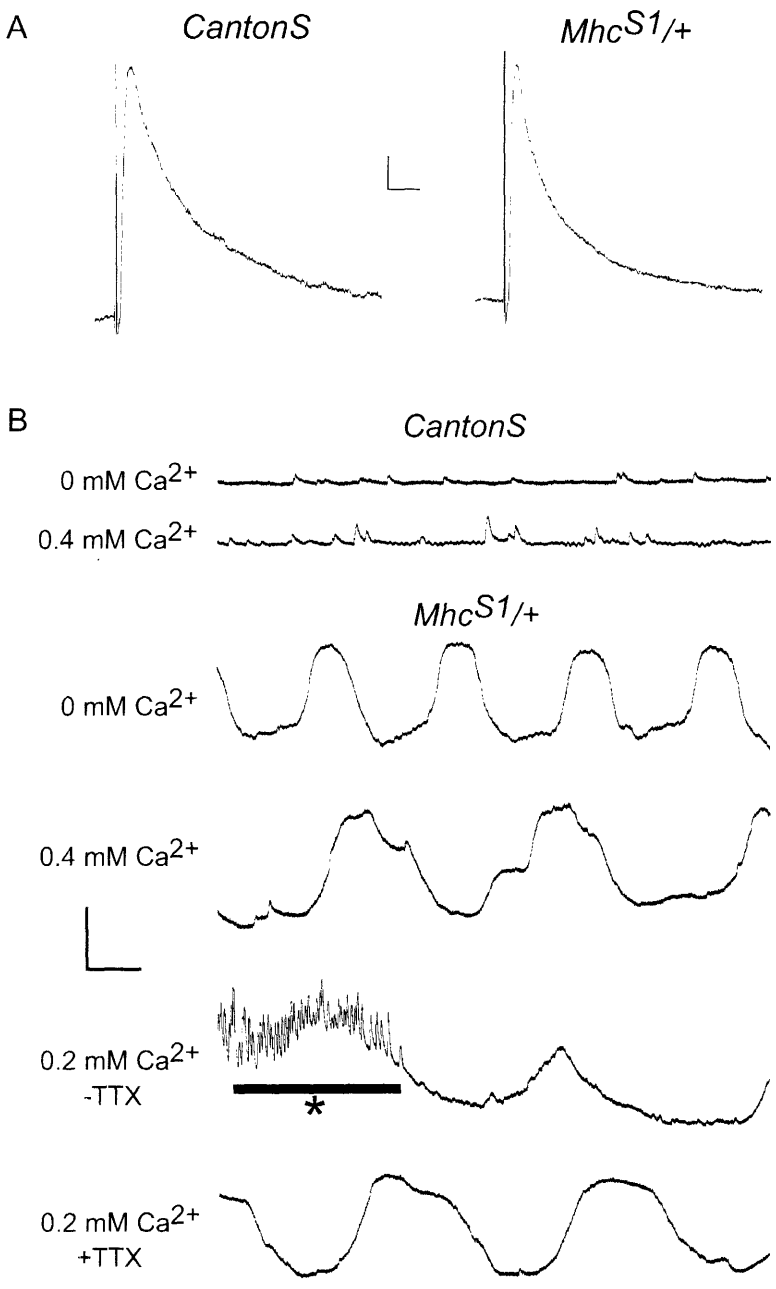

Figure 5: Electrophysiological properties of the *Mhc^{S1}*/+ third instar neuromuscular junction. Despite the increased presence of ectopic innervation, physiological properties are not altered in *Mhc^{S1}*/+. (A) Representative samples of EJPs in *CantonS* and *Mhc^{S1}*/+. Scale bar indicates 5mV, 200 ms. (B) Resting potential oscillations found in *Mhc^{S1}*/+ are present in both 0.4 mM and 0mM Ca^{2+}, as well as in the presence (-TTX) and absence (+TTX) of neuronal activity. Asterisk marks activity from the central pattern generator. Scale bar indicates 10mV, 500 ms.

Table I. Physiological properties of the NMJ[a]

Genotype	Resting Potential (mV)	Miniature frequency (mEJP/s)	mEJP Amplitude (mV)	EJP Amplitude (mV)
CantonS[b]	-69.4 ± 1.6	2.10 ± 0.21	0.95 ± 0.04	39.6 ± 1.8
MhcS1/+[c]	-62.6 ± 1.0**	1.53 ± 0.14*	0.79 ± 0.02**	34.2 ± 1.7*

a) Represented as Value±SEM b) n=8,23 c) n=11,29

* = P-value < 0.05, ** = P-value < 0.001

suggesting a defect in either intracellular Ca^{2+} homeostasis or the Ca^{2+} requirements of muscle contraction.

Discussion

Muscle contraction requires the coordinated action of many proteins under the regulation of defined stimuli. Dysregulation of this system leads to myopathy and dystrophy syndromes in humans. *Drosophila* provides an efficient model to dissect the molecular and cellular functions of the individual components and their roles in the coordinated machine that underlies this process. To this end, we have begun a molecular and cellular characterization of muscle dysfunction in *Drosophila* using the hypercontractive *Samba* mutants, Mhc^{S1} and Mhc^{S2}.

Hypercontraction and Mhc

Hypercontraction in the *Drosophila* IFM is thought to occur by two mechanisms. These mechanisms both lead to increased actomyosin force production by either 1) decreasing structural integrity of the sarcomere or 2) altering thin filament regulation of the crossbridge cycle. Mutations which lead to hypercontraction through the former mechanism include Mhc^{6}, $Mhc^{13\,(19)}$ and fln^{0}, whereas $wupA^{hdp2}$ and up^{101} occur through the latter mechanism (Kronert et al., 1995; Reedy et al., 2000). Hypercontraction by the latter group of mutations are suppressed by mutations in *Mhc* in a seemingly non-allele specific relationship, suggesting a decrease in actomyosin force is sufficient to suppress hypercontraction (Nongthomba et al., 2003). However, this model is complicated by data suppoting a role of Mhc in regulating thin filament dynamics

through a direct Mhc-TnI interaction (Kronert et al., 1999). Here we present work characterizing two new alleles of *Mhc*, Mhc^{S1} and Mhc^{S2}. These mutants represent dominant hypercontraction alleles, as defined by genetic interactions. These alleles enhance defects in $wupA^{hdp2}$ and up^{101}, both of which lead to hypercontraction as single mutants. Both $wupA^{hdp2}$ and up^{101} are fully suppressed by $Tm2^{D53}$, whereas the *Samba* mutants are only partially suppressed, suggesting that although these alleles lead to hypercontraction, they do so through a different molecular mechanism than $wupA^{hdp2}$ and up^{101}. In confirmation of the genetic data, the *Samba* mutants exhibit hypercontraction of the IFM when analyzed under polarized light microscopy. Due to their similarities with a previously isolated allele of *Mhc* (Mhc^{5}), we sequenced exon 4 of the locus, and identified two point mutations, V235E (*S1*) and E187K (*S2*), which map onto the ATP binding/hydrolysis site of the protein. Though hypercontraction occurs in Mhc^{6} and Mhc^{13}, these mutations do not display indented thoraces, suggesting that Mhc^{5}, Mhc^{S1}, and Mhc^{S2} represent a functionally distinct mechanism of hypercontraction. Another known enhancer of $wupA^{hdp2}$, Mhc^{8} (a mutation in the lever arm of Mhc) also leads to indented thoraces and is included with Mhc^{5}, Mhc^{S1}, and Mhc^{S2}, presumably by indirectly leading to similar changes in the functionality of Mhc as the point mutations which localize to the ATPase domain (Homyk and Emerson, 1988). Interestingly, two other alleles of *Mhc*, Mhc^{D41} and Mhc^{D45}, map to the ATP binding/hydrolysis site, but seem to have different effects on contraction as they are genetic suppressors of hypercontraction induced by $wupA^{hpd2}$ and up^{101} (Kronert et al.,

1999). This may be due to an opposite effect at the same step within the ATPase cycle in relation to the Mhc^{S1}, Mhc^{S2}, Mhc^{5}, and Mhc^{8} alleles. Alternatively, these mutations may affect a different step of the ATPase cycle, but lead to decreased contraction, rather than hypercontraction.

Given the large body of work surrounding the IFM and hypercontraction, coupled with the data presented here, we propose possible general models for hypercontraction based upon the allosteric/cooperative model previously described (Lehrer and Geeves, 1998) (Figure 6). In the wildtype sarcomere, a simplified 5 state model can be used to describe contraction. In the first state (A), the troponin complex is keeping the thin filament in the closed state. If myosin-nucleotide complex binds this state, it is referred to as "blocked," as it is not conducive to contraction. Neural stimulation shifts the equilibrium between state A to state B by allowing calcium to enter the sarcomere, which binds the troponin complex *via* troponin C, increasing the proportion of state B complexes. State B is open to contraction. Myosin binds state B in a non-cooperative manner, state C, provided myosin has bound and hydrolyzed its ATP substrate. Once state C is reached, cooperative mechanisms facilitate binding of multiple myosin heads, leading to state D, the low-force state of the sarcomere. From state D, state E is reached by release of P_i, entering a high-force contraction state of the muscle with myosin in its rigor state. Hypercontraction by up^{101} and $wupA^{hdp2}$ may occur by altering the state A/state B equilibrium in the absence of calcium, and thus increasing the fraction of blocked versus open states. If the proportion of complexes in state B were significantly high during unstimulated

Figure 6

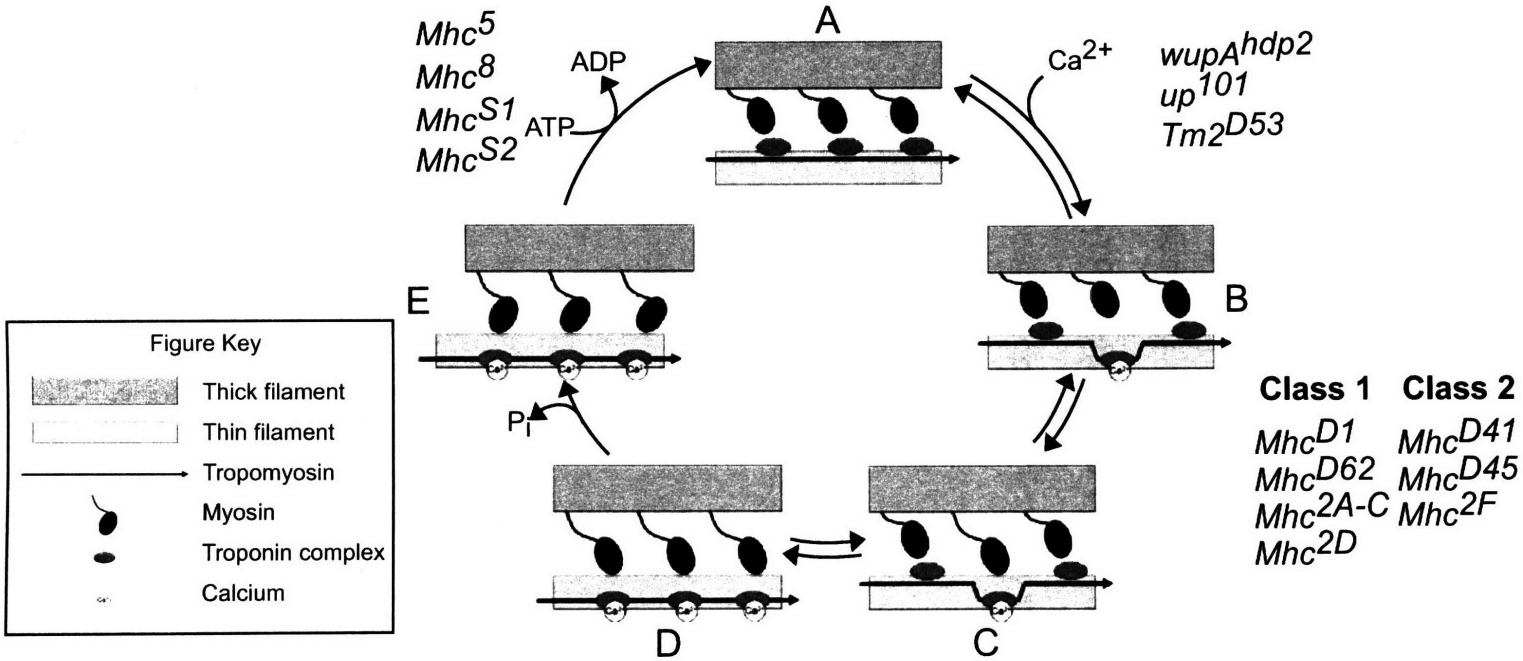

Figure 6: A working model for hypercontraction. A simplified 5-stage model of contraction is depicted. The resting state of muscle (A) contains myosin unbound to the thin filament. During activation of the muscle (B), intracellular Ca^{2+} increases, allowing a limited number of troponin complexes to shift into the open state. The open state allows non-cooperative binding of myosin (C) to the thin filament. When enough myosin heads bind, cooperative mechanisms facilitate binding of multiple heads (D). Release of P_i then allows contraction to occur (E), followed by ADP/ATP exchange to complete the cycle. *Drosophila* mutants are listed next to proposed steps at which they alter this simplified cycle.

phases of the muscle, then a large number of isolated myosin heads would bind and enter rigor state, increasing steady-state force on the thin filament during periods of relaxation. Mutations such as $Tm2^{D53}$ suppress this defect by shifting this altered equilibrium towards more wildtype values, possibly by increasing the energy required for the A→B transition. Mutations in *Mhc* can suppress this hypercontraction by decreasing the actomyosin force through 3 molecularly distinct ways. In one mechanism a mutation may prevent the state B to state C transition by altering the actin binding properties of Mhc. Thus, despite the increased proportion of state B complexes, there is a lower probability that Mhc molecules will bind and enter rigor state, therefore decreasing actomyosin forces during relaxation to tolerable levels in the presence of $wupA^{hdp2}$ or up^{101}. Mutations acting through this mechanism of altering actin binding properties include Mhc^{D1}, Mhc^{D62}, Mhc^{2A-C}, and Mhc^{2D}. In a second mechanism, mutations can decrease the number of available heads, and thus steady-state force can be decreased. The headless constructs suppress hypercontraction through this second mechanism. Finally, suppression can be obtained by decreasing the number of myosins which are able to bind at any given time by decreasing ATP binding ability or initial hydrolysis. These mutations include Mhc^{D41}, Mhc^{D45}, and Mhc^{2F} (Nongthomba et al., 2003).

Hypercontraction defects caused by *Mhc* mutations are manifested by two mechanisms. One mechanism, previously mentioned, leads to hypercontraction by decreasing the structural integrity of the thick filament (Mhc^{6} and $Mhc^{13\ (19)}$). The second mechanism involves the group of mutations Mhc^{5}, Mhc^{S1}, and

Mhc^{S2}. These mutations lead to hypercontraction by stabilizing a transition state between state E and state A by preventing ADP/ATP exchange. If a sufficient number of myosins remain bound, this state may perform a role similar to state C and allow contraction cycles to continue. During normal contraction, it has been estimated that 20-30% of myosins remain bound in order to allow for multiple contraction cycles during one stimulated muscle contraction event (Lehrer and Geeves, 1998). However, if the balance between structural support and contractile forces determines the number of contraction cycles per stimulation, this further stabilization can lead to an excess number of cycles and thus an excess in force production during the latter stages of a contraction event. In addition, this stabilization could lead to local contraction oscillations in muscle long after the Ca^{2+} transient has dissipated, increasing steady-state actomyosin force during relaxation states. This latter prediction is indeed true, as shown by the oscillatory muscle movement observed during intracellular recordings in third instar larvae. Alternatively, these mutations may cause A→C transitions by displacing the regulatory complex on the thin filament through direct interactions with troponin I as previously proposed. However, this seems unlikely as the *Mhc*^{5}, *Mhc*^{S1}, and *Mhc*^{S2} mutations are single amino acid substitutions localizing near the ATP binding/hydrolysis sites, as opposed to surfaces more accessible to a troponin I interaction. In double mutants of this class of *Mhc* alleles and either *wupA*^{hdp2} or *up*^{101}, lethality may reflect the additive effects of two distinct molecular mechanisms of hypercontraction. In addition, the partial suppression of *Tm2*^{D53} in the background of *Samba* supports these distinct mechanisms, as it

does not re-establish normal contraction mechanisms as observed with *wupA*^{hdp2} and *up*^{101}, but rather decreases the number and extent of unregulated contraction cycles. Therefore, hypercontraction by *Mhc*^{5} and the *Samba* mutants is caused by excess force at the end of a regulated contraction event as well as increased steady-state force resulting from unregulated contraction cycles, rather than alterations in thin filament state transitions through direct interactions with troponin I.

Excitability and hypercontraction mutants

The TS seizure activity in *Mhc*^{5}, *Mhc*^{S1}, and *Mhc*^{S2} as well as *up*^{101} and *wupA*^{hdp2} is likely to reflect a temperature-dependent defect caused by an alteration in the cellular state of a hypercontractive muscle, rather than direct temperature-dependent defects of mutant proteins. The model proposed for hypercontraction may account for the activity through a dysregulation of calcium homeostasis. In normal muscles, calcium levels dramatically increase in the sarcomere in order to increase the fraction of troponin complexes in state B during regulated contraction. However, in mutants such as *up*^{101} and *wupA*^{hdp2}, rather than calcium returning to intracellular stores, the calcium remains buffered in the sarcomere. This may be due to two possibilities. One possibility is that these mutations respond to lower calcium concentrations, where calcium ions are continually binding a mutant complex, transitioning to state B, released upon return to state A, then repeating this binding cycle long after the large calcium

transient has passed for regulated contraction. Although the $[Ca^{2+}]_{free}$ remains relatively low, there is an overall buffering of a significant amounts of calcium in the sarcomere by the troponin complex. The other possibility, though not mutually exclusive, is that these mutations lead to a lower activation energy for the A→B transition in the absence of calcium. State B, having a higher affinity for calcium, allows binding of calcium away from endogenous muscle calcium buffers. This can also lead to an overall aberrant buffering of calcium. Likewise, Mhc^{5}, Mhc^{S1}, and Mhc^{S2} lead to buffering because the sarcomere is continually cycling through states C→D→E→(C). After a single cycle of unregulated contraction, calcium may unbind the troponin complexes. However, a significant number of myosins remain bound in $Mhc^{S1,}$ Mhc^{S2}, Mhc^{5}, stimulating a second cycle through cooperative mechanisms, allowing state B troponin complexes to bind calcium. Buffered calcium in both mutant groups is thus continually binding and unbinding troponin complexes. During an increase in temperature, diffusion rates increase, allowing Ca^{2+} to diffuse farther from the contractile machinery when unbound. At sufficiently high temperatures, calcium may reach the membrane, effectively depolarizing the membrane and leading to a hyperexcitable state. This state would allow for multiple muscle action potentials once threshold is reached, but neuronal input would be required to stimulate the spike train. The suppression of seizure activity by $para^{ts1}$ occurs by preventing threshold through loss of presynaptic release.

Alternatively, though not mutually exclusive, excitability defects may be caused by further increases in ectopic innervation at the adult IFM. Although the

innervation defects at the third instar neuromuscular junction are modest, defects may be exacerbated at adult muscles. However, at the adult flight muscles, type II innervation seems to represent a more molecularly diverse set of synapses, and it is unknown whether muscle hypercontraction would induce increased innervation of any, a subset, or all type II- like synapses in the adult (Rivlin et al., 2004). Moreover, it is unclear how increases in type II innervation may alter excitability of muscles in a temperature-dependent fashion.

Although more experimentation will be required in order to discern between these possibilities as well as other potential mechanisms, it is clear that hypercontraction creates a distinct muscle state which is different from hypocontracted and normal muscles. In support of this, hypercontraction mutants have TS behavioral defects which are not evident in hypocontraction mutants or in wildtype flies. In addition, TS behavioral defects are not likely due to mixtures of differentially active myosins being expressed in the IFM, as Mhc^{D45}/+ heterozygotes do not display TS behavioral defects such as those found in Mhc^{S1}/+, Mhc^{S2}/+, and Mhc^{5}/+. Future studies in determining the components which contribute to this altered state will be critical in understanding the underlying causes of excitability defects in hypercontraction mutants. Characterization of genetic interactors of Mhc^{S1} and Mhc^{S2} mutants such as the *Swing* and *Breakdance* loci described here may also provide insights into the molecular pathways underlying hypercontraction myopathies, as well as contribute to understanding of the mechanisms underlying human muscle diseases such as hypertrophic cardiomyopathy.

Materials and methods

Fly strains and crosses

Flies were cultured on standard medium at 22°C. All crosses using appropriate genotypes were cultured at 25°C. Mhc^{S1} and Mhc^{S2} were generated in an F1 EMS screen for X-linked and autosomal dominant TS behavioral defects. *Samba* mutants were recombination mapped to 2-52 cM on the second chromosome with *Sp J L P* marker chromosomes, deficiency mapped to 36A8-36C4, and tested for non-complementation with $P\{w^{+mC}=lacW\}Mhc^{k10423}$ and Mhc^{1} (Mogami and Hotta, 1981; Spradling et al., 1999). The Swg^{X188} and $Brkd^{J29}$ mutations were also generated in screens for TS behavioral defects, and these have been mapped to 42A and 88F, respectively. In addition, revertants of Mhc^{S1} TS dysfunction were isolated by γ-irradiation. Mhc^{S1}/CyO males were exposed to 6000 rads, crossed to *Gla/CyO*, and F1 progeny were tested at 38°C for loss of TS behavior. Three revertants (Mhc^{rv1}, Mhc^{rv2}, and Mhc^{rv3}) were isolated. All three were embryonic lethal with normal morphological development, but showed complete loss of muscle wave propagation in late stage embryos. In addition, all three revertant alleles show non-complementation to Mhc^{1}. Suppression of lethality was scored as live flies which were able to survive eclosion and feed with enough motor coordination to prevent becoming trapped in the media.

Adult behavior analysis

Ten flies were placed into a preheated glass vial at 38°C. Flies showing TS behavioral defects were scored in fifteen second intervals. The analysis was done with ten repetitions for each genotype and each repetition contained an independent set of ten flies.

Polarized light miocrographs

Polarized light micrographs of the adult flight muscles were analyzed as previously described with the modification of using Xylenes as a clearing agent (Fyrberg et al., 1994). Thoraces were mounted using Permount (Fisher Scientific) and analyzed under Nomarski optics.

Mutation and crystal structure analysis

Mutations were determined by PCR and sequencing. Genomic DNA was isolated from *CantonS* and Mhc^{S1}/*Df(2L)H20* flies (Simpson, 1983). Exons 4-6 were amplified by PCR and the product was sequenced at the MIT Cancer Center sequencing facility. Genomic DNA from homozygous Mhc^{S2} embryos was isolated and similarly processed. Amino acids are numbered according to the Mhc-P11 sequence. Crystal structure analysis of the mutations was done using the Swiss PDB Viewer software available at http://us.expasy.org/spdbv/. Crystal structures 2MYS and 1MMG were downloaded from NCBI and mutations mapped according to BLAST alignments done through the NCBI BLAST website. (Fisher et al., 1995; Rayment et al., 1995; Rayment et al., 1993).

Antibodies and immunohistochemistry of third instar larvae

Wandering third instar larvae were raised at 25°C, then dissected and fixed by standard procedures. Affinity purified rabbit α-sytI antibodies (Littleton et al., 1993) were used at 1:1000 and Cy2-conjugated goat α-rabbit secondary antibodies at 1:200 (Jackson Labs). Texas red-conjugated phalloidin was incubated simultaneously with the secondary antibody at 1:500 (Molecular Probes). Visualization and quantification was performed under light microscopy using a 40X oil-immersion lens. Images were taken using confocal microscopy under similar conditions and processed with Zeiss PASCAL software.

Electrophysiology

Extracellular DLM recordings Extracellular DLM recordings were done in male flies raised at 25°C. 1-5MΩ electrodes were filled with 3M KCl. The recording electrode was inserted into the lateral thorax with the ground electrode inserted into the eye. Basal activity was recorded for two minutes at 22°C. Temperature was then shifted to 38°C for one minute, and returned to 22°C. Recordings were done using an Axoclamp-2B amplifier (Axon) and digitized with an Instrunet Model 100 digitizer at 10 kHz and analyzed with Superscope 3.0 software (GW Instruments). In order to attenuate extracellular signals from the eye, experiments were done in constant light.

Intracellular recordings Intracellular recordings were done at room temperature in wandering third instar larve raised at 25°C. Dissections and recordings were

done in 0.4 mM Ca^{2+} HL3 (Stewart et al., 1994) with 4 mM $MgCl_2$. Recordings were done from muscle 6 at segments A3-A5. 50-100MΩelectrodes were filled with 3 M KCl. Muscles were analyzed if the resting membrane potential was below -50mV. Data was digitized with a Digidata 1322, filtered at 10 kHz online, and analyzed using pCLAMP v8.0 software (Axon). mEJP amplitude and frequency was determined by manual analysis, analyzing representative samples from each muscle recording. EJP amplitude was similarly analyzed, utilizing the maximal response to suprathreshold stimulation (determined for each individual muscle). Ca^{2+}-free recordings were done in a similar manner. Failure to evoke release was used to verify that Ca^{2+} was minimal in the external solution. Recordings with an intact CNS were done in 0.2 mM Ca^{2+} to prevent substantial depolarization during central pattern activity in the presence or absence of 3 μM TTX.

Acknowledgements

We thank Ilaria Rebay, Avital Rodal, Motojiro Yoshihara, and Bill Adolfsen for helpful discussions about the manuscript. We would also like to thank the Bloomington Stock Center, S.I. Bernstein, and J.C. Sparrow for *Drosophila* strains. The α-DLG antibody developed by C.S. Goodman was obtained from the Developmental Studies Hybridoma Bank developed under the auspices of the NICHD and maintained by the University of Iowa, Department of Biological Sciences, Iowa City, IA 52242. This work was supported by grants from the NIH, the Human Frontiers Science Program, the Searle Scholars Program, and the Packard Foundation. J. Troy Littleton is an Alfred P. Sloan Research Fellow.

References

Beall, C.J., and E. Fyrberg. 1991. Muscle abnormalities in Drosophila melanogaster heldup mutants are caused by missing or aberrant troponin-I isoforms. *J Cell Biol.* 114:941-51.

Bernstein, S.I., K. Mogami, J.J. Donady, and C.P. Emerson, Jr. 1983. Drosophila muscle myosin heavy chain encoded by a single gene in a cluster of muscle mutations. *Nature.* 302:393-7.

Collier, V.L., W.A. Kronert, P.T. O'Donnell, K.A. Edwards, and S.I. Bernstein. 1990. Alternative myosin hinge regions are utilized in a tissue-specific fashion that correlates with muscle contraction speed. *Genes Dev.* 4:885-95.

Davis, G.W., A. DiAntonio, S.A. Petersen, and C.S. Goodman. 1998. Postsynaptic PKA controls quantal size and reveals a retrograde signal that regulates presynaptic transmitter release in Drosophila. *Neuron.* 20:305-15.

Deak, II, P.R. Bellamy, M. Bienz, Y. Dubuis, E. Fenner, M. Gollin, A. Rahmi, T. Ramp, C.A. Reinhardt, and B. Cotton. 1982. Mutations affecting the indirect flight muscles of Drosophila melanogaster. *J Embryol Exp Morphol.* 69:61-81.

Engel, J.E., and C.F. Wu. 1992. Interactions of membrane excitability mutations affecting potassium and sodium currents in the flight and giant fiber escape systems of Drosophila. *J Comp Physiol [A].* 171:93-104.

Fekete, E., and J. Szidonya. 1979. Abnormalities of ultrastructure and calcium distribution in the flight muscle of a flightless mutant of Drosophila melanogaster. *Acta Biol.* 30:47-57.

Ferrus, A., A. Acebes, M.C. Marin, and A. Hernandez-Hernandez. 2000. A genetic approach to detect muscle protein interactions in vivo. *Trends Cardiovasc Med.* 10:293-8.

Fisher, A.J., C.A. Smith, J.B. Thoden, R. Smith, K. Sutoh, H.M. Holden, and I. Rayment. 1995. X-ray structures of the myosin motor domain of

Dictyostelium discoideum complexed with MgADP.BeFx and MgADP.AlF4. *Biochemistry*. 34:8960-72.

Fyrberg, E.A., S.I. Bernstein, and K. VijayRaghavan. 1994. Basic methods for Drosophila muscle biology. *Methods Cell Biol*. 44:237-58.

Ganetzky, B., and C.F. Wu. 1983. Neurogenetic analysis of potassium currents in Drosophila: synergistic effects on neuromuscular transmission in double mutants. *J Neurogenet*. 1:17-28.

George, E.L., M.B. Ober, and C.P. Emerson, Jr. 1989. Functional domains of the Drosophila melanogaster muscle myosin heavy-chain gene are encoded by alternatively spliced exons. *Mol Cell Biol*. 9:2957-74.

Gramates, L.S., and V. Budnik. 1999. Assembly and maturation of the Drosophila larval neuromuscular junction. *Int Rev Neurobiol*. 43:93-117.

Hess, N.K., and S.I. Bernstein. 1991. Developmentally regulated alternative splicing of Drosophila myosin heavy chain transcripts: in vivo analysis of an unusual 3' splice site. *Dev Biol*. 146:339-44.

Homyk, T., Jr., and C.P. Emerson, Jr. 1988. Functional interactions between unlinked muscle genes within haploinsufficient regions of the Drosophila genome. *Genetics*. 119:105-21.

Homyk, T., Jr., J. Szidonya, and D.T. Suzuki. 1980. Behavioral mutants of Drosophila melanogaster. III. Isolation and mapping of mutations by direct visual observations of behavioral phenotypes. *Mol Gen Genet*. 177:553-65.

Hong, C.S., and B. Ganetzky. 1994. Spatial and temporal expression patterns of two sodium channel genes in Drosophila. *J Neurosci*. 14:5160-9.

Huxley, A.F. 2000. Cross-bridge action: present views, prospects, and unknowns. *J Biomech*. 33:1189-95.

Jarecki, J., and H. Keshishian. 1995. Role of neural activity during synaptogenesis in Drosophila. *J Neurosci*. 15:8177-90.

Kronert, W.A., A. Acebes, A. Ferrus, and S.I. Bernstein. 1999. Specific myosin heavy chain mutations suppress troponin I defects in Drosophila muscles. *J Cell Biol.* 144:989-1000.

Kronert, W.A., P.T. O'Donnell, A. Fieck, A. Lawn, J.O. Vigoreaux, J.C. Sparrow, and S.I. Bernstein. 1995. Defects in the Drosophila myosin rod permit sarcomere assembly but cause flight muscle degeneration. *J Mol Biol.* 249:111-25.

Lamb, G.D. 2000. Excitation-contraction coupling in skeletal muscle: comparisons with cardiac muscle. *Clin Exp Pharmacol Physiol.* 27:216-24.

Lehrer, S.S., and M.A. Geeves. 1998. The muscle thin filament as a classical cooperative/allosteric regulatory system. *J Mol Biol.* 277:1081-9.

Littleton, J.T., H.J. Bellen, and M.S. Perin. 1993. Expression of synaptotagmin in Drosophila reveals transport and localization of synaptic vesicles to the synapse. *Development.* 118:1077-88.

Littleton, J.T., E.R. Chapman, R. Kreber, M.B. Garment, S.D. Carlson, and B. Ganetzky. 1998. Temperature-sensitive paralytic mutations demonstrate that synaptic exocytosis requires SNARE complex assembly and disassembly. *Neuron.* 21:401-13.

Mogami, K., and Y. Hotta. 1981. Isolation of Drosophila flightless mutants which affect myofibrillar proteins of indirect flight muscle. *Mol Gen Genet.* 183:409-17.

Naimi, B., A. Harrison, M. Cummins, U. Nongthomba, S. Clark, I. Canal, A. Ferrus, and J.C. Sparrow. 2001. A tropomyosin-2 mutation suppresses a troponin I myopathy in Drosophila. *Mol Biol Cell.* 12:1529-39.

Nongthomba, U., M. Cummins, S. Clark, J.O. Vigoreaux, and J.C. Sparrow. 2003. Suppression of Muscle Hypercontraction by Mutations in the Myosin Heavy Chain Gene of Drosophila melanogaster. *Genetics.* 164:209-22.

Petersen, S.A., R.D. Fetter, J.N. Noordermeer, C.S. Goodman, and A. DiAntonio. 1997. Genetic analysis of glutamate receptors in Drosophila reveals a retrograde signal regulating presynaptic transmitter release. *Neuron.* 19:1237-48.

Poage, R.E., and S.D. Meriney. 2002. Presynaptic calcium influx, neurotransmitter release, and neuromuscular disease. *Physiol Behav.* 77:507-12.

Pollard, T.D. 2000. Reflections on a quarter century of research on contractile systems. *Trends Biochem Sci.* 25:607-11.

Rafael, J.A., E.R. Townsend, S.E. Squire, A.C. Potter, J.S. Chamberlain, and K.E. Davies. 2000. Dystrophin and utrophin influence fiber type composition and post-synaptic membrane structure. *Hum Mol Genet.* 9:1357-67.

Rayment, I., H.M. Holden, J.R. Sellers, L. Fananapazir, and N.D. Epstein. 1995. Structural interpretation of the mutations in the beta-cardiac myosin that have been implicated in familial hypertrophic cardiomyopathy. *Proc Natl Acad Sci U S A.* 92:3864-8.

Rayment, I., W.R. Rypniewski, K. Schmidt-Base, R. Smith, D.R. Tomchick, M.M. Benning, D.A. Winkelmann, G. Wesenberg, and H.M. Holden. 1993. Three-dimensional structure of myosin subfragment-1: a molecular motor. *Science.* 261:50-8.

Reedy, M.C., B. Bullard, and J.O. Vigoreaux. 2000. Flightin is essential for thick filament assembly and sarcomere stability in Drosophila flight muscles. *J Cell Biol.* 151:1483-500.

Rivlin, P.K., R.M. St Clair, I. Vilinsky, and D.L. Deitcher. 2004. Morphology and molecular organization of the adult neuromuscular junction of Drosophila. *J Comp Neurol.* 468:596-613.

Rozek, C.E., and N. Davidson. 1983. Drosophila has one myosin heavy-chain gene with three developmentally regulated transcripts. *Cell.* 32:23-34.

Ruff, R.L. 2003. Neurophysiology of the neuromuscular junction: overview. *Ann N Y Acad Sci.* 998:1-10.

Seidman, J.G., and C. Seidman. 2001. The genetic basis for cardiomyopathy: from mutation identification to mechanistic paradigms. *Cell.* 104:557-67.

Simpson, P. 1983. Maternal-Zygotic Gene Interactions During Formation of the Dorsoventral Pattern in Drosophila Embryos. *Genetics*. 105:615-632.

Spradling, A.C., D. Stern, A. Beaton, E.J. Rhem, T. Laverty, N. Mozden, S. Misra, and G.M. Rubin. 1999. The Berkeley Drosophila Genome Project gene disruption project: Single P-element insertions mutating 25% of vital Drosophila genes. *Genetics*. 153:135-77.

Stewart, B.A., H.L. Atwood, J.J. Renger, J. Wang, and C.F. Wu. 1994. Improved stability of Drosophila larval neuromuscular preparations in haemolymph-like physiological solutions. *J Comp Physiol [A]*. 175:179-91.

Suzuki, D.T., T. Grigliatti, and R. Williamson. 1971. Temperature-sensitive mutations in Drosophila melanogaster. VII. A mutation (para-ts) causing reversible adult paralysis. *Proc Natl Acad Sci U S A*. 68:890-3.

Vigoreaux, J.O. 2001. Genetics of the Drosophila flight muscle myofibril: a window into the biology of complex systems. *Bioessays*. 23:1047-63.

Wassenberg, D.R., 2nd, W.A. Kronert, P.T. O'Donnell, and S.I. Bernstein. 1987. Analysis of the 5' end of the Drosophila muscle myosin heavy chain gene. Alternatively spliced transcripts initiate at a single site and intron locations are conserved compared to myosin genes of other organisms. *J Biol Chem*. 262:10741-7.

Wu, C.F., B. Ganetzky, F.N. Haugland, and A.X. Liu. 1983. Potassium currents in Drosophila: different components affected by mutations of two genes. *Science*. 220:1076-8.

Zhang, S., and S.I. Bernstein. 2001. Spatially and temporally regulated expression of myosin heavy chain alternative exons during Drosophila embryogenesis. *Mech Dev*. 101:35-45.

Expression Profiling of a Hypercontraction-induced Myopathy in *Drosophila* Suggests an Actin Remodeling Response

Enrico S. Montana[1] & J. Troy Littleton[1,2]

[1]Department of Biology, [1]Picower Center for Learning and Memory, [2]Department of Brain and Cognitive Sciences, Massachusetts Institute of Technology, Cambridge, MA 02139, USA

The work in this chapter is work I had done under the guidance of Troy. Jessica Slind and Eun J. Lee provided some assistance in cloning the UAS constructs. The antibody to the MSP-300 protein was a gift provided by Talila Volk. Affymetrix provided some useful advice in setting up the microarray analysis in the lab. This work has been submitted to and reviewed by *JBC.* It is currently under revision.

Abstract

We have recently identified and characterized mutations in *Myosin Heavy Chain* that lead to hypercontraction of the indirect flight muscles in *Drosophila*. These *Mhc* mutations disrupt Ca^{2+}-dependent calcium contraction cycles in the larval body wall muscles and cause temperature-induced myogenic seizure activity in adult animals. Analysis of the hypercontraction mutants *wings up A*^{helpdup2} and *upheld*^{101} revealed temperature-sensitive behavioral defects occur specifically in hypercontraction mutants, suggesting a fundamental difference between hypercontraction and normal or hypocontracted muscles. To characterize the genomic response to hypercontraction-induced muscle myopathy, we have utilized expression analysis with high-density oligonucleotide microarrays. The transcriptional profile indicates a remodeling of the muscle architecture in response to hypercontraction. Specifically, a subset of the highly upregulated genes has been shown or is putatively involved in actin regulation and structural support for the contractile machinery. Further, we show that these genes may be involved in remodeling key structural sites within the muscle.

Introduction

Human cardiomyopathies can occur from single gene mutations which alter the properties of the contractile machinery. These diseases are often characterized as either hypertrophic (increase in myocyte size) or dilated (increase in ventricular volume). Mutated genes responsible for these diseased states include Myosin heavy chain, troponin I, troponin T, tropomyosin and myosin light chain (Seidman and Seidman, 2001). In response to these defects, cardiac cells undergo a transcriptional response which includes the upregulation of fetal cardiac genes and immune response genes, as well as a downregulation of nuclear-encoded mitochondrial genes and calcium handling proteins (Aronow et al., 2001; Barrans et al., 2002; Chien et al., 1991; Komuro et al., 1991; Lowes et al., 2002; Sadoshima and Izumo, 1997; Sadoshima et al., 1992). This response, however, has been heterogeneous between studies in mammals. This may be due to differences in both the experimental procedures and the cardiomyopathy models utilized for each study, as well as differences in the pathogenic progression at which the study was performed. Alternatively, this heterogeneity may reflect distinct mechanisms underlying specific cardiomyopathies. In addition, due to differences in microarray production, annotation, and incomplete genomic information, cross-referencing these studies remains difficult. Regardless, the molecular signaling which mediates the transcriptional response is thought to involve a calcineurin-dependent signaling

cascade, leading to the deacetylation of histones, and the consequent activation of genes which are normally expressed at low levels in adult tissue (Frey et al., 2000; Molkentin et al., 1998; Zhang et al., 2002a). Defining the transcriptional response across the entire genome and the signals that mediate this re-profiling is essential for determining the functional consequences of differential gene expression in the mechanisms of disease pathogenesis.

Analysis of flightless behavior in *Drosophila* has provided a genetic model system to study the molecular mechanisms underlying cardiac dysfunction in humans. Many of the genes that are mutated in cardiac dysfunction in humans also lead to flightless defects in *Drosophila*. Among these genes are *Myosin Heavy Chain* (*Mhc*), *actin88F* (*act88F*), *wings up A* (*wupA*: troponin I), and *upheld* (*up*: troponin T) (Ferrus et al., 2000; Vigoreaux, 2001). As the molecular lesions provide strong parallels between the underlying molecular causes of cardiomyopathies and flightlessness in *Drosophila*, there may also be parallels in the concomitant cellular changes in response to these single gene mutations.

Recently, we have identified mutations in *Mhc* which lead to hypercontraction of the adult indirect flight muscles (IFM) (Montana and Littleton, 2004). This hypercontraction is likely due to unregulated contraction cycles that occur in mutant muscles. These mutations were isolated as dominant, temperature-sensitive (TS) behavioral mutants which showed TS seizure-like behavior at restrictive temperatures. In an analysis of several known muscle mutants, this TS state is specific to hypercontraction mutations, as all hypercontraction mutants assayed showed similar TS defects. These data

suggested that hypercontracted muscles are fundamentally different than hypocontracted and normal muscles. Further, this difference may reflect the underlying cellular mechanisms which lead to human diseases such as hypertrophic cardiomyopathy.

In order to characterize the differences between hypercontracted and normal muscles, we have begun a genome-wide expression analysis of a *Drosophila* hypercontraction-induced myopathy utilizing high-density oligonucleotide DNA microarrays. Definition of the transcriptional response to hypercontraction-induced myopathy in *Drosophila* may identify conserved cellular responses to muscle dysfunction, and could potentially reveal novel targets for therapeutic treatment of muscle diseases.

Results

Expression analysis of Mhc^{S1} and Mhc^{S2}

Previous data suggests a fundamental difference exists between hypercontracted muscles and normal or hypocontracted muscles. This difference may reflect abnormal Ca^{2+} regulation, causing myogenic seizures in a temperature-dependent manner (Montana and Littleton, 2004). This altered muscle state may also parallel differences between normal human cardiac muscles and cardiomyopathies, providing not only a genetic model system for identifying new genes involved in mammalian cardiac dysfunction, but also a cellular model in which to understand the cellular mechanisms underlying diseased states in response to altered contractile function. In order to characterize the differences between these muscles states in *Drosophila*, we performed expression profiling with Affymetrix® high-density oligonucleotide GeneChip® arrays. These microarrays contain representative sequences for most of the 14,000 genes thought to be encoded in the *Drosophila* genome. In our expression analysis, we utilized two independent alleles of *Mhc*, Mhc^{S1} and Mhc^{S2}, that lead to indirect flight muscle (IFM) hypercontractions. These alleles are both missense mutations (V235E and E187K) that localize near the ATP binding/hydrolysis domain of the Mhc protein. Using two independent alleles has allowed us to look for conserved responses to Mhc dysfunction by reducing

background and allele specific changes. In addition, these two mutations map to a region in the Mhc protein in which at least nine different mutations have been identified that lead to hypertrophic cardiomyopathy (Figure 1; Rayment et al., 1995). A total of 8 independent arrays were performed: 4 *CantonS*, 2 Mhc^{S1}/+, and 2 Mhc^{S2}/+. The data were processed using the Affymetrix® statistical expression algorithm in a total of 16 pairwise comparisons between mutant and wildtype arrays. To analyze the four mutant chips as a group against the four wildtype controls, SAM v1.20 analysis was used using the two-class unpaired response type (Tusher et al., 2001). To increase the chances of making relevant gene change calls, we set stringent conditions to analyze the data. For a gene to be differentially regulated, it must have been called up- or downregulated by the Affymetrix® algorithm in 75% of the pairwise comparisons. To further rank this data, it was subdivided into two categories: 1) differentially regulated in 75% of all pairwise comparisons and, 2) differentially regulated in only one of the two mutants. We analyzed which of the genes identified by the Affymetrix® statistical expression algorithm were also identified by the SAM analysis. Once the gene set was defined, we individually placed each gene through a BLAST analysis to look for similarities with known proteins or known protein domains. Finally, genes were functionally categorized according to known or putative functions based on current literature or sequence similarity. Under theses criteria, 228 genes were upregulated and 118 were downregulated in response to hypercontraction-induced myopathy (Table I, Figure 2).

Figure 1

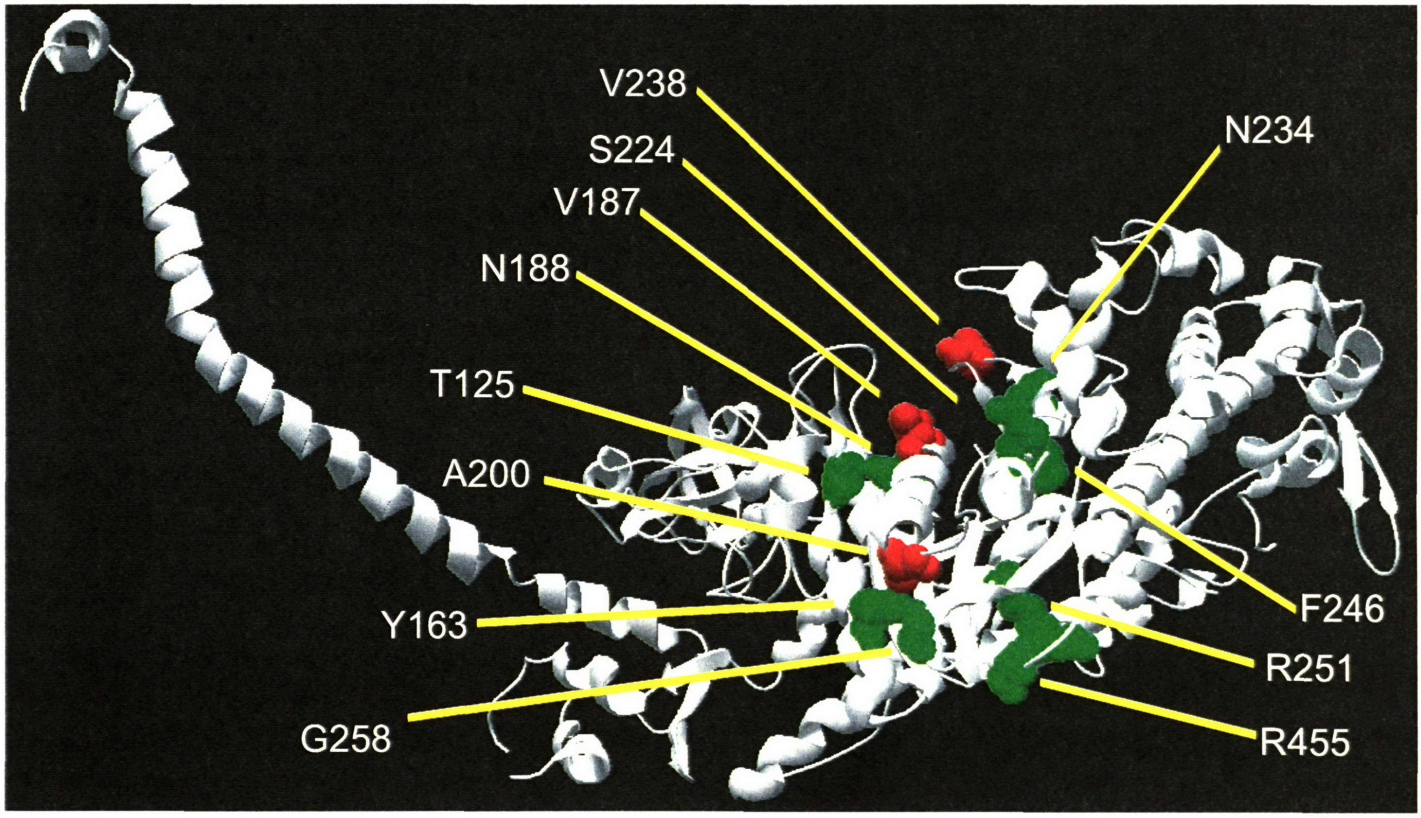

Figure 1: *Mhc* mutations mapped onto the chicken Mhc crystal structure

Nine known mutations that map near or in the ATPase active site in human hypertrophic cardiomyopathes and three dominant hypercontraction mutations in *Drosophila* are mapped onto a crystal structure of Mhc (Rayment et al., 1995; Rayment et al., 1993). The locations of the human mutations are shown in green and the *Drosophila* mutations are shown in red.

Table I. Microarray Summary

Upregulated Genes	
Category	Number
Muscle Structure/Function	35
Serine Proteases	24
Novel	54
Chaperones	8
Nuclear Biology	13
Metabolism and Energy	55
Immune Response	15
Signaling	8
Other	16
Total	228

Downregulated Genes	
Category	Number
Metabolism and Energy	77
Muscle Structure/Function	6
Other	22
Novel	13
Total	118

To verify that vectorial changes in gene expression were correct, seven genes were tested using semi-quantitave RT-PCR. These seven genes showed similar vector changes, confirming that the expression profiles reflect the representation of transcripts isolated (Figure 2). Analysis of the identified genes shows similarities between this analysis and expression analyses performed in mammalian hypertrophic cardiomyopathies and muscular dystrophies. In mammalian cardiomyopathies, differential gene regulation has focused on the activation of fetal protein isoforms involved in cardiac function (Lim et al., 2001; Molkentin et al., 1998). In addition to fetal gene activation, induction of immediate-early genes has also been implicated in response to cardiomyopathies (Sadoshima and Izumo, 1997). Interestingly, there are parallels between cardiac dysfunction and skeletal muscle dysfunction. Many skeletal muscular dystrophies include cardiomyopathy within the pathology, likely reflecting shared components and mechanisms underlying the function of these types of tissues (Fadic et al., 1996; van der Kooi et al., 1997). Expression analysis of muscular dystrophies has revealed a downregulation of nuclear-encoded mitochondrial genes and alterations in developmentally-regulated components of the contractile machinery (Campanaro et al., 2002; Chamberlain, 2000; Chen et al., 2000; Noguchi et al., 2003). For both skeletal and cardiac dysfunction, dysregulation of intracellular Ca^{2+} homeostasis has been suggested to be important for pathogenesis and altered transcriptional regulation (Frey et al., 2000; Gailly, 2002; Leinwand, 2001; Martonosi and Pikula, 2003; Semsarian et al., 2002).

Figure 2

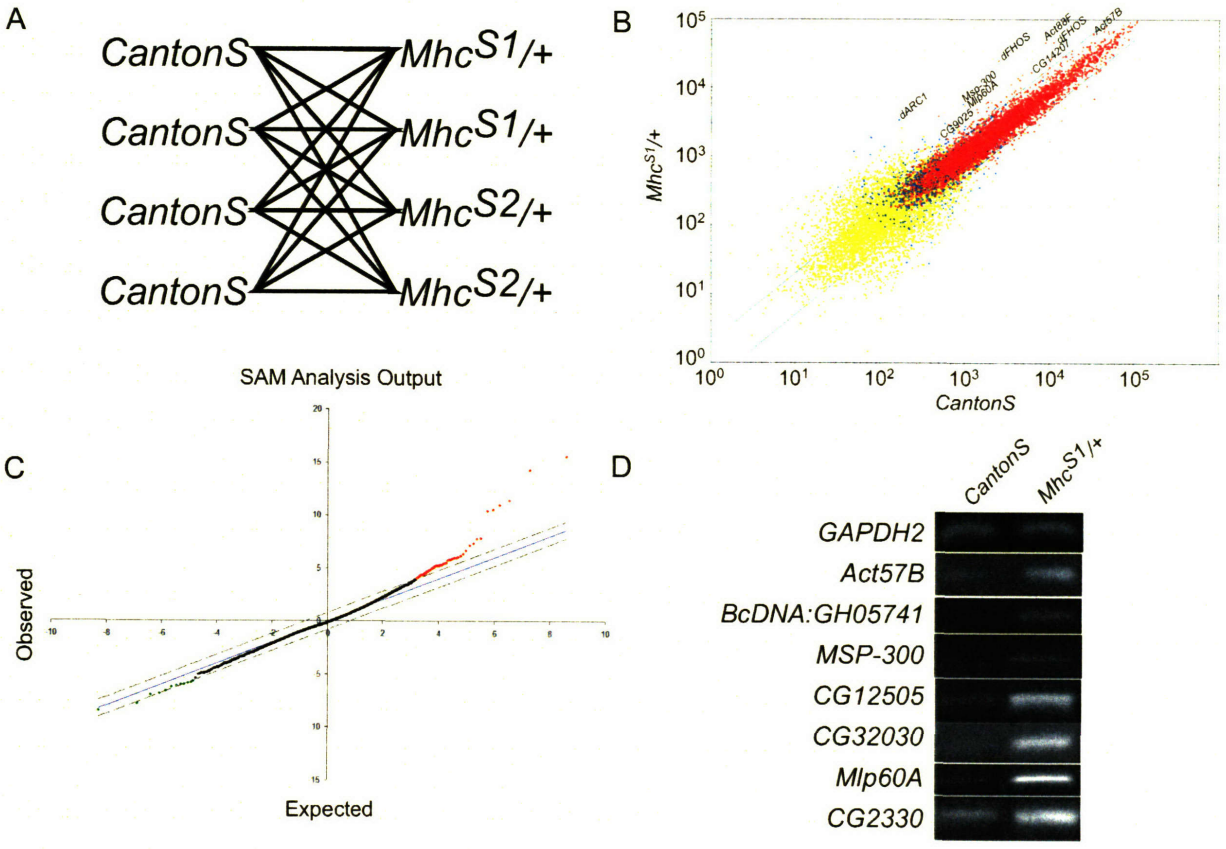

Figure 2: Expression analysis of the Samba mutants using Affymetrix® high-density oligonucleotide GeneChip® microarrays. (A) Schematic depicting the pairwise comparison matrix used to analyze the microarray data with the Affymetrix® statistical algorithm. (B) A sample pairwise comparison between *CantonS* and Mhc^{S1}/+ expression analyses. Green lines indicate a 2-fold difference in expression. (C) The output of SAM analysis v.1.20 using a two-class unpaired data set and Δ-value set to give ~25% false detection rate. (D) Semi-quantitative RT-PCR shows similar vector changes identified by the microarrays. *GAPDH2*, *Act57B*, and *CG2330* represent quantitative comparisons, as both control and mutant reactions are within the linear regions of the RT-PCR.

The differential regulation in the Mhc^{S1} and Mhc^{S2} mutants includes the upregulation of developmentally controlled genes which are required for earlier stages of development. *Mlp60A* and *Mlp84B*, which normally show high expression during the initial setup of embryonic and adult musculature, are upregulated in the *Mhc* mutants (Stronach et al., 1996). Likewise, *Act57B*, the predominant actin of the larval body wall musculature, rather than the adult musculature, also shows upregulation (Labuhn and Brack, 1997). In cardiomyopathies and muscular dystrophies, embryonic sarcomeric genes are upregulated (Chen et al., 2000; Chien et al., 1991). Although we see an upregulation of developmentally-regulated transcripts, this does not include the sarcomeric genes. This may be due to the fact that the *Drosophila* genome only encodes a single gene for muscle Mhc, TnI, and TnT. If embryonic splice variants were upregulated by myopathy in *Drosophila*, they would not be detectable by this assay, as the microarrays do not distinguish between alternative transcripts encoded by the same locus.

Interestingly, a subset of the genes altered in our hypercontraction-induced myopathy model has been implicated in activity-dependent synaptic plasticity in several mammalian model systems. These include the *Drosophila* homologs of the mammalian proteins ARC (*CG12505* and *CG13941*), neurochondrin/norbin (*CG2330*), and CPG2 (*Msp-300*) (Lyford et al., 1995; Nedivi et al., 1996; Shinozaki et al., 1997; Zhang et al., 2002b). These activity-regulated genes are thought to modulate actin dynamics to strengthen activated synapses during plasticity (Lyford et al., 1995; Shinozaki et al., 1997).

Overall, the most striking gene set identified is the upregulation of genes known or predicted to be involved in muscle structure and function on the level of the actin cytoskeleton, suggesting a remodeling of the actin cytoskeleton and its structural support occurs in response to hypercontraction (Figure 3, Table II). Of the ten most upregulated genes across all statistical analyses, six fall within this category. Another class of upregulated genes we have includes chaperones and serine proteases, further supporting a remodeling of the muscle architecture (Table S1).

Like muscular dystrophies, *Drosophila* hypercontraction mutants exhibit an upregulation of immune-response related genes. In Duchenne's muscular dystrophy, this response is thought to reflect infiltration of degrading muscle tissue by activated dendritic cells, as immunohistochemical analysis of muscle biopsies show increases in dendritic cell infiltration into the muscle (Chen et al., 2000). Whether the immune-response related genes upregulated in *Drosophila* reflect a similar biological phenomenon is unknown. Known and putative metabolic genes form the majority of downregulated genes (77/118), many of which are known or predicted to function in the mitochondria. This response has been shown to occur in Duchenne's and Limb-girdle muscular dystrophies, suggesting a metabolic crisis in myopathic flight muscles similar to muscular dystrophies.

One additional gene of interest is the downregulation of the calcium pump responsible for transporting calcium back into the sarcoplasmic reticulum, *Ca-P60A* (Aronow et al., 2001). This downregulation may contribute to or reflect

Figure 3

A

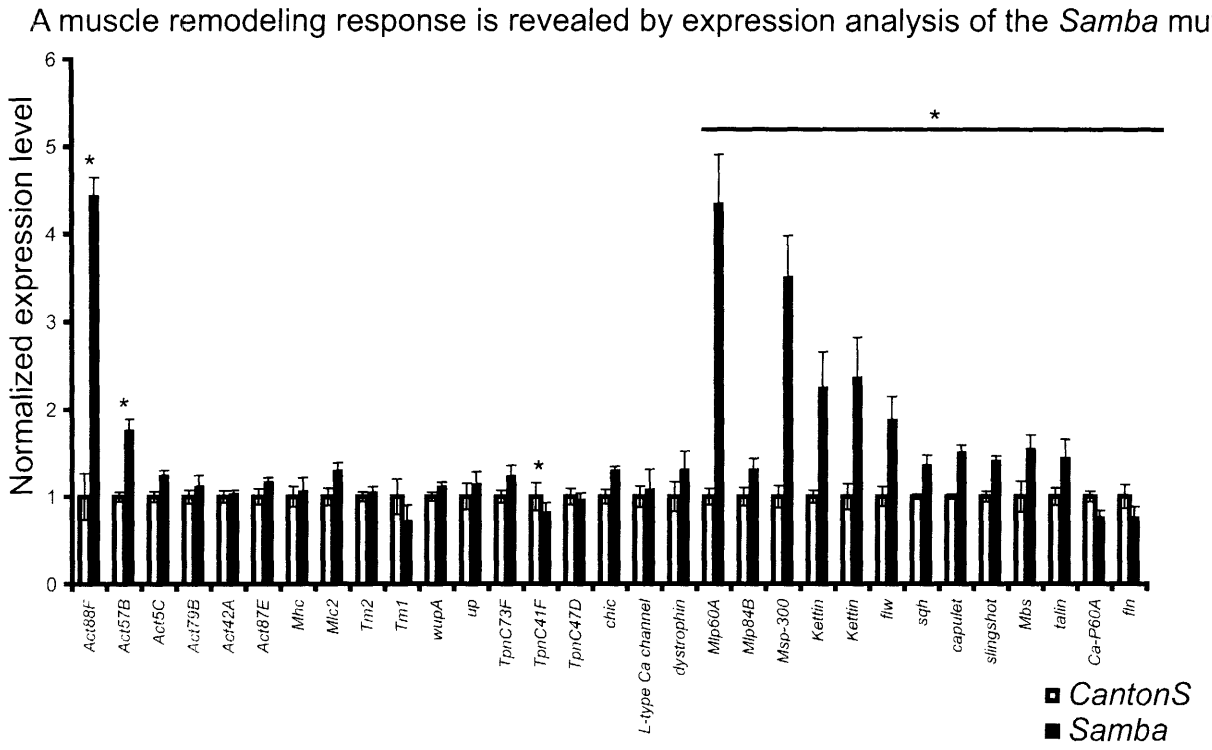

B

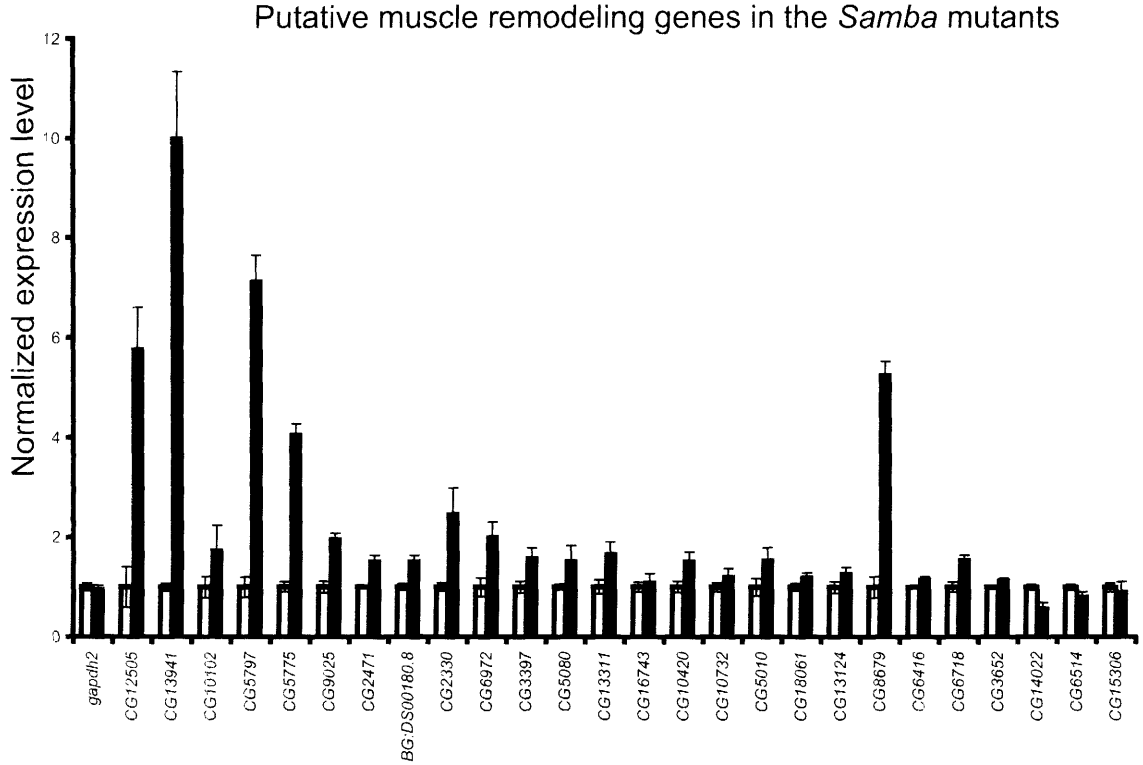

Figure 3: A potential muscle remodeling response in the *Mhc* mutants (A) A subset of known muscle genes shows differential-regulation in mutant tissue. Note that most contractile genes are not upregulated. Genes identified as significantly altered in expression level are indicated (*). (B) A putative set of genes with domain structures which suggest a muscle remodeling role that show altered transcription in the *Mhc* mutants. Both graphs depict normalized expression values ± SEM.

Table II. Differentially-regulated genes in the *Samba* mutants with known or predicted roles in muscle structure/function

Gene	Description	CS Signal Average	CS SD[a]	Mutant Signal Average	Mutant SD[a]	Signal FC[b]	Algorithm[c]
CG12505	*dARC1*	579.33	473.21	3353.4	950.89	5.79	ABCD
CG5797	*dFHOS*	3160.75	1297.21	22587.27	3160.28	7.15	ABCD
Act88F	Actin	10493.42	5568.01	46679.65	4187.62	4.45	ABCD
CG5775	*dFHOS*	11088.03	2289.31	45266.9	4213.05	4.08	ABCD
Mlp60A	*Muscle LIM protein at 60A*	1224.45	228.54	5334.03	1359	4.36	ABCD
Msp-300	*Nesprin/MSP-300*	51.25	6.06	216.33	99.8	4.22	ABCD
CG9025	*dFEM-1*	681.72	163.60	1353	137.3	1.98	ABCD
CG2471	*dSCLP*	1747.93	110.18	2697.7	325.83	1.54	ABCD
Act57B	Actin	36098.75	3998.79	63933.4	8460.42	1.77	ABCD
flw	*flap wing*	1542.88	346.60	2914.55	793.42	1.89	ABC
CG18242	*Kettin*	25.17	19.90	60.45	50.53	2.4	ABC
Ket	*Kettin*	824.38	245.79	1956.93	735.75	2.37	ABC
CG13941	*dARC2*	63.37	10.11	634.6	167.74	10.01	ACD
sqh	*spaghetti squash*	5915.5	300.85	8105.55	1250.23	1.37	AB
BcDNA:LD24380	*capulet*	2484.6	149.96	3768.85	373.77	1.52	BD
BG:DS00180.8	wnt-binding protein	3368.77	437.94	5163.53	694.75	1.53	BD
CG2330	*dNeurochondrin*	1732.22	290.35	4316.98	1700.51	2.49	B
CG6972	ARM-repeat containing protein	1003.53	365.06	2027.1	569.87	2.02	B
CG3397	K^+ channel β–subunit	1146.35	262.79	1837.82	412.87	1.6	B
Mlp84B	*Muscle LIM protein at 84B*	10213.85	2175.26	13503.95	2411.89	1.32	B
CG5080	myosin-like	3773.05	434.98	5810.4	2137.56	1.54	B
CG13311	peritrophic matrix structural protein	1023.7	294.95	1722.98	444.21	1.68	B
CG16743	proline-rich protein	2764.35	516.68	3091.07	829.46	1.12	B
CG10420	ARM repeat, ER chaperone	381.52	85.20	587.03	124.8	1.54	B
CG10732	AIP3-like	682.28	158.19	1358.2	478.58	1.99	B
CG5600	*Myosin binding subunit*	921.72	322.79	1436.57	271.83	1.56	B
CG6831	*Talin*	1285.95	255.85	1864.32	532.21	1.45	B
CG5010	proline-rich protein	4339.55	1490.98	6745.4	2017.47	1.55	B
CG18061	*Paxillin*	2908.05	413.85	3550.1	385.37	1.22	B
CG13124	ARM repeat, middle domain of eIF4G	5648.97	1278.30	7262.42	1263.31	1.29	B
CG8679	LEM domain, ankyrin repeat	39.73	17.30	209.45	19.82	5.27	D
CG6238	*slingshot*	2558.8	308.93	3621.9	277.15	1.42	D
CG6416	PDZ domain, zasp domain (α-actinin binding)	20587.03	68.51	24181.48	1498.94	1.17	D
CG6718	Ankyrin repeats, calcium independent phospholipase A2	170.57	46.14	163.9	58.36	0.96	D
CG3652	YIP1-like	2323.3	158.46	2702.08	71	1.16	D
CG14022	muscle-specific acylphosphatase-like	5774.52	585.28	3454.55	1142.12	0.60	ABC
Ca-P60A	SERCA pump	34574.30	4200.06	26608.38	5156.32	0.77	B
CG6514	troponin C-like molecule	2489.32	293.14	2070.82	413.95	0.83	B
fln	*flightin*	6678.17	1837.91	5141.45	1520.69	0.77	B
CG15306	CH domain containing protein	18707.78	3201.35	17391.75	6728.25	0.93	B
TpnC41C	*troponinC at 41C*	16283.97	5267.47	13494.35	3284.33	0.83	B

a)SD=Standard deviation

b)Average Signal FC= CS Signal Average/Mutant Signal Average See supplemental table for a more comprehensive table.

c)A=Indentified in 75% of total pairwise comparisons. B=Identified in 75% of MhcS1 pairwise comparisons. C=Identified in 75% of MhcS1 pairwise comparisons D=Identified in SAM analysis

general Ca^{2+} homeostasis dysfunction in the flight muscles. Indeed, our previous work suggested that intracellular Ca^{2+} is likely to be dysregulated in *Mhc* mutant fibers, as third instar body wall muscles exhibited spontaneous contraction cycles in the absence of external Ca^{2+} (Montana and Littleton, 2004).

A subset of differentially-regulated genes are expressed in somatic musculature

Most of the genes that have been found to be differentially regulated in this analysis are largely uncharacterized. To determine whether these genes may be important for muscle function, we analyzed the expression patterns of several with domain structures that suggested a role in the muscle. These include *CG12505* (*dARC1*), *CG2330* (*dNeurochondrin*), *CG32030* (*CG5797* and *CG5775*; *dFHOS*), *CG2471* (*dSCLP*), *CG6972* and *CG9025* (*dFEM-1*).

FEM-1, an ankrin repeat protein, was originally isolated in *C. elegans* and has been shown to be important in sex determination through programmed cell death (Kimble et al., 1984). *dSCLP*, a leucine rich repeat-containing protein, is a homolog of SCLP, a gene originally identified in *Manduca* that was found to be upregulated in skeletal muscle cells undergoing programmed cell death (Kuelzer et al., 1999). Although *dFEM-1* showed differential expression in the CNS, it does not exclude the possibility of function within the mesoderm. *dSCLP*, however, showed strong expression in the mesoderm, suggesting its primary function resides in the muscle. *CG6972* is an insect specific protein, with a homolog found in *Anopheles*. This gene contains a low homology armadillo

repeat. The expression pattern shows expression only in somatic musculature, suggesting a function in the muscle.

dARC1 is one of three homologs (*CG12505*, *CG13941*, and *CG10102*) of the mammalian ARC gene The *in situ* hybridization expression pattern for *dARC1* shows a broad expression pattern with many tissue types. However, there is differential expression in both somatic and visceral musculature. Additionally, there is a higher expression in the CNS. Interestingly, the CNS expression pattern is localized to the synaptic regions of the ventral ganglion within the CNS. In the mammalian CNS, ARC mRNA is trafficked to activated synapses and locally translated in the dendrites (Steward and Worley, 2002). This suggests a potential conservation of ARC function in synaptic plasticity and provides a secondary system in which to analyze *dARC1* function *in vivo.*

Neurochondrin was originally isolated as a transcript that is upregulated in neurons that have undergone tetraethylammonium-induced long-term potentiation. Additionally, neurochondrin overexpression in Neuro2a cells induces neurite outgrowth (Shinozaki et al., 1997). The *Drosophila* homolog, *dNeurochondrin*, shows expression in both somatic and visceral musculature, suggesting it functions primarily within the muscle.

dFHOS is an FH1 and FH2-domain containing protein with armadillo repeats in the N-terminus. This gene is the *Drosophila* homolog of FHOS, a human "formin-homology containing protein overexpressed in the spleen" (Westendorf et al., 1999). Recent evidence has shown that formin-containing proteins regulate polymerization of non-branched actin filaments (Pruyne et al.,

Figure 4

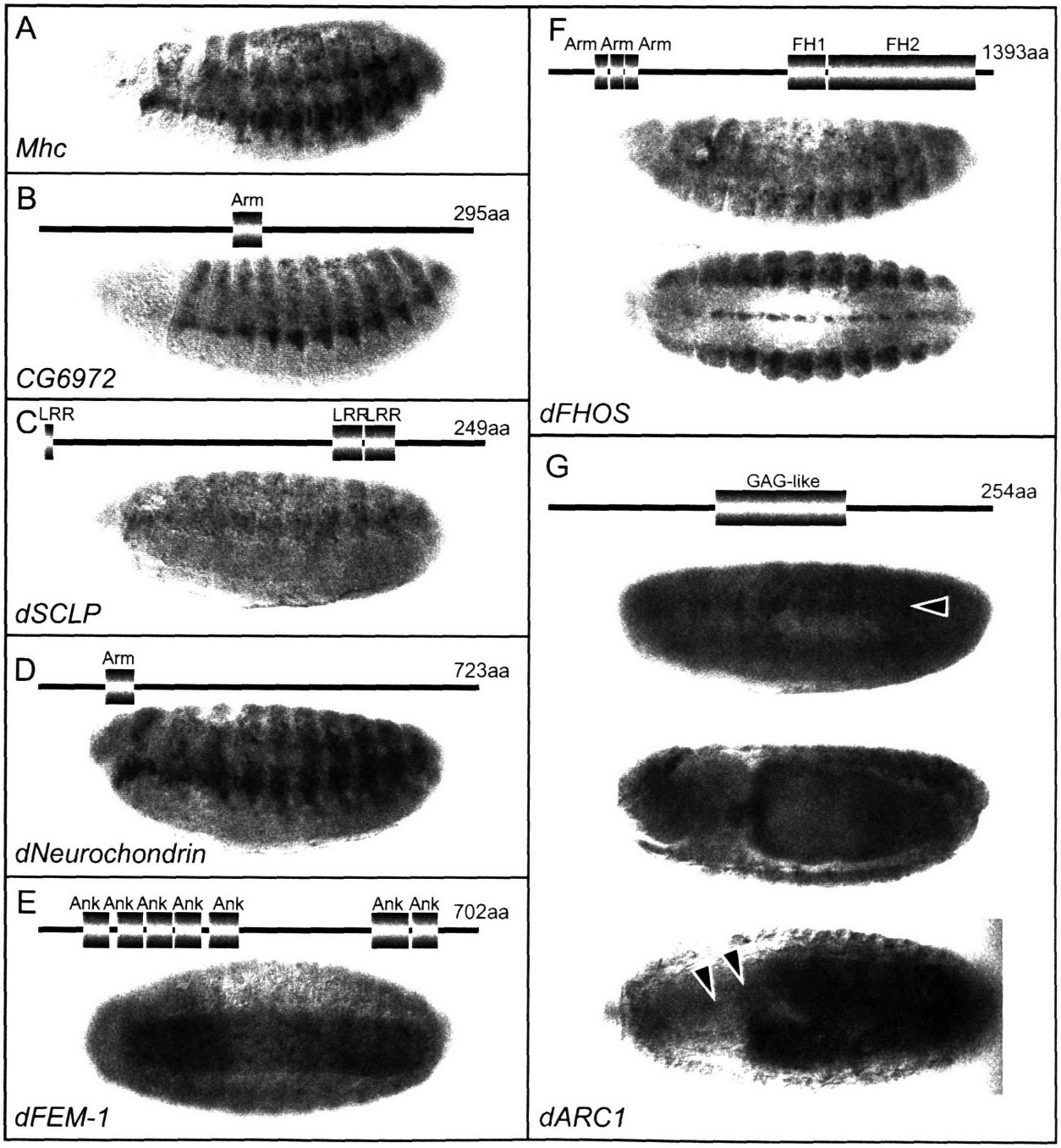

Figure 4: *In situ* analysis confirms that many of the putative muscle remodeling genes are expressed in the somatic mesoderm. Above each *in situ* is a schematic showing the overall domain structure of the protein. Expression patterns are (A) *Mhc,* stage 15, (B) *CG6972*, stage 14, (C) *dSCLP*, stage 16 (D) *dNeurochondrin*, stage 16, (E) *dFEM-1*, stage 16, (F) *dFHOS*, both stage 13, and (G) *dARC1*, late stage 15 (*top* and *middle* are same embryo at different focal planes) and stage 16 (*bottom*). Note the differential expression in somatic mesoderm as well as in the axonal tracts (arrows). Most embryos are positioned anterior to the left and dorsal to the top, except *dFEM-1,* the second *dFHOS*, and the third *dARC1* embryos, which show the ventral face and anterior to the left.

2002; Sagot et al., 2002). The expression pattern of *dFHOS* shows strong somatic muscle expression, as well as cells along the midline of the CNS. These midline CNS cells may represent mesectodermal cells that are thought to differentiate into glial cell fates.

With the exception of *dFEM-1*, the somatic muscle expression of these genes occurs during late mesodermal differentiation, turning on around stage 13 of embryogenesis, when the body wall myoblasts begin to fuse and form the body wall musculature. This indicates that these genes are more likely to be involved with the structure or function of muscle cells, rather than the specification and determination of mesodermal derivatives (Figure 4).

The expression profiling data indicate that the hypercontraction *Mhc* mutants lead to a specific transcriptional response that is similar to that of human muscular dystrophies and hypertrophic cardiomyopathies. This response does not represent a re-activation of the entire developmental program of the mesoderm, as early mesodemal determinants are not upregulated. Rather, it seems to be a program of genes which are required for the structure or function of muscle cells. It is still unclear how this transcriptional response affects the function of the muscle. Future studies will determine whether the differentially-regulated genes contribute to dysfunction, or are involved in the remodeling of damaged and diseased tissue.

Muscle remodeling may occur on the actin cytoskeleton or at key structural sites

To begin understanding the role of differentially-regulated genes in muscle dysfunction, it is important to identify the possible sites of action at which the proteins these genes encode may act within the muscle. For this, we analyzed the immunolocalization of MSP-300, the *Drosophila* nesprin (Rosenberg-Hasson et al., 1996; Zhang et al., 2002b). As previously reported, localization of MSP-300 was found in four distinct places in larval body wall muscles (Figure 5). These sites include the Z-line, the muscle attachment sites, the nucleus, and at an unknown structure resembling an attachment site between muscles 6 and 7. This data suggests that possible sites of action for this subset of genes that are differentially regulated in post-differentiated diseased or damaged muscle may be these four sites. In support of this, the muscle LIM protein Mlp84B has been shown to accumulate at muscle attachment sites and Z-lines as well (Stronach et al., 1999). Additionally, *flap wing* has been shown to be important for the integrity of muscle attachment sites and the organization of the Z-lines in the IFM (Raghavan et al., 2000). The *Drosophila* titin (*sls, Kettin, and titin*) has been shown to be important for both myoblast fusion as well as structural integrity of the sarcomere, with immunolocalization to Z-lines (Hakeda et al., 2000; Lakey et al., 1993; van Straaten et al., 1999).

As many of the genes we have identified as potential muscle remodeling genes are uncharacterized, we assayed whether the most upregulated gene, *dARC1* can potentially localize to the actin cytoskeleton. For this analysis, we created transgenic flies which express dARC1 fused to the N-terminus of GFP under the UAS/GAL4 expression system (Phelps and Brand, 1998). In addition,

Figure 5

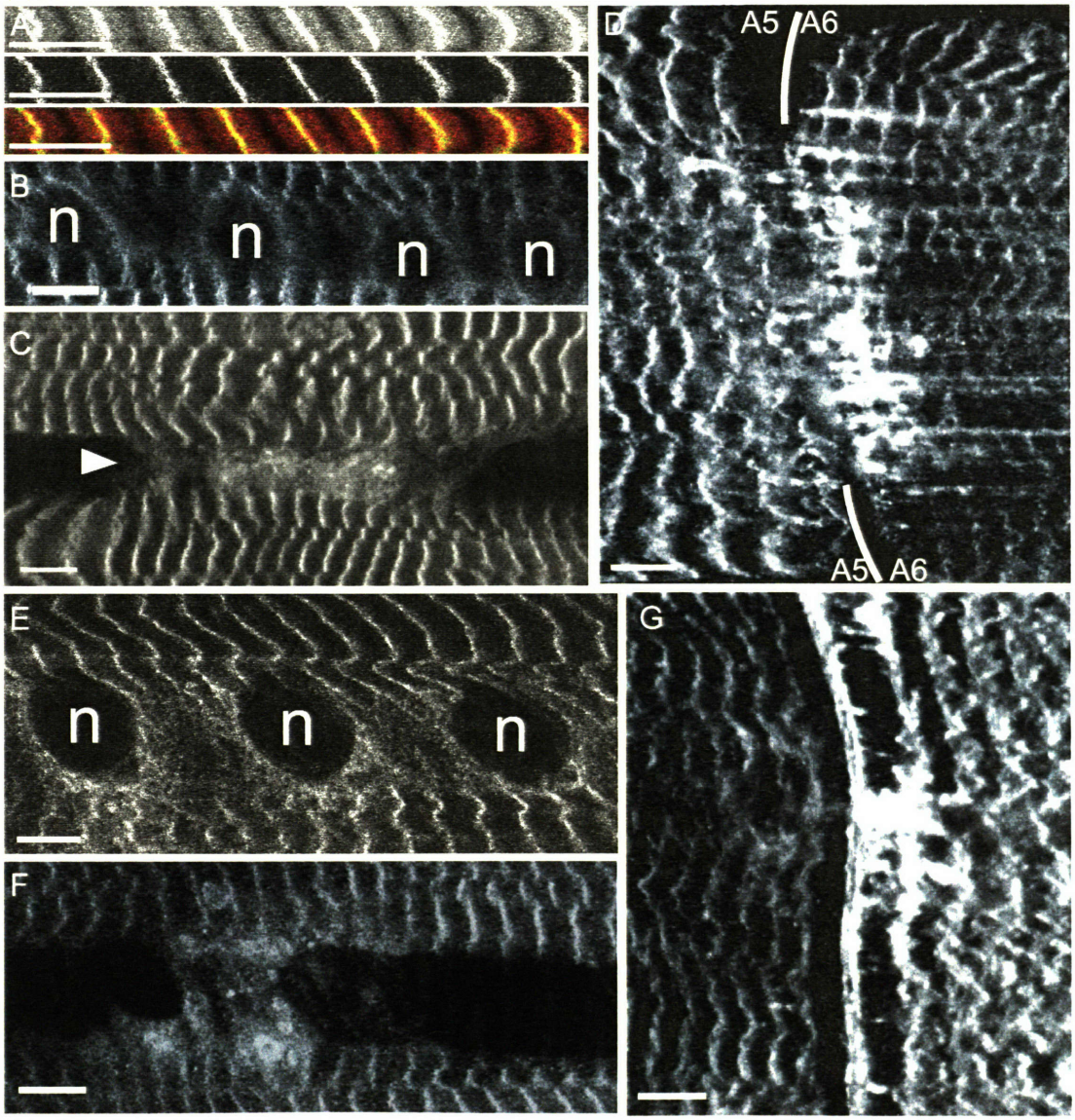

Figure 5: Potential sites of action for muscle remodeling in hypercontraction mutants. Four distinct structures are labeled with antisera raised against the MSP-300 protein. Redistribution of the protein is not detected in mutant animals. (A) Phalloidin-labeled actin cytoskeleton (top), α-MSP-300 (middle), and merge (bottom) indicate the presence of MSP-300 at the Z-line. (B,E) Structures around the nuclei are α-MSP-300 positive (nuclei labeled with n). (C,F) MSP-300 is found at inter-muscular connections between muscles 6 and 7, and (D,G) at intersegmental muscle attachment sites. Genotypes are (A-D) *Canton S*, (E,G) Mhc^{S1}/+, and (F) Mhc^{S2}/+. Scale bars indicate 10μm.

we generated flies which overexpress non-tagged dARC1. The GFP-tagged dARC1 protein did not fold correctly when overexpressed in the muscle (Figure 6). However, when co-expressed with untagged dARC1, the GFP localization resembled sarcomeric structures in the muscle. Co-staining with Texas-red phalloidin was not possible, as fixation disrupted the GFP localization, causing GFP-dARC1 to disassociate from this structure and form aggregates (data not shown). Interestingly, the co-expression of these proteins in the CNS shows GFP fluorescence at synaptic sites (Figure 6). This suggests that *dARC1* may mediate a function in *Drosophila* synapses, consistent with data in mammals (Guzowski et al., 2000; Lyford et al., 1995). Given this data, it is likely that dARC1 may bind to the sarcomere *in vivo*. Future experiments to co-localize this signal with known markers of sarcomeric substructures will determine the precise localization of dARC1 in this overexpression system.

Figure 6

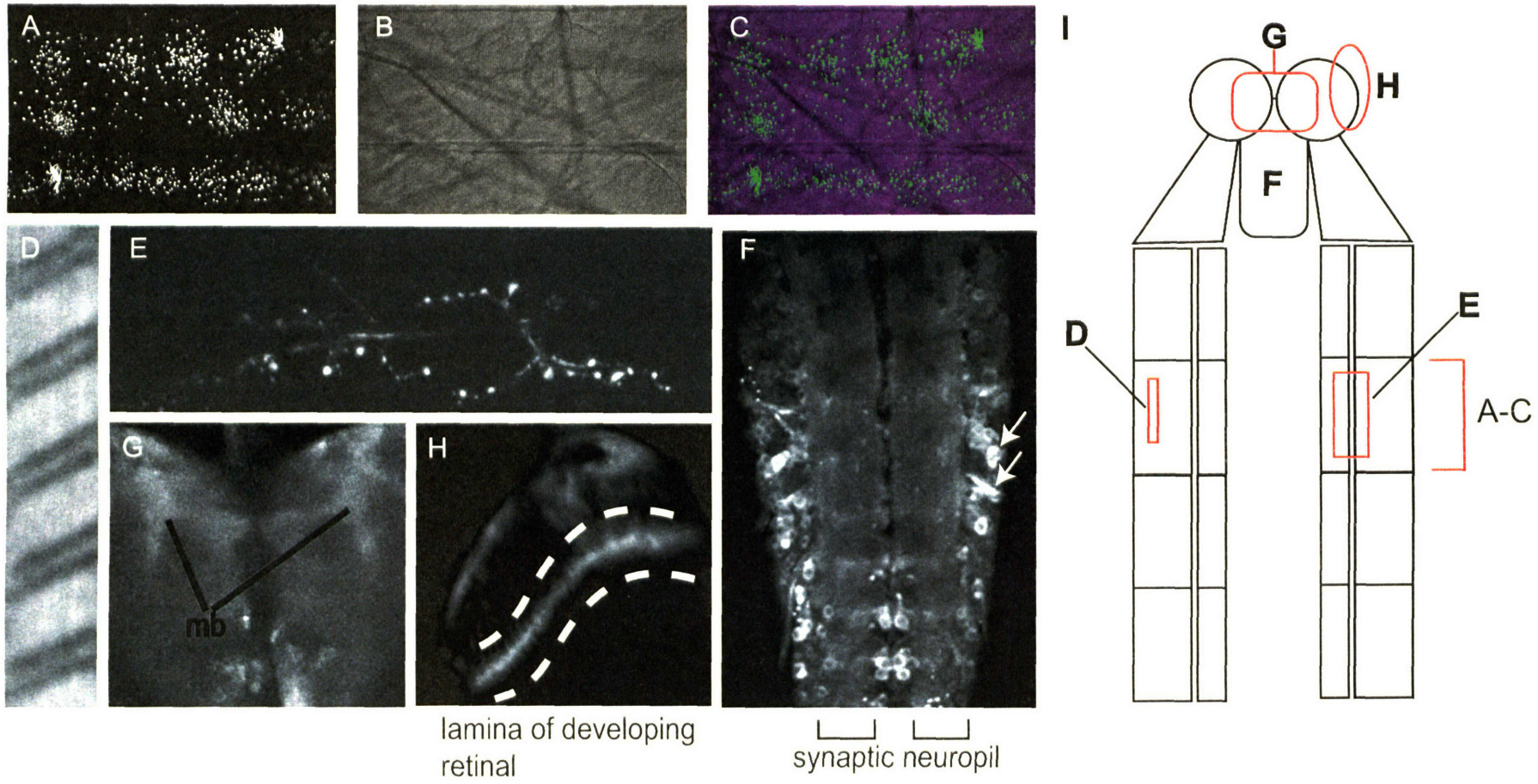

Figure 6: dARC1 potentially localizes to the sarcomere in the muscle and synaptic regions within the CNS (A) Expression of dARC1-GFP fusions were unstable in the muscle, forming aggregates within the muscle. (B) DIC image of the muscle containing dARC1-GFP aggregates. (C) Merged image of (A) and (B). (D) Co-expression of both dARC1 and dARC1-GFP shows localization to structures resembling the sarcomere in the muscle. In addition, co-expression in the CNS shows synaptic-like localization in the (E) neuromuscular junction, (F) neurophil region of the ventral ganglion, (G) mushroom bodies of the brain lobes, and (H) the developing visual system. Genotypes shown are (A-C) *w;Mhc-GAL4,+/+, UAS-dARC1-GFP* (D) *w; Mhc-GAL4, UAS-dARC1,+/+,+,UAS-dARC1-GFP* and (E-H) *C155; UAS-dARC1,+/+,UAS-dARC1-GFP*.

Discussion

Muscle contraction is a highly-coordinated and specialized process that requires the proper functioning of a large number of proteins. Mutations which affect this process lead to a large array of diseases which include muscular dystrophies and cardiomyopathies. Although the molecular lesions underlying a number of these diseases are well known, the downstream consequences underlying disease pathogenesis are less understood. Often, changes in the overall transcriptional profile occur in response to genetic lesions. Defining the alterations in gene expression can aid in understanding the pathogenesis of disease. In addition, functional studies on differentially-regulated genes with can help in identifying novel therapeutic targets for treatment of the disease.

Altered gene expression in response to hypercontraction in Drosophila

In a previous study, we showed that hypercontraction mutations in *Drosophila* lead to an altered muscle state when compared with normal muscles. This state alteration was reflected in temperature-sensitive seizures in the adult animal and external Ca^{2+}-independent contraction cycles in the larval body wall muscles. By using microarray analyses, we can begin to gain insight into this altered state and identify differences which may contribute to muscle dysfunction, as well as differences in gene expression which functionally compensate for alterations induced by mutation.

The striking difference between normal and hypercontraction muscles identified is the robust upregulation of genes that are either known to or putatively act at the level of the actin cytoskeleton. Some of the previously characterized genes that we have identified as differentially-regulated in response to myopathy include *Mlp60A, Mlp84B, Kettin, MSP-300, flw, sqh, capulet, slingshot, act88F, act57B, Mbs,* and *talin*. *Mlp60A, Mlp84B, Kettin, MSP-300, flw, capulet,* and *talin,* have all been shown to play roles in providing or modulating the structural supports of the cytoskeleton (Baum et al., 2000; Brown et al., 2002; Lakey et al., 1993; Raghavan et al., 2000; Rosenberg-Hasson et al., 1996; Stronach et al., 1999). This suggests that in *Drosophila* muscles, hypercontraction and degredation can trigger a transcriptional response to remodel the cytoskeleton and its associated support structures. This may represent a functionally beneficial compensation mechanism by which the muscle responds to the increased forces induced by hypercontraction. The upregulation of *sqh* supports the idea of compensatory mechanisms. In wildtype animals, *sqh* normally acts as a regulatory light chain of the non-muscle type II myosin, *zipper* (Karess et al., 1991). This upregulation could potentially alter the overall activity and force output of the muscle by changing the properties of Mhc. On the other hand, the downregulation of *fln* may reflect a deleterious alteration in transcription. Loss-of-function mutations in *fln* lead to sarcomeric instability and defects in thick filament assembly (Baum et al., 2000). In addition to the increased forces produced by mutant Mhc, decreasing *fln* transcription may lead destabilization of the thick filament structure.

Among the known genes we have identified through the microarray, several have defined expression patterns through development, but normally are not highly expressed in the adult animal. The muscle LIM proteins, for example, have peak expressions at the terminal stages of muscle development in the embryo and pupa (Stronach et al., 1996). In addition, *act57B* is the predominant actin for the larval somatic musculature, while *act88F* is predominantly an adult actin (Tobin et al., 1990). This may indicate that, like fiber regeneration by satellite cells in human muscular dystrophy, *Drosophila* could have mechanisms for fiber regeneration in response to myopathy (Jejurikar and Kuzon, 2003). However, early mesodermal determinants do not show upregulation, suggesting this is unlikely. Further, many of the genes which encode the contractile machinery are not upregulated, suggesting that the subset of upregulated genes function within the mature myopathic fibers rather than function in fiber replenishment.

Many of the genes which we have identified as differentially-regulated in response to hypercontraction are novel and have not been characterized. However, it seems likely that many will act within this muscle remodeling pathway. The domain structure and homology of these genes suggest they play roles in regulating or supporting the cytoskeleton. Further, the *in situ* hybridization experiments indicate that many of these are differentially expressed in the muscle. Therefore, not only do the novel genes have sequences which indicate a role in cytoskeletal regulation and show similar regulatory patterns in response to myopathy, but they also are preferentially expressed in muscle. One

of these genes, *dFHOS*, is a formin-domain containing protein. Recent data has shown that formin domains promote the formation of unbranched actin polymers in an ARP2/3-independent manner (Pruyne et al., 2002; Sagot et al., 2002). This may indicate that *dFHOS* plays a role in polymerizing the unbranched actin filaments in the sarcomere. Current work in the lab will address the role of *dFHOS* in *Drosophila* muscles.

Therefore, the transcriptional profile seems to indicate that in *Drosophila,* hypercontraction-induced myopathy leads to a remodeling of the cytoskeletal architecture. This remodeling most likely occurs on the level of modulation and support of the actin cytoskeleton. Further, the likely subcellular domains at which they act include muscle attachment sites, nuclear membrane, and at the Z-line structures of the sarcomere—known localization sites for many of the differentially-regulated transcripts which have been previously characterized.

In addition to the potential muscle remodeling response, the upregulation of immune response genes suggests an infiltration of immune cells involved in degradation of dying muscle cells. The downregulation of nuclear-encoded mitochondrial genes and genes involved in energy and metabolism indicates a general metabolic crisis of the animal. Whether this occurs due to the declining health of the IFM, or if this response is causative to the myopathy is unknown. This downregulation may also be indicative of Ca^{2+} overloading of the mitochondria and subsequent Ca^{2+}-activated cell death. Mitochondrial staining in *Mhc* mutant third instar body wall muscles appears normal (unpublished data), suggesting that this downregulation does not correspond to decreased

mitochondrial number, but rather supports a loss of metabolic function and subsequent energy depletion in the muscle.

Synaptic plasticity and muscle remodeling

An intriguing observation in the expression profile was an upregulation of a subset of genes which have been isolated in mammalian systems as activity-regulated transcripts in the nervous system. These genes include *dARC1, dNeurochondrin,* and *MSP-300*. The mammalian homologs (ARC, neurochondrin/norbin and CPG2) are upregulated in response to synaptic activity. Although loss-of-function studies have not been done on these genes, cell culture studies suggest the proteins are involved in regulating the morphological properties of the synapse in an activity-dependent manner (Fosnaugh et al., 1995; Lyford et al., 1995; Nedivi et al., 1996; Shinozaki et al., 1997; Steward, 2002; Steward et al., 1998; Steward and Worley, 2002; Wallace et al., 1998). Activity-dependent synaptic modification is dependent upon Ca^{2+} signals originating from influx through NMDA receptors at synapses (Malenka, 1991). Potentially, the Ca^{2+}-dependent processes that have been implicated in muscular dystrophies and cardiomyopathies may also function in activity-dependent synaptic plasticity, utilized to remodel actin-dependent structures in response to defined stimuli.

Drosophila as a model system to study human muscle diseases

The transcriptional response to hypercontraction-induced myopathy in *Drosophila* suggests a conserved cellular response to muscle dysfunction from flies to humans. The general classes of genes which show differential regulation include an upregulation of developmentally-regulated muscle transcripts, an upregulation of immune response genes, and a downregulation of energy and metabolism genes. These responses have been seen in both muscular dystrophies and cardiomyopathies. Further, the expression analysis has indicated a potential remodeling of the cytoskeleton and its support architecture. This response could be indicative of compensatory mechanisms utilized to slow the degredation process. Alternatively, it may reflect an endogenous response that normally occurs in muscle injury, but may not be sufficient to compensate for genetic lesions. The parallels found in *Drosophila* to human muscle diseases suggests that the cellular responses to genetic lesions affecting muscle function and, subsequently, leading to myopathic states, may be conserved. Therefore, *Drosophila*, offers a system in which to perform high-throughput pharmaceutical discovery for compounds which alleviate the defects of contractile dysfunction. Further, using the molecular genetic tools available, we can begin to understand the functional consequences of altered transcription in context of muscle disease, as well as to dissect the pathways activated by the primary mutations which lead to the altered state observed in hypercontraction.

Materials and methods

Fly strains and crosses

Flies were cultured on standard medium at 22°C. All crosses using appropriate genotypes were cultured at 25°C. Overexpression of *dARC1* was done using the C155 driver for neuronal expression. Muscle expression was driven using the Mhc-GAL4 driver.

Mutation and crystal structure analysis

Crystal structure analysis of the mutations was done using the Swiss PDB Viewer software available at http://us.expasy.org/spdbv/. The 2MYS crystal structure was downloaded from NCBI and mutations mapped according to BLAST alignments done through the NCBI BLAST website. (Fisher et al., 1995; Rayment et al., 1995; Rayment et al., 1993).

Tissue samples

Tissue was derived from 3-4 day old adult male flies of the appropriate genotype raised at 25°C. Flies were frozen in liquid nitrogen and vortexed in order to obtain isolated heads and bodies (wings and legs were discarded). Circadian differences were minimized by processing tissue between 11am-2pm.

A total of 8 independent microarrays were analyzed (four control, two Mhc^{S1}/+, and two Mhc^{S2}/+).

Tissue processing

Total RNA was isolated using Trizol (GibcoBRL). 7-12 flies were processed in 200μl of Trizol. Five batches (1ml) of processed tissue were then used to isolate the total RNA. From the total RNA, mRNA was isolated using the Qiagen Oligotex mRNA extraction kit. cDNA was created with random hexamer and T7-polyT oligonucleotides using the GibcoBRL/Invitrogen cDNA kit. cDNA was then purified by phenol/chloroform extraction and Phase Lock Gel extraction tubes (Eppendorf) as suggested by Affymetrix®. Biotin-labeled cRNA was made with the Enzo High-yield Bioarray kit using the supplied protocol with the modification of running half reaction mixes. Reactions were cleaned with the Qiagen RNEasy kit, precipitated overnight, and resuspended into 13μl of DEPC-treated ddH_2O. Fragmentation was done with fragmentation buffer (200 mM Tris-acetate, pH 8.1, 500 mM KOAc, 150 mM MgOAc) at 94°C for 35 min then brought up into 33μl total volume, and appropriate amount of cRNA was then sent to the Affymetrix® processing lab at MIT for hybridization and signal detection.

Expression Analysis

Statistical analysis was done with the Affymetrix® Microarrary Suite software using the following normalization values:

Scaling target: 1500

Alpha1: 0.04

Alpha2: 0.06

Tau: 0.015

Gamma1L: 0.0025

Gamma1H: 0.0025

Gamma2L: 0.0030

Gamma2H: 0.0030

Perturbation: 1.1

Gene changes were called based upon the stringency criteria that differential regulation must be reported by Affymetrix software for at least 75% of the pairwise comparisons. Additionally, an analysis utilizing Significance Analysis of Microarrays (SAM) v.120 was done in order to provide an independent analysis of the normalized data, giving higher stringency in differential regulation hits. Analysis with SAM was done as two-class, unpaired data sets, setting delta to ~25% false positive rate. Raw and normalized data can be obtained by request at http://web.mit.edu/flybrain/littletonlab/.

Semi-quantitative RT-PCR

Semi-quantitative RT-PCR was utilized to verify select genes from the microarray analysis. PCR primers were designed to sequences used in the design of probe pairs by Affymetrix. cDNA isolated was diluted into the equivalent amount isolated from 1μg total RNA per 1μl. This solution was

further diluted 1:100 and 0.1 to 1 μl used in the reactions depending upon transcript abundance and primer efficiency. Reaction samples were taken from cycles 21-30 in order to determine linear regions of the reactions. If linear regions were overlapping, comparisons were made in those cycles. If linear regions were not overlapping, reactions were run until mutant reactions were within linear cycles.

In situ analysis

In situ expression analysis was performed using standard procedures. Probes were designed to ~200 bp fragments, amplified by PCR using a 3' primer that includes the T7 sequence. Sequences used for *in situ* hybridization coincide to sequences used by Affymetrix for probe pair design. In most cases, the same sequence used for semi-quantitative RT-PCR was used for in situ analysis. Primer sequences for semi-quantitative RT-PCR and *in situ* probe production can be obtained upon request.

Immunostaining of third instar larvae

Immunostaining of third instar larval fillets was done as previously described (Montana and Littleton, 2004). For labeling MSP-300, we utilized α-MSP-300 antisera at 1:500 (Volk, 1992). Secondary goat α-rabbit conjugated to Cy2 was used at 1:500 (Jackson Labs). F-actin was labeled with Texas red-conjugated phalloidin at 1:500, incubated simulateously with the secondary antibody (Molecular Probes).

Overexpression of dARC1

Transgenic flies were generated by cloning the *dARC1* open reading frame and the *dARC1-GFP* fusion construct into the pUAST vector. Both constructs were cloned using XhoI/XbaI restriction sites built into the primers. The fusion of *dARC1* and *GFP* was created by using standard gene-fusion PCR techniques. Transgenic flies were obtained using Genetic Services, Inc. (Cambridge, MA). Imaging of GFP was done similar to immunostained larvae with the exception that the larvae were mounted live and visualized under a 40X/0.8NA water-immersion lens (Zeiss).

Acknowledgements

We thank Avital Rodal, Motojiro Yoshihara, and Bill Adolfsen for helpful discussions about the manuscript and Affymetrix® for help in setting up the software and taking the time to help us get acquainted with its use. We would also like to thank the Bloomington Stock Center and T. Volk for *Drosophila* strains. The α-MSP-300 antibody was a gift from T. Volk. This work was supported by grants from the NIH, the Human Frontiers Science Program, the Searle Scholars Program, and the Packard Foundation. J. Troy Littleton is an Alfred P. Sloan Research Fellow.

Aronow, B.J., T. Toyokawa, A. Canning, K. Haghighi, U. Delling, E. Kranias, J.D. Molkentin, and G.W. Dorn, 2nd. 2001. Divergent transcriptional responses to independent genetic causes of cardiac hypertrophy. *Physiol Genomics.* 6:19-28.

Barrans, J.D., P.D. Allen, D. Stamatiou, V.J. Dzau, and C.C. Liew. 2002. Global gene expression profiling of end-stage dilated cardiomyopathy using a human cardiovascular-based cDNA microarray. *Am J Pathol.* 160:2035-43.

Baum, B., W. Li, and N. Perrimon. 2000. A cyclase-associated protein regulates actin and cell polarity during Drosophila oogenesis and in yeast. *Curr Biol.* 10:964-73.

Brown, N.H., S.L. Gregory, W.L. Rickoll, L.I. Fessler, M. Prout, R.A. White, and J.W. Fristrom. 2002. Talin is essential for integrin function in Drosophila. *Dev Cell.* 3:569-79.

Campanaro, S., C. Romualdi, M. Fanin, B. Celegato, B. Pacchioni, S. Trevisan, P. Laveder, C. De Pitta, E. Pegoraro, Y.K. Hayashi, G. Valle, C. Angelini, and G. Lanfranchi. 2002. Gene expression profiling in dysferlinopathies using a dedicated muscle microarray. *Hum Mol Genet.* 11:3283-98.

Chamberlain, J.S. 2000. Muscular dystrophy meets the gene chip. New insights into disease pathogenesis. *J Cell Biol.* 151:F43-6.

Chen, Y.W., P. Zhao, R. Borup, and E.P. Hoffman. 2000. Expression profiling in the muscular dystrophies: identification of novel aspects of molecular pathophysiology. *J Cell Biol.* 151:1321-36.

Chien, K.R., K.U. Knowlton, H. Zhu, and S. Chien. 1991. Regulation of cardiac gene expression during myocardial growth and hypertrophy: molecular studies of an adaptive physiologic response. *Faseb J.* 5:3037-46.

Fadic, R., Y. Sunada, A.J. Waclawik, S. Buck, P.J. Lewandoski, K.P. Campbell, and B.P. Lotz. 1996. Brief report: deficiency of a dystrophin-associated glycoprotein (adhalin) in a patient with muscular dystrophy and cardiomyopathy. *N Engl J Med.* 334:362-6.

Ferrus, A., A. Acebes, M.C. Marin, and A. Hernandez-Hernandez. 2000. A genetic approach to detect muscle protein interactions in vivo. *Trends Cardiovasc Med*. 10:293-8.

Fosnaugh, J.S., R.V. Bhat, K. Yamagata, P.F. Worley, and J.M. Baraban. 1995. Activation of arc, a putative "effector" immediate early gene, by cocaine in rat brain. *J Neurochem*. 64:2377-80.

Frey, N., T.A. McKinsey, and E.N. Olson. 2000. Decoding calcium signals involved in cardiac growth and function. *Nat Med*. 6:1221-7.

Gailly, P. 2002. New aspects of calcium signaling in skeletal muscle cells: implications in Duchenne muscular dystrophy. *Biochim Biophys Acta*. 1600:38-44.

Guzowski, J.F., G.L. Lyford, G.D. Stevenson, F.P. Houston, J.L. McGaugh, P.F. Worley, and C.A. Barnes. 2000. Inhibition of activity-dependent arc protein expression in the rat hippocampus impairs the maintenance of long-term potentiation and the consolidation of long-term memory. *J Neurosci*. 20:3993-4001.

Hakeda, S., S. Endo, and K. Saigo. 2000. Requirements of Kettin, a giant muscle protein highly conserved in overall structure in evolution, for normal muscle function, viability, and flight activity of Drosophila. *J Cell Biol*. 148:101-14.

Jejurikar, S.S., and W.M. Kuzon, Jr. 2003. Satellite cell depletion in degenerative skeletal muscle. *Apoptosis*. 8:573-8.

Karess, R.E., X.J. Chang, K.A. Edwards, S. Kulkarni, I. Aguilera, and D.P. Kiehart. 1991. The regulatory light chain of nonmuscle myosin is encoded by spaghetti-squash, a gene required for cytokinesis in Drosophila. *Cell*. 65:1177-89.

Kimble, J., L. Edgar, and D. Hirsh. 1984. Specification of male development in Caenorhabditis elegans: the fem genes. *Dev Biol*. 105:234-9.

Komuro, I., Y. Katoh, T. Kaida, Y. Shibazaki, M. Kurabayashi, E. Hoh, F. Takaku, and Y. Yazaki. 1991. Mechanical loading stimulates cell hypertrophy and

specific gene expression in cultured rat cardiac myocytes. Possible role of protein kinase C activation. *J Biol Chem*. 266:1265-8.

Kuelzer, F., P. Kuah, S.T. Bishoff, L. Cheng, J.R. Nambu, and L.M. Schwartz. 1999. Cloning and analysis of small cytoplasmic leucine-rich repeat protein (SCLP), a novel, phylogenetically-conserved protein that is dramatically up-regulated during the programmed death of moth skeletal muscle. *J Neurobiol*. 41:482-94.

Labuhn, M., and C. Brack. 1997. Age-related changes in the mRNA expression of actin isoforms in Drosophila melanogaster. *Gerontology*. 43:261-7.

Lakey, A., S. Labeit, M. Gautel, C. Ferguson, D.P. Barlow, K. Leonard, and B. Bullard. 1993. Kettin, a large modular protein in the Z-disc of insect muscles. *Embo J*. 12:2863-71.

Leinwand, L.A. 2001. Calcineurin inhibition and cardiac hypertrophy: a matter of balance. *Proc Natl Acad Sci U S A*. 98:2947-9.

Lim, D.S., R. Roberts, and A.J. Marian. 2001. Expression profiling of cardiac genes in human hypertrophic cardiomyopathy: insight into the pathogenesis of phenotypes. *J Am Coll Cardiol*. 38:1175-80.

Lowes, B.D., E.M. Gilbert, W.T. Abraham, W.A. Minobe, P. Larrabee, D. Ferguson, E.E. Wolfel, J. Lindenfeld, T. Tsvetkova, A.D. Robertson, R.A. Quaife, and M.R. Bristow. 2002. Myocardial gene expression in dilated cardiomyopathy treated with beta-blocking agents. *N Engl J Med*. 346:1357-65.

Lyford, G.L., K. Yamagata, W.E. Kaufmann, C.A. Barnes, L.K. Sanders, N.G. Copeland, D.J. Gilbert, N.A. Jenkins, A.A. Lanahan, and P.F. Worley. 1995. Arc, a growth factor and activity-regulated gene, encodes a novel cytoskeleton-associated protein that is enriched in neuronal dendrites. *Neuron*. 14:433-45.

Malenka, R.C. 1991. The role of postsynaptic calcium in the induction of long-term potentiation. *Mol Neurobiol*. 5:289-95.

Martonosi, A.N., and S. Pikula. 2003. The network of calcium regulation in muscle. *Acta Biochim Pol*. 50:1-30.

Molkentin, J.D., J.R. Lu, C.L. Antos, B. Markham, J. Richardson, J. Robbins, S.R. Grant, and E.N. Olson. 1998. A calcineurin-dependent transcriptional pathway for cardiac hypertrophy. *Cell*. 93:215-28.

Montana, E.S., and J.T. Littleton. 2004. Characterization of a hypercontraction-induced myopathy in Drosophila caused by mutations in Mhc. *J Cell Biol*. 164:1045-54.

Nedivi, E., S. Fieldust, L.E. Theill, and D. Hevron. 1996. A set of genes expressed in response to light in the adult cerebral cortex and regulated during development. *Proc Natl Acad Sci U S A*. 93:2048-53.

Noguchi, S., T. Tsukahara, M. Fujita, R. Kurokawa, M. Tachikawa, T. Toda, A. Tsujimoto, K. Arahata, and I. Nishino. 2003. cDNA microarray analysis of individual Duchenne muscular dystrophy patients. *Hum Mol Genet*. 12:595-600.

Phelps, C.B., and A.H. Brand. 1998. Ectopic gene expression in Drosophila using GAL4 system. *Methods*. 14:367-79.

Pruyne, D., M. Evangelista, C. Yang, E. Bi, S. Zigmond, A. Bretscher, and C. Boone. 2002. Role of formins in actin assembly: nucleation and barbed-end association. *Science*. 297:612-5.

Raghavan, S., I. Williams, H. Aslam, D. Thomas, B. Szoor, G. Morgan, S. Gross, J. Turner, J. Fernandes, K. VijayRaghavan, and L. Alphey. 2000. Protein phosphatase 1beta is required for the maintenance of muscle attachments. *Curr Biol*. 10:269-72.

Rayment, I., H.M. Holden, J.R. Sellers, L. Fananapazir, and N.D. Epstein. 1995. Structural interpretation of the mutations in the beta-cardiac myosin that have been implicated in familial hypertrophic cardiomyopathy. *Proc Natl Acad Sci U S A*. 92:3864-8.

Rayment, I., W.R. Rypniewski, K. Schmidt-Base, R. Smith, D.R. Tomchick, M.M. Benning, D.A. Winkelmann, G. Wesenberg, and H.M. Holden. 1993. Three-dimensional structure of myosin subfragment-1: a molecular motor. *Science*. 261:50-8.

Rosenberg-Hasson, Y., M. Renert-Pasca, and T. Volk. 1996. A Drosophila dystrophin-related protein, MSP-300, is required for embryonic muscle morphogenesis. *Mech Dev*. 60:83-94.

Sadoshima, J., and S. Izumo. 1997. The cellular and molecular response of cardiac myocytes to mechanical stress. *Annu Rev Physiol*. 59:551-71.

Sadoshima, J., L. Jahn, T. Takahashi, T.J. Kulik, and S. Izumo. 1992. Molecular characterization of the stretch-induced adaptation of cultured cardiac cells. An in vitro model of load-induced cardiac hypertrophy. *J Biol Chem*. 267:10551-60.

Sagot, I., A.A. Rodal, J. Moseley, B.L. Goode, and D. Pellman. 2002. An actin nucleation mechanism mediated by Bni1 and profilin. *Nat Cell Biol*. 4:626-31.

Seidman, J.G., and C. Seidman. 2001. The genetic basis for cardiomyopathy: from mutation identification to mechanistic paradigms. *Cell*. 104:557-67.

Semsarian, C., I. Ahmad, M. Giewat, D. Georgakopoulos, J.P. Schmitt, B.K. McConnell, S. Reiken, U. Mende, A.R. Marks, D.A. Kass, C.E. Seidman, and J.G. Seidman. 2002. The L-type calcium channel inhibitor diltiazem prevents cardiomyopathy in a mouse model. *J Clin Invest*. 109:1013-20.

Shinozaki, K., K. Maruyama, H. Kume, H. Kuzume, and K. Obata. 1997. A novel brain gene, norbin, induced by treatment of tetraethylammonium in rat hippocampal slice and accompanied with neurite-outgrowth in neuro 2a cells. *Biochem Biophys Res Commun*. 240:766-71.

Steward, O. 2002. mRNA at synapses, synaptic plasticity, and memory consolidation. *Neuron*. 36:338-40.

Steward, O., C.S. Wallace, G.L. Lyford, and P.F. Worley. 1998. Synaptic activation causes the mRNA for the IEG Arc to localize selectively near activated postsynaptic sites on dendrites. *Neuron*. 21:741-51.

Steward, O., and P. Worley. 2002. Local synthesis of proteins at synaptic sites on dendrites: role in synaptic plasticity and memory consolidation? *Neurobiol Learn Mem*. 78:508-27.

Stronach, B.E., P.J. Renfranz, B. Lilly, and M.C. Beckerle. 1999. Muscle LIM proteins are associated with muscle sarcomeres and require dMEF2 for their expression during Drosophila myogenesis. *Mol Biol Cell.* 10:2329-42.

Stronach, B.E., S.E. Siegrist, and M.C. Beckerle. 1996. Two muscle-specific LIM proteins in Drosophila. *J Cell Biol.* 134:1179-95.

Tobin, S.L., P.J. Cook, and T.C. Burn. 1990. Transcripts of individual Drosophila actin genes are differentially distributed during embryogenesis. *Dev Genet.* 11:15-26.

Tusher, V.G., R. Tibshirani, and G. Chu. 2001. Significance analysis of microarrays applied to the ionizing radiation response. *Proc Natl Acad Sci U S A.* 98:5116-21.

van der Kooi, A.J., M. van Meegen, T.M. Ledderhof, E.M. McNally, M. de Visser, and P.A. Bolhuis. 1997. Genetic localization of a newly recognized autosomal dominant limb-girdle muscular dystrophy with cardiac involvement (LGMD1B) to chromosome 1q11-21. *Am J Hum Genet.* 60:891-5.

van Straaten, M., D. Goulding, B. Kolmerer, S. Labeit, J. Clayton, K. Leonard, and B. Bullard. 1999. Association of kettin with actin in the Z-disc of insect flight muscle. *J Mol Biol.* 285:1549-62.

Vigoreaux, J.O. 2001. Genetics of the Drosophila flight muscle myofibril: a window into the biology of complex systems. *Bioessays.* 23:1047-63.

Volk, T. 1992. A new member of the spectrin superfamily may participate in the formation of embryonic muscle attachments in Drosophila. *Development.* 116:721-30.

Wallace, C.S., G.L. Lyford, P.F. Worley, and O. Steward. 1998. Differential intracellular sorting of immediate early gene mRNAs depends on signals in the mRNA sequence. *J Neurosci.* 18:26-35.

Westendorf, J.J., R. Mernaugh, and S.W. Hiebert. 1999. Identification and characterization of a protein containing formin homology (FH1/FH2) domains. *Gene.* 232:173-82.

Zhang, C.L., T.A. McKinsey, S. Chang, C.L. Antos, J.A. Hill, and E.N. Olson. 2002a. Class II histone deacetylases act as signal-responsive repressors of cardiac hypertrophy. *Cell*. 110:479-88.

Zhang, Q., C. Ragnauth, M.J. Greener, C.M. Shanahan, and R.G. Roberts. 2002b. The nesprins are giant actin-binding proteins, orthologous to Drosophila melanogaster muscle protein MSP-300. *Genomics*. 80:473-81.

Characterization of the *Drosophila* ARC Homolog, *dARC1*

Enrico S. Montana[1*], Mark Mattaliano[3*], Jose Augusto[3], Leslie Griffith[3], & J. Troy Littleton[1,2]

[1]Department of Biology, [1]Picower Center for Learning and Memory, [2]Department of Brain and Cognitive Sciences , [3]Department of Biology, [3]Brandeis University, Waltham, MA, 02454, [1,2]Massachusetts Institute of Technology, Cambridge, MA 02139, USA

*These authors contributed equally to this work

This work initially started as two parallel projects. As the projects progressed, it became clear that we would need to fully collaborate on this characterization. Presented here is mostly the work I have done on my half of this collaboration with a few exceptions. Mark generated the antibody that is utilized in the *in vivo* immunohistochemistry, as well as performed the behavioral analyses of the *dARC1* mutants. Further studies on the characterization of the *dARC1* mutant are still in progress. This work will be published pending the results of Mark and Leslie.

Abstract

The *dARC1* gene is one of two *Drosophila* homologs of the mammalian activity-regulated cytoskeleton-associated gene ARC, an immediate-early gene that has been implicated in the process of long-term memory consolidation. The *dARC1* gene was identified in two independent expression analyses as differentially-regulated in response to three stimuli, including heat, neuronal activity, and hypercontraction-induced myopathy. Here, we present the characterization of a loss-of-function mutation in *dARC1* in the context of synaptic function and plasticity. The dARC1 protein is expressed in a large subset of cells within the CNS, the larval body wall muscles, and epidermal cells of the larvae. Loss-of-function mutations in *dARC1* result in no defects associated with synaptic transmission, high-frequency stimulation-induced vesicle depletion in the presynaptic terminal, paired-pulse facilitation, and post-tetanic potentiation. In addition, overexpression of *dARC1* does not alter synaptic transmission. Further, loss or overexpression of *dARC1* does not change the structural parameters of the third instar neuromuscular junction (NMJ). Finally, loss of *dARC1* results in no learning and memory defects in courtship conditioning, nor defects in circadian rhythm. These results indicate that in *Drosophila*, *dARC1* does not play a central role in synaptic transmission, nor mediates short- or long-term plasticity mechanisms.

Introduction

Synaptic plasticity can be divided into short-term and long-term components, depending upon the longevity of the plasticity trace. Short-term changes can occur *via* several mechanisms, including alterations in release probability, changes in postsynaptic receptor sensitivity, and alterations in Ca^{+} concentrations in the presynaptic terminal (Blitz et al., 2004). Long-term changes, however, can last for the lifetime of the organisms and requires the synthesis of new transcripts and proteins (Steward, 2002; Steward and Worley, 2002). These long-term alterations can be manifested in both changes in activity and structure (Bailey et al., 2004; Malenka and Bear, 2004). Understanding the mechanisms by which the brain works to form and modify memories may facilitate the development of treatments for learning deficiencies and diseased states such as Parkinson's and Alzheimer's diseases.

During the transition from short-term to long-term plasticity, the first round of transcription prior to the initial protein synthesis includes a large, heterogeneous group of genes known as immediate-early genes (IEG) (Lanahan and Worley, 1998). Activity-regulated cytoskeleton-associated protein (ARC) is one of these IEGs, originally identified as a gene highly upregulated in response to strong neuronal activity (Lyford et al., 1995).

Since its original identification, ARC has been shown to be regulated by a diverse number of neuronal stimuli. These include activation in response to seizure induction, brain-derived neurotrophic factor (BDNF), light, and cocaine

(Donai et al., 2003; Guzowski et al., 2000; Nedivi et al., 1996; Nishimura et al., 2003; Ying et al., 2002). In addition, immunohistochemical and *in situ* hybridization studies on the ARC transcript and protein have localized the ARC mRNA and protein to recently activated dendritic spines (Donai et al., 2003; Moga et al., 2004; Steward et al., 1998). Biochemical analysis suggests ARC associates with the actin cytoskeleton *in vitro* (Lyford et al., 1995). In cell culture studies, overexpression of ARC and CamKII (calmodulin-dependent kinase II) in neuroblastoma cells modulates neuritic outgrowth (Donai et al., 2003). These studies suggest ARC may mediate long-term synaptic changes by modifying the actin cytoskeleton in response to synaptic activation. When antisense DNA oligomers are used to disrupt ARC expression in hippocampal slices, the maintenance phase of long-term potentiation (LTP) is disrupted, without effects on induction. Further, intrahippocampal infusions of these interfering oligomers into mice can disrupt memory in spatial water maze tasks at 48hr without affecting the initial training or short-term memory (Guzowski et al., 2000). These findings suggest ARC plays a critical role in forming long-term memories in mice by modulating the actin cytoskeleton in activated postsynaptic dendrites. However, genetic loss-of-function studies have yet to be performed to verify these findings.

The genetic tractability of *Drosophila* makes it a unique system to study the *in vivo* roles of ARC. The large breadth of genetic tools allows both loss-of-function and gain-of-function studies to be done within a relatively short period of time. Previously, work in *Drosophila* has shown that the homolog of ARC,

dARC1, is upregulated in response to muscle dysfunction induced by hypercontraction mutations in *Myosin Heavy Chain* (*Mhc*) (Chapter 3). Expression analysis studies on *Mhc* revealed a potential actin-remodeling pathway in response to hypercontraction (Chapter 3). Many of the genes identified had been previously shown to associate with key structural support sites for the muscle actin cytoskeleton. In addition, BLAST analysis on a number of novel transcripts suggested a similar role in actin remodeling. Expression patterns of some of these genes showed differential expression in the muscle, suggesting a role in the biology of the muscle. Further, this transcriptional response included a subset of genes whose mammalian homologs have been shown to be regulated by neuronal activity. These include the *Drosophila* homologs of ARC, neurochondrin, and CPG2 (Lyford et al., 1995; Nedivi et al., 1996; Shinozaki et al., 1997). Work in mammalian muscle dysfunction models suggests that calcium plays a critical role in the pathogenesis of muscle disease (Frey et al., 2000; Gailly, 2002; Leinwand, 2001). These data suggest that both synaptic plasticity and muscle dysfunction may require a shared signaling pathway that activates the expression of genes involved in actin remodeling.

Here, we describe the characterization of a *dARC1* mutation in *Drosophila*. Using a P-element transposon located upstream of the open reading frame, we have generated loss-of-function mutations in *dARC1.* Further, we have created transgenic animals which overexpress the dARC1 protein in a spatially and temporally restricted manner, allowing us to analyze the gain-of-function consequences of dARC1 upregulation. The characterization of dARC1

suggests that it may play a role in subtle modifications of the synapse, but does not participate in essential roles which govern synaptic function and plasticity.

Results

Isolation of loss-of-function mutation in dARC1

We previously identified *CG12505* as a transcript that was highly upregulated in response to hypercontraction-induced myopathy caused by point mutations in the *Mhc* locus (Chapter 3). In parallel studies, we have also identified the *CG12505* transcript as a transcript upregulated in response to heat-induced neuronal activity in temperature-sensitive seizure mutants. Although *CG12505* seems to be regulated by heat shock protocols in wildtype flies, its induction is higher in the background of the activity mutants *seizure* and *slowpoke* (Figure 1). *CG12505* encodes a protein with homology to the mammalian gene ARC (activity-regulated cytoskeletal-associated protein; Figure 1). The homology consists of 23% identity and 40% similarity. In addition, the N-terminal 218 amino acids of the mouse ARC protein are not represented in the *Drosophila* gene *CG12505*. We have renamed this gene *dARC1*. The *dARC1* gene is situated within a complex locus containing three potential homologs of the mammalian ARC gene (Figure 1). *CG13941* and *CG10102* also show homology to the mammalian ARC gene, and we have named these *dARC2* and *dARC3*, respectively. However, *dARC3* (*CG10102*) has never been detected above the noise limit of any of the microarrays we have performed (unpublished data). In addition, no corresponding cDNAs have been isolated, suggesting that this gene may not be expressed and represents a partial open reading frame due

to the duplication of a portion of the *dARC1* gene. In order to facilitate the generation of a mutation in the *dARC1* locus, we obtained a P-element transposon insertion which was situated about 250 base pairs upstream of the *dARC1* coding region (Figure 1). To create a loss-of-function (lof) mutation, we utilized standard P-element excision screens to generate imprecise excision events detectable by PCR. In total, we isolated six viable lof mutations from our screen. The extent of these deletions as determined by PCR analysis is summarized (Figure 1). In addition, we isolated eight lethal mutations from the screen. Complementation testing revealed three complementation groups, with only one group which did not complement a deficiency that removes the *dARC1* locus. Further complementation testing revealed that the lethality within this group can be attributed to loss of the *Tfb1* locus (which resides upstream of *dARC1,* immediately downstream of *dARC2*), as they fail to complement a lethal P-element insertion within *Tfb1.*

In order to verify our six potential mutations, we utilized Northern analysis to assay whether deletions of *dARC1* corresponded to a loss of transcript. Sequence analysis of the deletions was complicated by the presence of the direct duplication within the genomic region (Figure 2). Indeed, the deletions removed *dARC1* transcript as assayed by Northern blot, confirming that we have isolated lof mutations in *dARC1.*

Next, we assayed whether these mutations removed dARC1 protein in adult flies. For this analysis, rabbit antisera was raised against a peptide corresponding to the N-terminal region of dARC1. The antisera was further

Figure 1

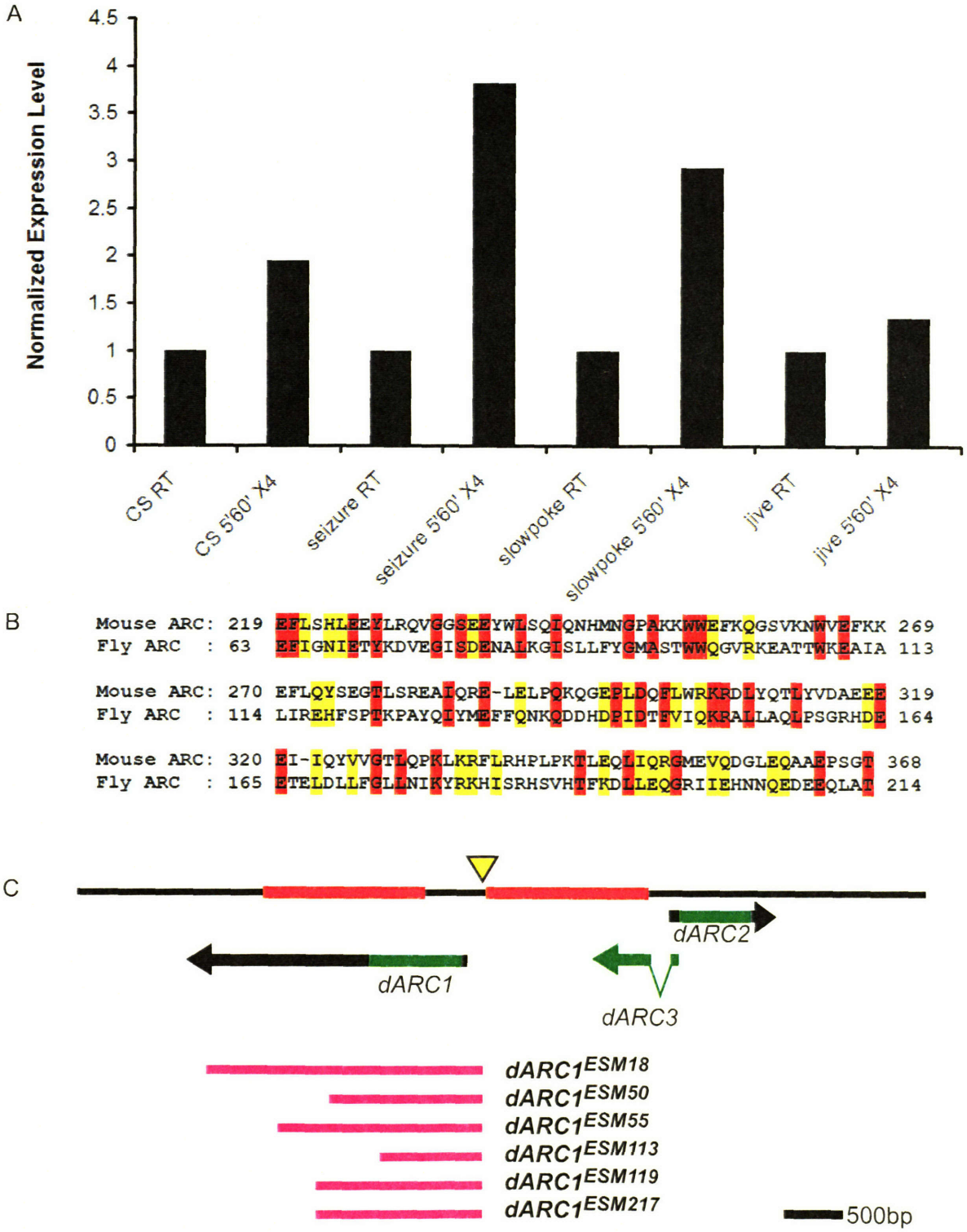

Figure 1: Identification and mutation of the *dARC1* locus (A) The *dARC1* gene was identified as a transcript upregulated in response to both heatshock and neuronal activity. Although the temperature shift induces *dARC1* expression in *CantonS*, the amount of induction in $seizure^{TS1}$ and $slowpoke^{TS1}$ is greater than heatshock alone. (B) The alignment between the mouse ARC and *dARC1* showing the amount of conservation between these homologs. Note that the homology begins only after the first 218 amino acids of ARC. (C) A schematic diagram of the *dARC* cluster in the *Drosophila* genome. Black arrows represent the mRNA while green represents the open reading frame. A yellow triangle marks the position of the P-element used to create a lof mutation in *dARC1*. The red blocks represent the sequence duplication. The pink bars show the extent of the deletions isolated as deduced by PCR analysis.

purified using affinity purification to either the peptide utilized in the antibody generation or full-length GST-fused recombinant dARC1 protein. Western blot analysis on whole fly extracts using affinity purified antibodies revealed loss of dARC1 protein in these six deletions, further confirming we have isolated six independent lof mutations in *dARC1* (Figure 2). For most of the following analysis, we used the *ESM18* deletion allele and the *ESM115* precise excision in our experiments unless otherwise indicated.

Localization of the dARC1 protein

Previously, we have shown that the *dARC1* transcript is expressed ubiquitously throughout late-stage embryos with differential expression within the body-wall muscles and central nervous system (CNS) (unpublished data). In order to determine the subcellular localization of dARC1 protein, we performed immunocytochemistry on third-intar larval preparations and adult brain dissections using antisera raised to the N-terminal region of dARC1 which was specific to dARC1 and not present within the coding regions of dARC2 and dARC3. Previous studies on the mammalian ARC protein have shown that ARC localizes to dendritic spines, within the region associated with actin-based structures (Lyford et al., 1995; Moga et al., 2004). In addition, ARC has been found to localize to actin-based structures in non-neuronal tissues (Maier et al., 2003). In third instar larvae, dARC1 protein was diffusely expressed in the cytoplasm at low levels throughout the body-wall muscles, in a large subset of

Figure 2

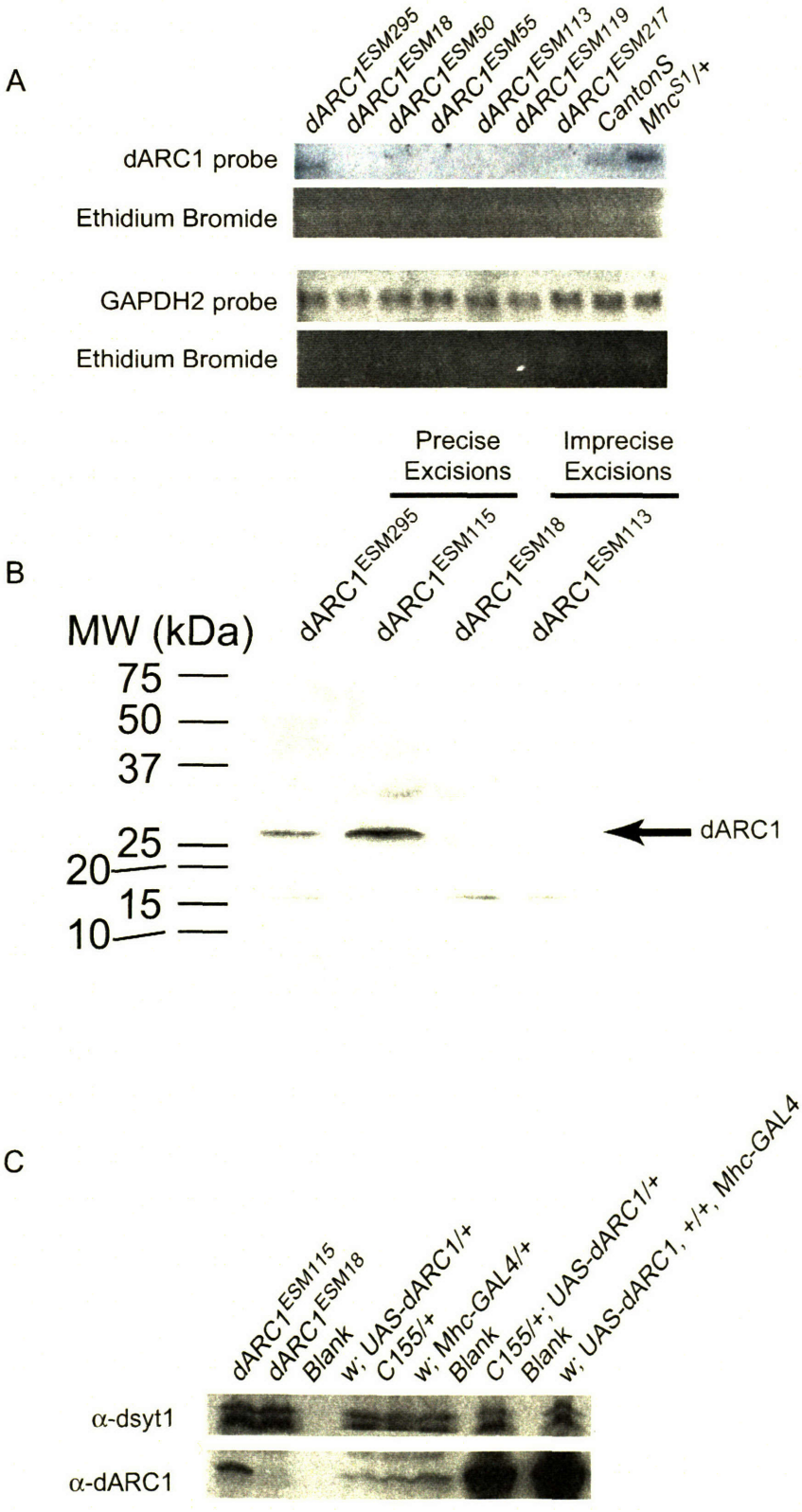

Figure 2: Verification of the *dARC1* mutation (A) Northern blot analysis confirms that the small deletions isolated in the P-element excision screen are lof mutations in the *dARC1* locus. Note the upregulation of *dARC1* transcript in Mhc^{S1}/+ as compared to *CantonS*. (B) Western blot analysis of two precise excisions as well as the largest and smallest deletions isolated in the screen. The predicted size of dARC1 is about 28kDA, which corresponds to the band that is missing in the mutant extracts. (C) Further confirmation of the mutation, as well as antibody specificity using a western blot. The 28kDa band that is absent in the mutant also shows upregulation in the transgenic overexpression lines.

unidentified neurons in the brain lobes and ventral ganglion, and in the epidermis (Figure 3).

To assay the subcellular localization of dARC1 under higher expression levels, we utilized overexpression constructs of dARC1 under the control of the yeast GAL4/UAS system (Phelps and Brand, 1998). Overexpression of dARC1 using the C155 driver, a brain-specific GAL4 expression construct, reveals localization of dARC1 to synaptic regions in the CNS and NMJs (Figure 3). When overexpressed in the muscle, dARC1 localized to structures resembling the contractile machinery in the sarcomere. However, in both overexpression conditions, substantial diffuse cytoplasmic staining was still observed throughout the cells. Therefore, the overexpression localization suggests that dARC1 may localize to synaptic regions and the actin cytoskeleton, consistent with the known localization of mammalian ARC to dendritic spines and the actin cytoskeleton.

Electrophysiological analysis of the dARC1^{ESM18} *mutant*

Previous studies in mammals have focused predominantly on the regulation of ARC transcript and protein. These studies have shown that in response to synaptic activity, ARC transcript localizes to the activated dendrite within 30 minutes of activation in response to light. In addition, ARC protein accumulates within these dendrites in a similar time-frame (Moga et al., 2004). These studies suggest that ARC may function to modify synapses in an activity-dependent manner by altering the cytoskeleton in the dendritic spines. However,

Figure 3

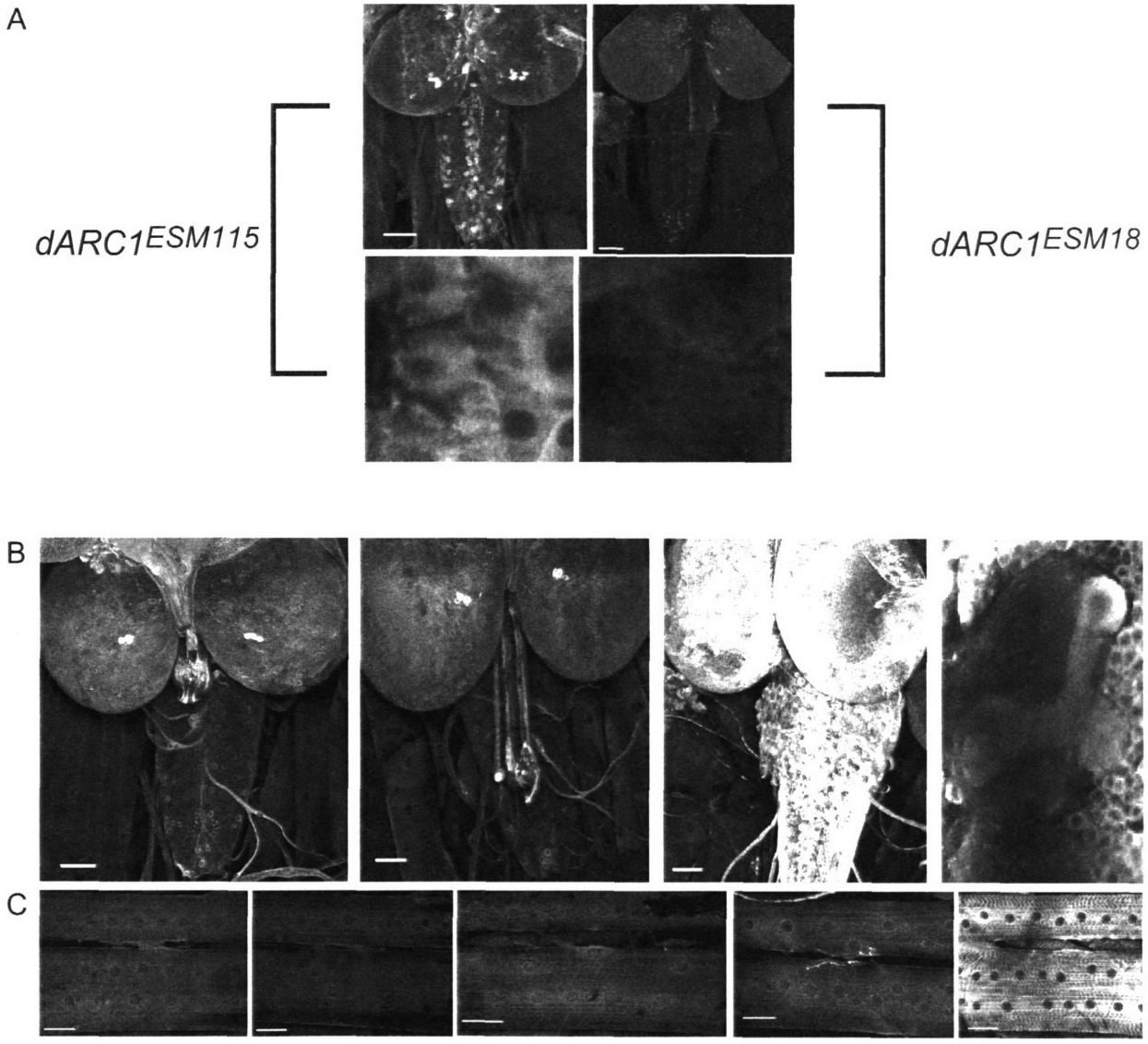

Figure 3: Localization of dARC1 (A) The localization of dARC1 *in vivo* shows expression in a subset of neurons in the central brain lobes and ventral ganglion in the brain lobes that goes away in the *dARC1*^{ESM18} mutant. Note the staining in the synaptic region of the visual system. In addition, diffuse staining in the muscle as well as in epithelial cells is absent in the mutant when compared with the precise excision. (B) Overexpression of *dARC1* can lead to dARC1 expression throughout the brain, with staining in the synaptic region of the mushroom body. Genotypes shown are (l-r) *w;UAS-dARC1/+*, *C155/+*, and *C155/w; UAS-dARC1/+*. Note the mushroom body staining in the far right panel. (C) Overexpression localization in the muscle and motor neuron in the body wall muscles 6/7. Genotypes shown are (l-r) *w;UAS-dARC1/+*, *C155/+*, *w; Mhc-GAL4/+*, *C155/w; UAS-dARC1/+*, and *w; Mhc-GAL4/UAS-dARC1*. Note that CNS overexpression can lead to staining in at the NMJ. Scale bars 50μm.

genetic loss-of-function studies of ARC in synaptic modification have yet to be performed. Using the lof mutation, *dARC1*^{ESM18}, we assayed the physiological consequences of loss of dARC1 function at the third instar NMJ. Although the regulation suggests that dARC1 may mediate long-term synaptic modification, we utilized physiological analyses to determine if loss of dARC1 alters synaptic function on several time-scales. We reasoned that dARC1 may play a role in developmental plasticity, as synaptic maturation occurs in an activity-dependent manner throughout development of *Drosophila*. Loss of dARC1 may, therefore, lead to alterations of the structure or function of the synapse due to chronic defects over the course of development.

First, we analyzed the effect of lof dARC1 on spontaneous miniature excitatory junctional potentials (mEJP). Given the localization and regulation of ARC in mammals, ARC may play a role in modifying the density of glutamate receptors in the postsynaptic membrane. For this analysis, we recorded mEJPs from CNS-intact third instar larvae in the presence of 1.5mM $[Ca^{2+}]_{ext}$ and 3μM TTX. No statistical differences were found in mEJP amplitude between control and *dARC1*^{ESM18} larvae (KS-test p-value > 0.05; Figure 4). In addition, overexpression of dARC1 in either the muscle or the CNS did not reveal differences in the amplitude of mEJPs, suggesting that dARC1 does not play a role in regulating the density of glutamate receptors at third instar NMJs (KS-test p-values > 0.05).

Next, we assayed whether dARC1 plays a role in basal synaptic transmission. For this analysis, we measured excitatory junctional potentials

Figure 4

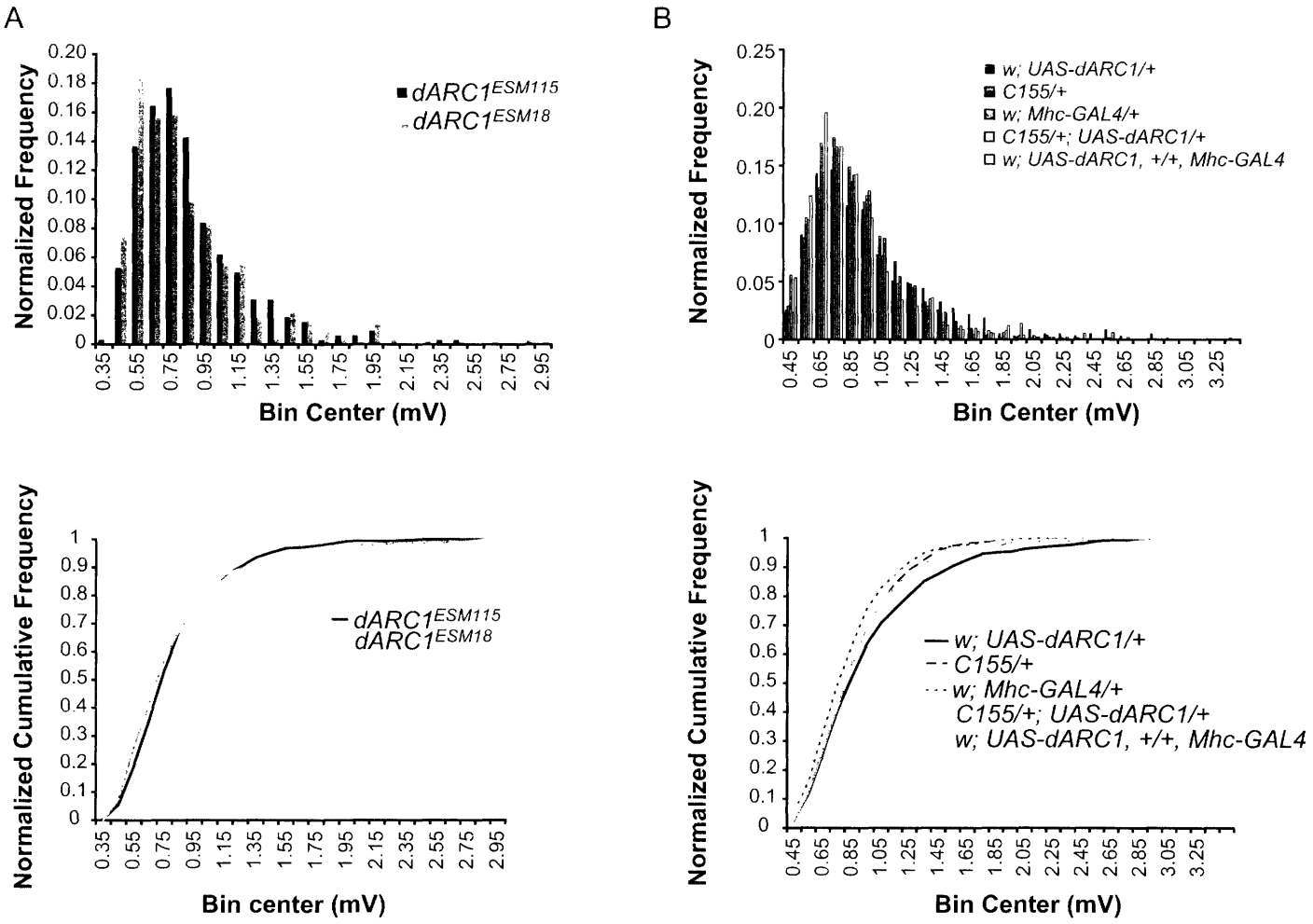

Figure 4: mEJP analysis of the *dARC1* mutant and overexpression shows no change in mEJP amplitude (A) Normalized miniature histogram of mEJP events recorded in the precise excision and $dARC1^{ESM18}$ flies shows no change in mEJP amplitude (top). The same data is represented as a cumulative histogram (bottom). (B) Normalized miniature histogram of mEJP events recorded from flies overexpressing dARC1 in either the CNS or the muscle shows no change in mEJP amplitude (top). The same data is represented as a cumulative histogram (bottom).

(EJP) in the presence of varying levels of external [Ca^{2+}] (0.1mM, 0.2mM, 0.4mM and 1.5mM). For the high Ca^{2+} condition, we increased the Mg^{2+} concentration from 4mM to 20mM, as a single action potential was often sufficient to illicit a contraction event in the muscle, perturbing the electrophysiological recording. Loss of dARC1 did not change the amplitude of EJPs, suggesting that dARC1 does not play a role in basal synaptic transmission (Student's t-test p-values > 0.05; Figure 5, Supplementary Tables S3 and S4). Furthermore, overexpression of dARC1 in either the muscle or the CNS does not alter EJP amplitude, confirming that dARC1 does not play an integral role in synaptic transmission (ANOVA p-values > 0.05; Figure 6).

We then assayed whether dARC1 plays a role in vesicular trafficking during high-frequency stimulation. Vesicular trafficking is known to be an actin-dependent process (Bader et al., 2004). Alterations in presynaptic actin dynamics can be seen by changes in the ability of the synapse to recycle synaptic vesicles under high calcium, high-frequency stimulation conditions. For this analysis, we used 1.5mM Ca^{2+} and 20mM Mg^{2+} to prevent the muscle from contracting under high Ca^{2+} conditions. No differences were found between control and mutant larvae, as both mutant and control larvae released about 30% less than baseline after five minutes of 10 Hz stimulation. These data suggest that dARC1 does not play a role in synaptic vesicle trafficking (Figure 5).

Our findings suggest dARC1 does not play an essential role in basal synaptic transmission, though it may function in mature synapses to mediate long-term plasticity mechanisms. In order to address activity-dependent

Figure 5

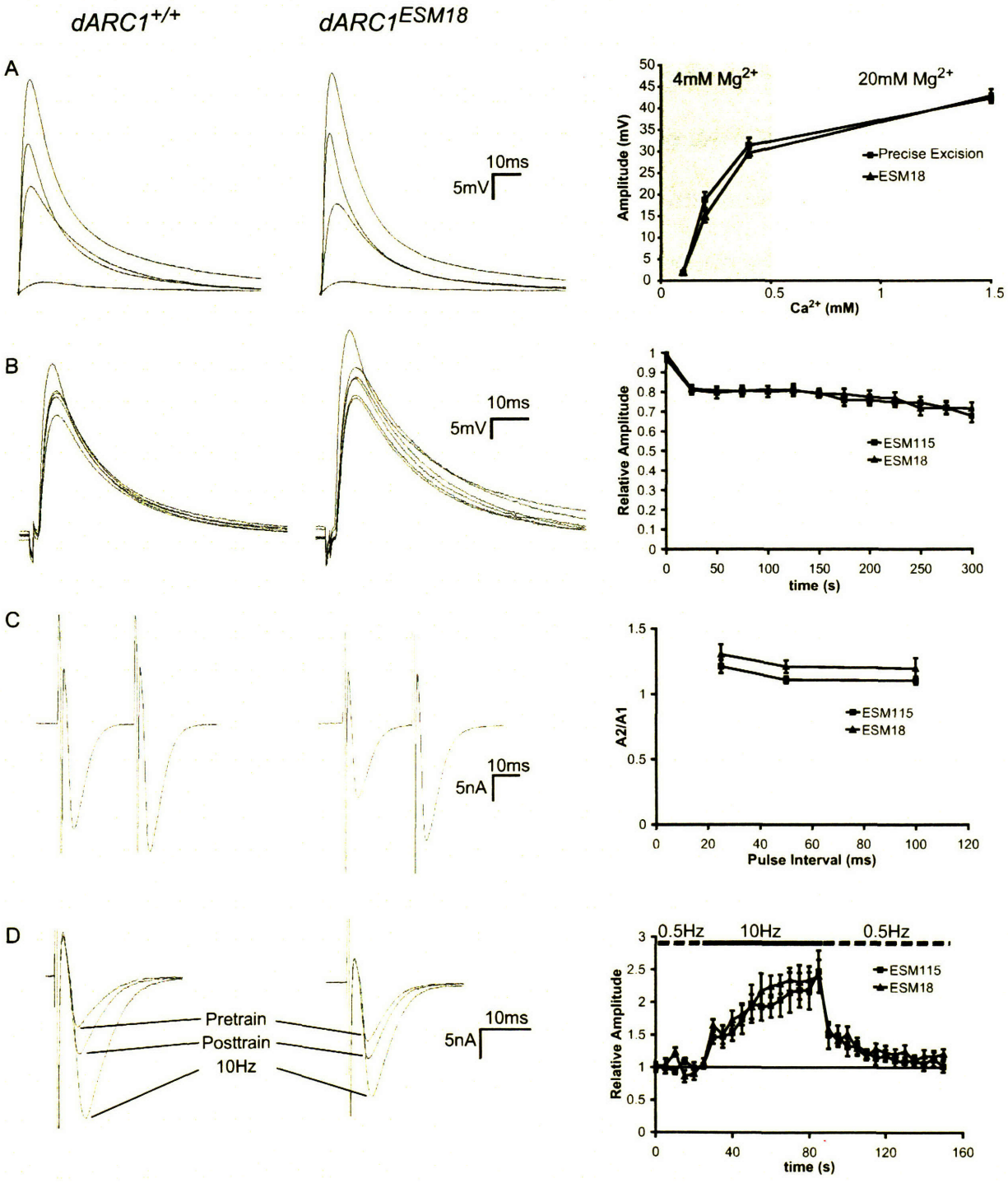

Figure 5: Electrophysiological analysis of the *dARC1* mutant Electrophysiological analysis shows no change in (A) basal synaptic transmission, (B) high-frequency dependent vesicle recycling, (C) paired-pulse facilitation, and (D) post-tetanic potentiation. Data shown for each of these analyses include (l-r) traces from a precise excision, the $dARC1^{ESM18}$ mutant, and quantification of the results. Scale bars 10ms, 5mV as shown. (A) Overlayed are the averaged traces from ten events in a single muscle at each of the Ca^{2+} concentrations. (B) Traces from a single muscle are overlayed from the time points t=0, 60s, 120s, 180s, 240s, and 300s. (C) Traces shown are the average of ten events recorded from a single muscle with a 25ms delay between stimuli. (D) Traces shown are from a single muscle. Pretrain is an average of the 10 events prior to the 10Hz stimulation. 10Hz is the average of the last 10 events at high-frequency. Posttrain is the average of the 10 events immediately following the high-frequency stimulation.

Figure 6

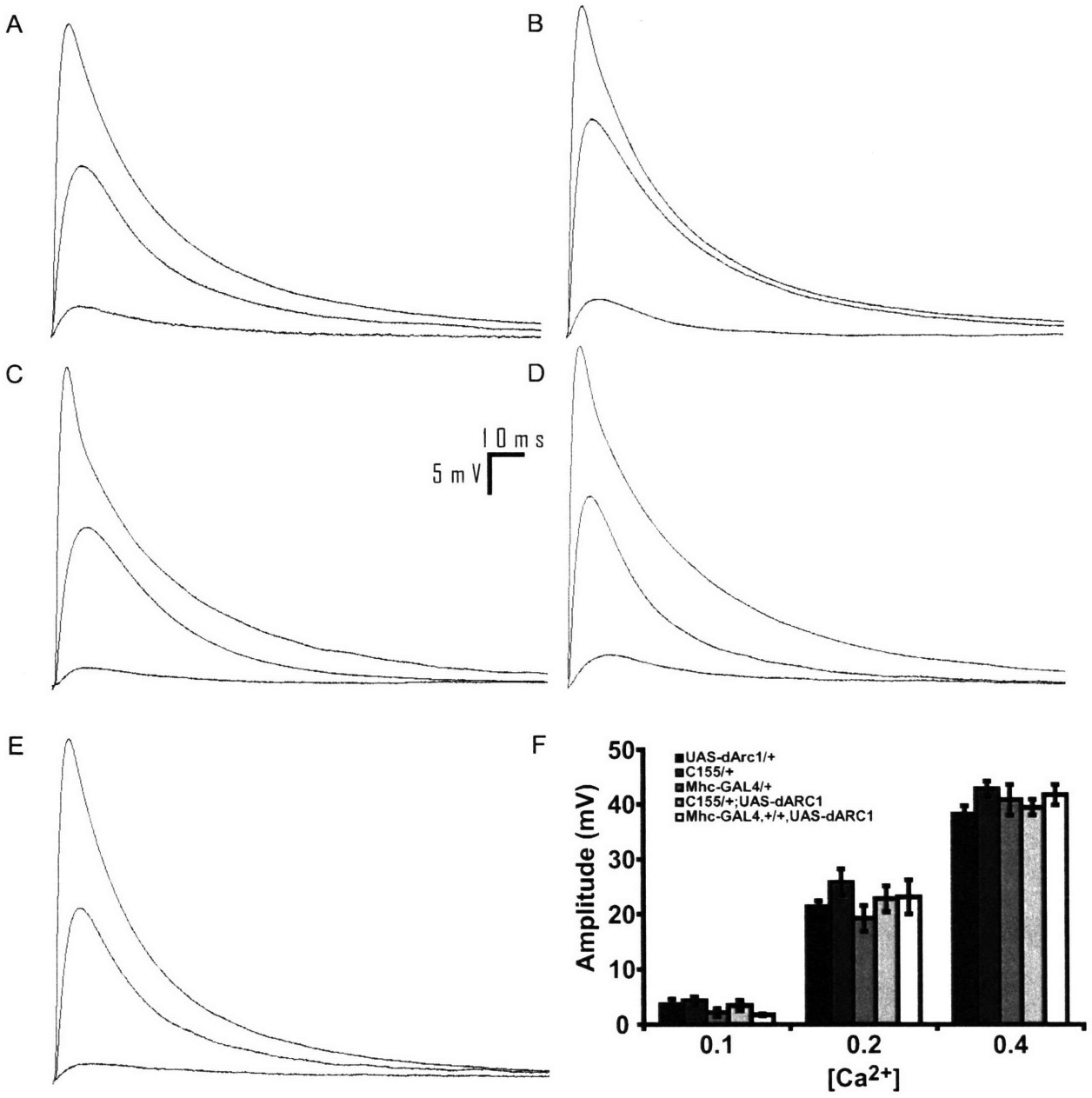

Figure 6: Overexpression of *dARC1* does not alter basal synaptic transmission The EJP amplitude was measured at 0.1mM, 0.2mM, and 0.4mM Ca^{2+} to assay the effect of overexpression of *dARC1* in synaptic transmission. Genotypes assayed are (A) *w;UAS-dARC1/+*, (B) *C155/+*, (C) *w; Mhc-GAL4/+,* (D) *C155/w; UAS-dARC1/+*, and (E) *w; Mhc-GAL4/UAS-dARC1*. (F) Quantification of the EJP amplitude data in the overexpression study. (A-E) Averaged traces from ten events in a single muscle at each of the Ca^{2+} concentrations are overlayed.

mechanisms, we analyzed mutant larvae for alterations in two forms of plasticity. The first, paired-pulse facilitation has been shown to occur on the timescale of milliseconds. In this paradigm, two action potentials are stimulated within a defined interval. During close succession intervals, the second release event is normally larger than the first under low calcium conditions. The second, post-tetanic potentiation, occurs on the timescale of minutes. This paradigm involves low-frequency test (0.5Hz) stimulation, followed by high-frequency stimulation (10Hz), and then resumes baseline stimulation (0.5Hz). After high-frequency stimulation, low-frequency release events remain larger than the test stimulation for one to two minutes (Bogdanik et al., 2004). Like paired-pulse facilitation, this form of plasticity is seen under low calcium conditions and is likely to be dependent upon residual Ca^{2+} effects (Zucker and Regehr, 2002).

For the paired-pulse facilitation paradigms *dARC1*^{ESM18} did not show any differences from control larvae, suggesting that dARC1 does not play a significant role in this form of short-term plasticity (A_2/A_1 for 25ms: *ESM18* 1.30 $\pm$ 0.08mV *ESM115* 1.21 $\pm$ 0.05mV; p-value > 0.05) (Figure 5). During post-tetanic potentiation, both mutant and control animals showed over a 2-fold facilitation during the high-frequency stimulation, and a 130% potentiation which slowly decayed over one minute. These two short-term plasticity protocols are likely due to residual intracellular calcium and mGLUR activity (post-tetanic potentiation), rather than being mediated by long-term synaptic modification mechanisms (Bogdanik et al., 2004; Zucker and Regehr, 2002).

The electrophysiological data we have presented suggests that dARC1 does not perform an integral role in basal synaptic transmission, nor short-term plasticity mechanisms at the *Drosophila* third instar neuromuscular junction. Alternatively, dARC1 may modulate these processes, but the subtlety with which it acts may not be accessible in this preparation. This could be due to the inherent stability of neuromuscular transmission, which has a much higher safety factor than central mammalian synapses. Further, homeostatic mechanisms may counteract the alterations due to loss of dARC1 to restore the functionality of the synapse. In addition, there have not been protocols described for the *Drosophila* neuromuscular junction with which we can assay long-term synaptic modification with similar time-scales as what is predicted for the activity-dependent regulation of dARC1 protein

.

Synaptic structure analysis of dARC1^{ESM18}

Although dARC1 may not play a role in synaptic transmission, it could function in altering the structural properties of the synapse by modulation of the underlying actin cytoskeleton. The development of *Drosophila* neuromuscular junctions is highly reproducible between samples, allowing reliable quantification of changes in the number of boutons at third instar NMJs. In order to assay the role of dARC1 in the structural morphology of synapses, we quantified the number of boutons of the muscle 6/7 NMJ in segment A3. For this analysis, we used α-synaptotagmin 1 (syt1) to label and visualize synapses. Compared with

controls, no statistical differences were found in the number of boutons at the synapse (*dARC1*^{ESM295} 71.6± 4.0, *dARC1*^{ESM18} 72.7 ± 5.4 boutons, Student's t-test p-value > 0.05; Figure 7). In mammalian synapses, ARC is upregulated in response to activity. It may be that ARC plays a role in modifying the structural parameters of synapses after maturation at higher levels of expression. In order to test this, we overexpressed dARC1 presynaptically in the CNS and postsynaptically in the muscle, and assayed for changes in bouton number. As the case for loss of dARC1 function, no significant changes were found when overexpressed in the nervous system (ANOVA p-value > 0.05). However, when overexpressed in the muscle, the control line, w; *Mhc-GAL4/+* had significantly reduced bouton number than w; *UAS-dARC1/+* and *w; Mhc-GAL4,+/+, UAS-dARC1* (Tukey-test p-value < 0.05). This reduction is subtle and may not have biological significance, as the overexpression larvae are not statistically different from the *w; UAS-dARC1/+* larvae (*w; UAS-dARC1* 107.4 ± 4.7; *C155/+*100.9 ± 3.5; *w; Mhc-GAL4/+* 90.3 ± 2.8; *C155/+; UAS-dARC1/+* 107.3 ± 3.5; *w; Mhc-GAL4,+/+, UAS-dARC1* 105.4 ± 5.2; Figure 7).

The structural data suggests that dARC1 does not function in modifying synaptic structure at the *Drosophila* NMJ. Multiple homeostatic mechanisms may play a role in compensation for loss of dARC1. In addition, the lof and overexpression of dARC1 in our experiments occur constitutively throughout development. Synaptic modification may be more sensitive to acute changes in levels of dARC1. Inducible loss and overexpression of dARC1 with more precise

Figure 7

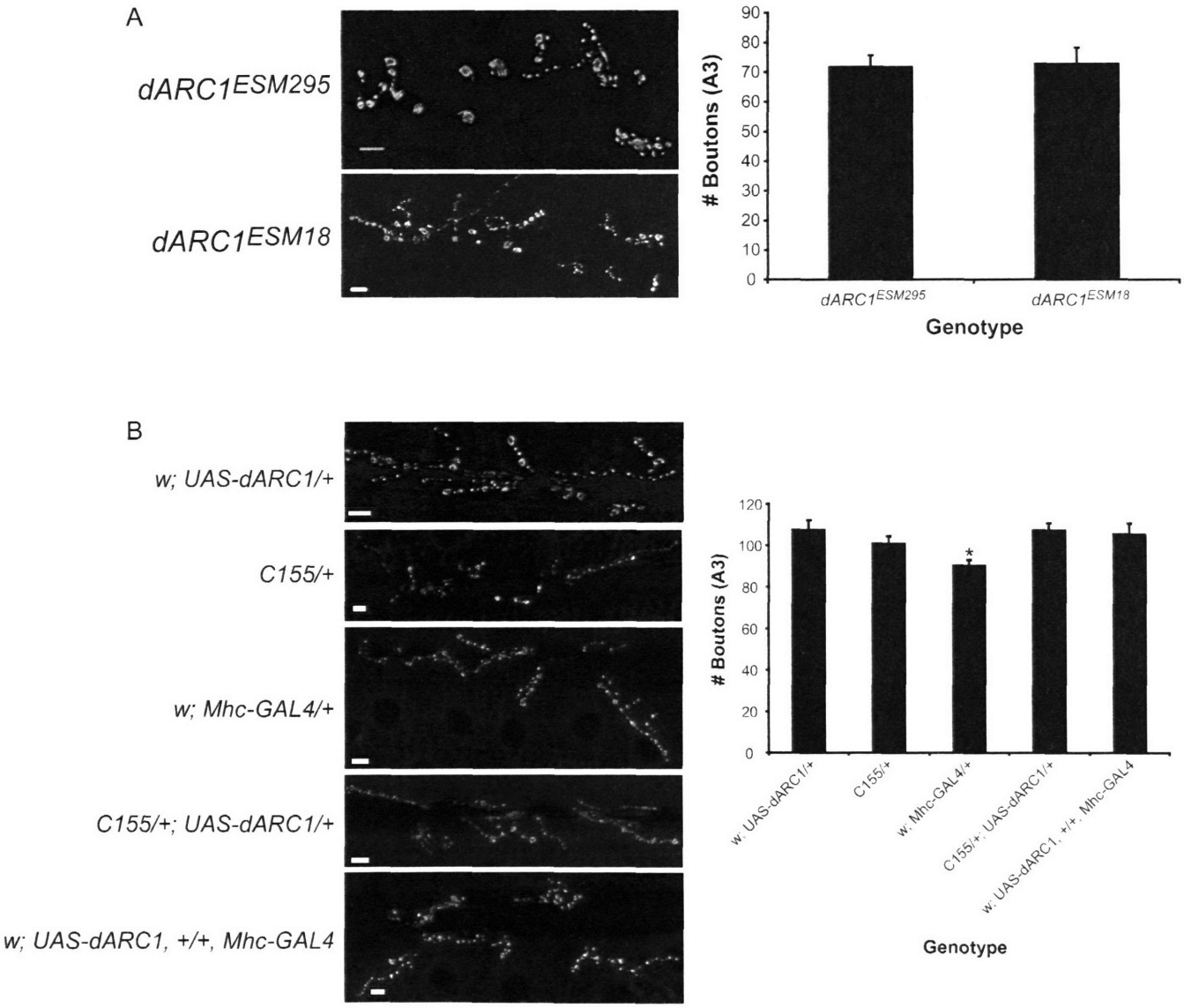

Figure 7: Structural analysis of third instar neuromuscular junctions at the body wall muscles 6/7 in *dARC1* mutant and overexpression larvae

Synaptic structure was visualized using α-sytI antisera, which labels synaptic vesicles in the presynaptic terminals. All boutons were counted under a 40X/1.2NA oil immersion lens. (A) Comparisons between $dARC1^{ESM295}$ precise excision larve to $dARC1^{ESM18}$ mutant larvae show no difference in bouton number (graphed at right). (B) Likewise, overexpression of *dARC1* does not have significant effects on bouton number at the third instar muscle 6/7neuromuscular junction (graphed at right). Scale bars 10μm.

temporal control may be required to examine acute roles for ARC in synaptic physiology.

Behavioral analysis of dARC1

The electrophysiological and structural analysis did not show large differences in synaptic properties between *dARC1*^{ESM18} and control animals. In addition, overexpression of dARC1 did not show significant differences. However, these assays may not be sensitive enough to detect subtle alterations in synaptic function mediated by *dARC1*. To address this issue, we studied two aspects of the behavioral output of *dARC1*^{ESM18} flies.

Male courtship behavior can used to assay learning and memory in *Drosophila*. The behavior is highly stereotypical, with chemical, tactile, auditory, and visual cues required for plasticity in the males (Hall, 1994). Although this behavior is stereotypical, males are conducive to cues which control whether initiation of courtship occurs. This gating of the courtship behavior is mediated by an unknown aversive cue which decreases the probability of mating initiation by the male fly (Tompkins et al., 1983). It is hypothesized that males that have been in contact with mated females are exposed to non-visual aversive cues, thus becoming conditioned to decrease mating initiation (Joiner MI and Griffith, 1997). Utilizing this behavioral paradigm, we assessed the ability of *dARC1*^{ESM18} flies in memory formation and consolidation of mating behavior.

The mating behavior is quantified as a courtship index (CI) ratio. CI represents the fraction of time a male spends in courtship behavior over a 10 minute observation period. The ratio of CI_{test}:CI_{sham} provides a quantitative measure of behavioral modification due to training (sham males are placed in the mating chamber without a female trainer). Thus, if no modification of behavior occurs during training, then the CI ratio is equal to 1. In addition, all testing of trained and sham controls were done with decapitated females in order to reduce variations due to female rejection behaviors. Both *dARC1*^{ESM115} and *dARC1*^{ESM18} males trained on mated females showed a decrease in courtship when subsequently exposed to mature virgin females, suggesting *dARC1* does not play a significant role in initial learning of mating behavior modification. In addition, both wildtype and *dARC1*^{ESM18} showed indistinguishable decay in memory at ten minutes and two hours after training, suggesting that *dARC1* does not play a significant role in short-term or long-term memory of mating behavior learning (Figure 8).

The circadian behavior of *Drosophila* is mediated by an endogenous clock used for predicting daily changes in the environment. Though sensitive to exogenous cues such as light, the pacemaking clock can maintain rhythmicity under controlled conditions which provide no external indications of time (Allada et al., 2001). Since 1971, genetic analysis of the *Drosophila* circadian clock has provided a robust system in which to study the circadian clock of an organism, allowing the identification of genes which alter the clock on the order of 20% or less, a magnitude of change few behavioral assays can distinguish (Konopka

Figure 8

A

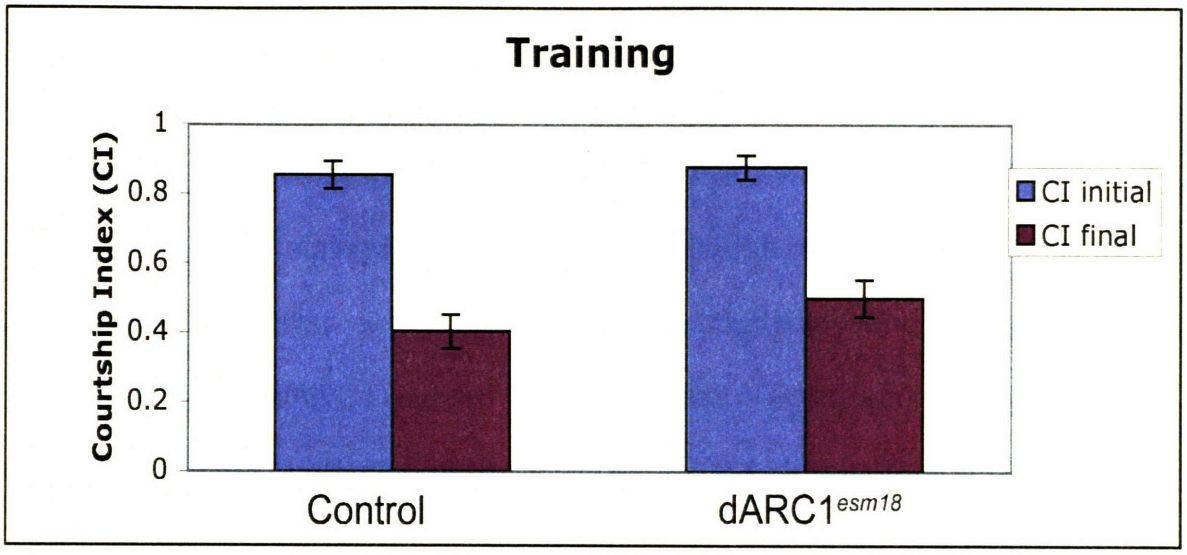

B

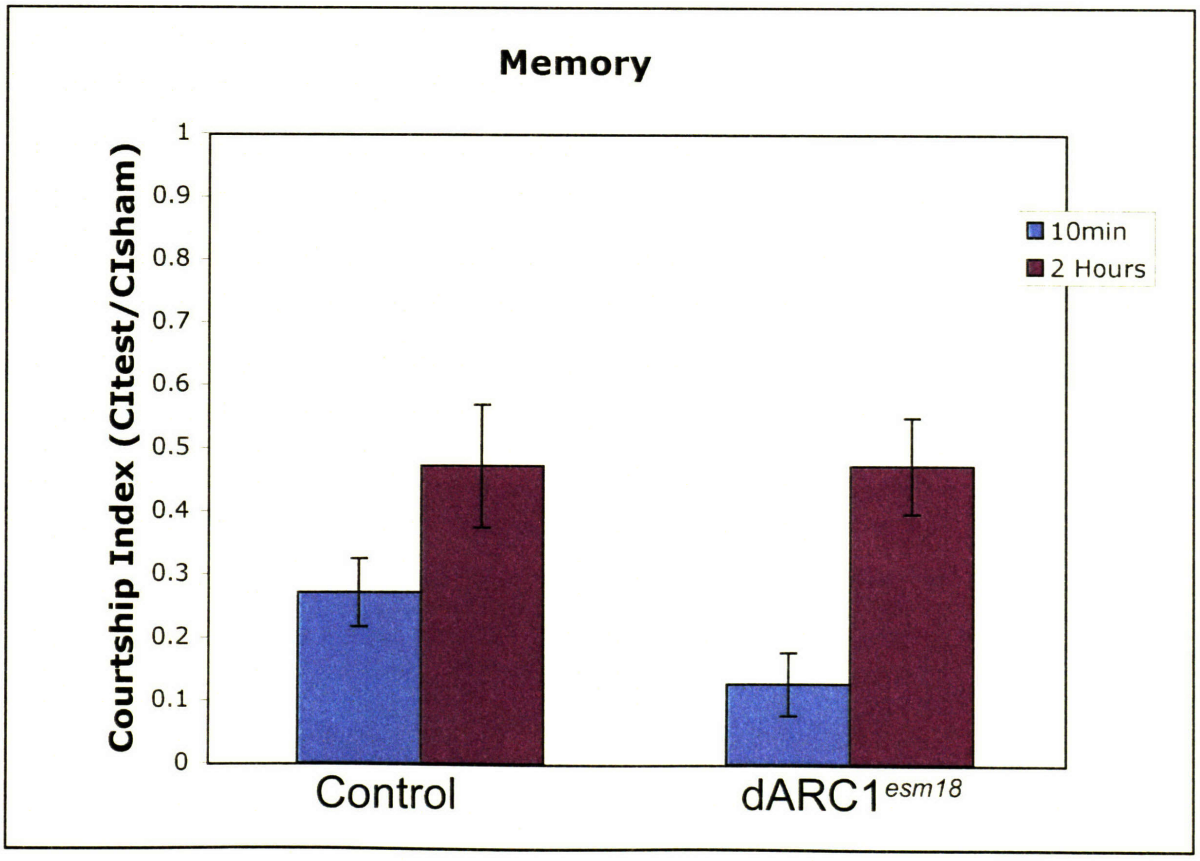

Figure 8: Courtship conditioning is not affected in *dARC1* mutants The *dARC1* mutants were assayed for potential defects in learning and memory using courtship conditioning. The courtship index (CI) represents the fraction of time in a 10 minute test period that a male spends in mating behavior. Memory is expressed as the ratio of the CI of males trained to a mated female to the CI of sham males. (A) Training of males to mated females decreased the CI of both genotypes to a similar extent, indicating that courtship conditioning remains unchanged in a lof *dARC1* mutant. (B) Short-term (10min) and long-term (2hrs) memory is likewise unaffected during loss of *dARC1* function.

and Benzer, 1971). Using the locomotor activity as a read-out of circadian rhythm, we assayed the role of *dARC1* in maintenance of a stable, 24 hour periodicity in *Drosophila*.

Wiltype and $dARC1^{ESM18}$ flies were trained on a light-dark (LD) cycle before being placed into a constant dark (DD) cycle. Automated tracking of the locomotor activity continued for 13 days in DD. Normally, *Drosophila* exhibits an anticipation to both the L-D and D-D transition by steady increases in locomotory activity (Suri et al., 2000). Both $dARC1^{ESM115}$ and $dARC1^{ESM18}$ showed normal anticipation of these transitions when kept in DD for 13 days, indicating no defects in the normal functioning of the internal clock. In addition, $dARC1^{ESM18}$ did not show a skew in the activity plots over time, indicating that the functioning clock did not have an alteration of the periodicity. Finally, analysis of the overall locomotory activity showed that $dARC1^{ESM18}$ does not change general locomotory activity in *Drosophila* (Figure 9). These data indicate that *dARC1* does not play an integral role in circadian rhythm function or maintenance. In addition, loss of *dARC1* does not result in overall changes in locomotory activity.

Figure 9

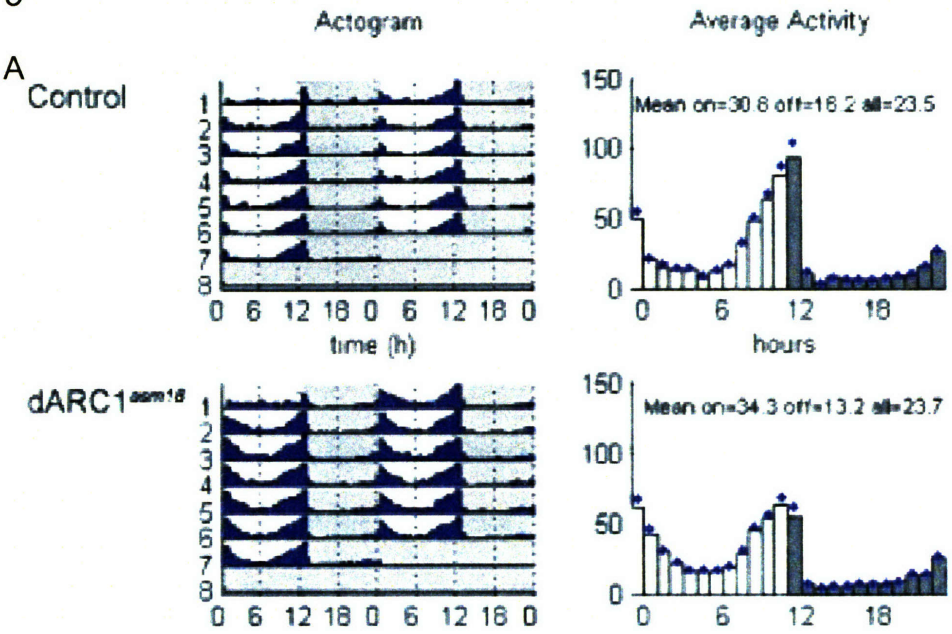

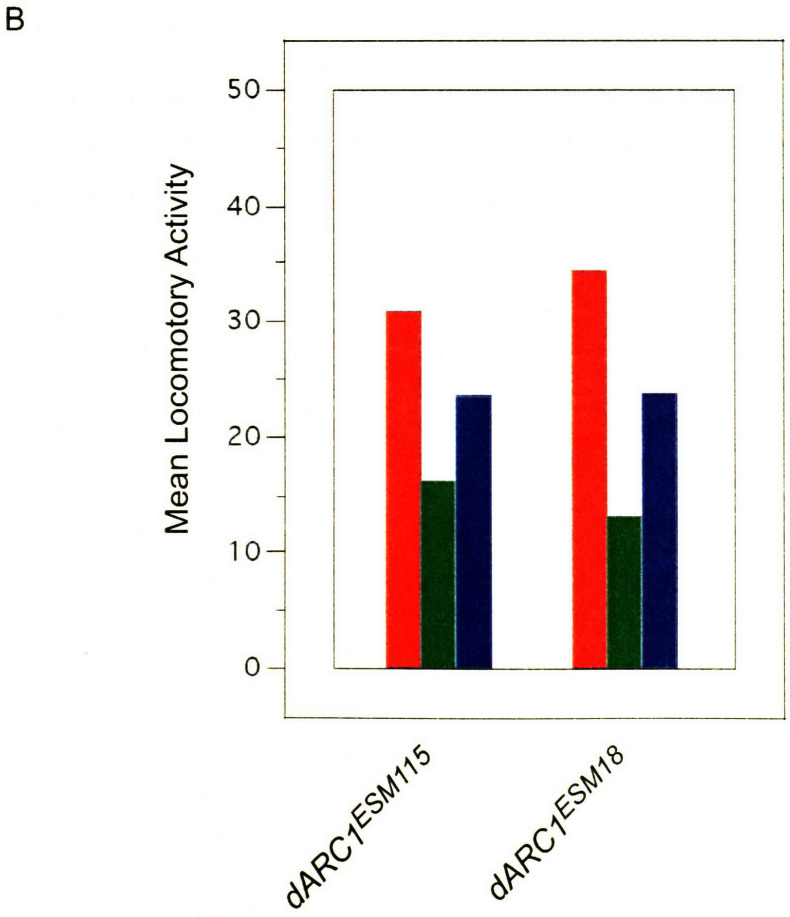

Figure 9: Loss of *dARC1* results in no change to the circadian rhythm in *Drosophila* Mutant *dARC1* flies were assayed for changes in circadian clock function through measurement of overall locomotor activity. (A) Daily locomotor activity for *dARC1* mutants trained on LD cycles did not show significant changes in clock perpetuation when shifted to DD. (left) Sample locomotor activity for the indicated genotype over the 13 day test period and (right) the average of the daily activity for the genotype is shown. (B) Overall locomotion is also unchanged for $dARC1^{ESM18}$ flies, indicating that dARC1 does not play a role in overall regulation of locomotion. Shown in the graph are mean locomotory activity for Light hours (Red), Dark hours (Green) and overall average (Blue).

Discussion

The *dARC1* gene is one of two homologs of the mammalian activity-regulated cytoskeleton associated gene ARC. We identified *dARC1* in two independent expression analyses showing that *dARC1* transcription can be upregulated in response to heat, central nervous system activity, and hypercontraction-induced myopathy. In mammals, studies have shown that ARC is regulated by neuronal activity (Lyford et al., 1995; Moga et al., 2004; Nedivi et al., 1996; Nishimura et al., 2003; Steward et al., 1998; Tan et al., 2000). The ARC mRNA and proteins localize to activated synapses within actin-rich domains of postsynaptic dendritic spines (Lyford et al., 1995; Moga et al., 2004; Steward et al., 1998). In addition, knock-down of ARC using antisense deoxynucleotide oligomers leads to defects in LTP maintenance, correlating with a loss of long-term memory consolidation in a spatial water maze (Guzowski et al., 2000). However, genetic lof studies on the mammalian ARC have yet to be performed.

dARC1 *is not required for synaptic transmission, short-term plasticity, courtship modification and memory, and circadian rhythms*

Although the role of ARC has been implicated in long-term memory consolidation, we assayed the role of *dARC1* in the *Drosophila* CNS across multiple levels, given that this is the first genetic lof study of ARC function. Our studies indicate that dARC1 does not perform an integral role in synaptic

transmission, short-term plasticity, and synaptic structure at the third instar neuromuscular junction. However, the large safety factor of the neuromuscular junction may obscure subtle alterations mediated by dARC1. In addition, synaptic roles of dARC1 at other synapses have not been assayed. Further, compensatory mechanisms may alleviate defects which occur due to loss of dARC1 function at the synapse. Indeed, the effects of these homeostatic mechanisms have been observed in maintaining proper function at the *Drosophila* neuromuscular junction (Daniels et al., 2004; Davis et al., 1998; Davis and Goodman, 1998a; Davis and Goodman, 1998b; Davis et al., 1996; Paradis et al., 2001; Schuster et al., 1996a; Schuster et al., 1996b).

The behavioral analysis further supports the hypothesis that *dARC1* does not play a significant role in synaptic plasticity, as two complex behaviors are not affected by loss of *dARC1*. However, *dARC1* may play a more modulatory role in these processes, rather than a central role in the overall behaviors. Recent work in courtship behavior has demonstrated metaplasticity mechanisms may mediate the consolidation of memories in the context of multiple related experiences (Ejima et al., 2005). It remains a distinct possibility that *dARC1* mediates long-term memory consolidation when presented with multiple related experiences, rather than underlying the memory consolidation process directly.

Conflicting evidence for the role of mammalian ARC and dARC1

This data presents a direct conflict with the roles proposed for the mammalian ARC gene. Several reasons may account for this discrepancy. First, the *Drosophila* genome encodes two homologs of the mammalian ARC gene. This may lead to functional replacement/redundancy issues when analyzing the single loss of *dARC1*. In the absence of *dARC1*, *dARC2* expression may be sufficient to compensate for defects associated with *dARC1*. Further, our analysis has been performed on genetic lof mutations in *dARC1*, whereas the mammalian studies have been done using interfering dexoynucleotide oligomers (Guzowski et al., 2000). There may be differences in defects associated with acute versus chronic loss of ARC function at synapses. It may be that genetic loss of *dARC1* stimulates homeostatic compensatory mechanisms which can functionally replace the roles mediated by *dARC1.* Studies using conditional loss of *dARC1* may help in determining whether this occurs *in vivo.*

Understanding the molecular pathways which underlie the learning and memory process may facilitate the development of therapeutic treatments towards learning deficiencies and diseased states. The mammalian gene ARC has been implicated in the process of long-term memory consolidation. Based on the mammalian data, loss of *dARC1* should result in long-term memory defects without effect on synaptic transmission, short-term plasticity, or initial learning and short-term memory. However, our data suggest that the *Drosophila* homolog, *dARC1* does not play a role in synaptic structure and function, courtship learning and memory, and circadian rhythms. Future studies on

dARC1 and *dARC2* will help in determining whether these proteins modulate the memory formation and consolidation process through metaplastic mechanisms. In addition, studies in sensitized backgrounds such as temperature-sensitive activity mutants may reveal subtle modulation mediated by dARC1. Finally, studies of *dARC1* mutants in the role of muscle remodeling in *Drosophila* may yield insights into the cellular functions mediated by dARC1.

Materials and methods

Fly strains and crosses

Flies were cultured on standard medium at 22°C. All crosses using appropriate genotypes were cultured at 25°C. The P-element strain *w[1118]; P{w[+mGT]=GT1}BG01371* was obtained from the Bloomington fly stock center. The excision of the P-element was done using a standard F_3 P-element excision screen. PCR analysis was done using primers obtained from IDT DNA Technologies (sequences can be obtained upon request). The overexpression lines were made by cloning the *dARC1* open reading frame into the pUAST vector. The transgenic flies were generated at Genetic Services, Inc. (Cambridge, MA).

Microarray analysis

The expression of *dARC1* was assayed using protocols previously described (unpublished data). The experiment was done using *CantonS*, *seizure*^{TS1}, *slowpoke*^{TS1}, and *sesB*^{jive} (Elkins et al., 1986; Jackson et al., 1985; Rikhy et al., 2003). The transcriptional profile of *CantonS* and TS mutants were obtained from flies raised both at room temperature and treated with four 5min heat shocks separated by 60min rest periods. The labeled RNA was processed in the MIT Cancer Center Biopolymers Lab and data obtained processed using the Affymetrix Micoarray Suite software v5.0.

Cloning of dARC1 for creating transgenic flies and protein purification

Primers consisting of the first and final 30bp of the *dARC1* open reading frame were used to clone the coding region of *dARC1* from the cDNA libraries obtained from the microarray analysis in the *Mhc* mutants (unpublished data). Sequences corresponding to the restriction sites BamHI/SalI and XhoI/XbaI were used to clone the sequence in frame to GST into the pGEX-4T vector (Pharmacia) and the pUAST vector, respectively. Restriction enzymes were obtained from New England BioLabs.

Northern and Western blot analyis

Total RNA was isolated from wildtype and $dARC1^{ESM18}$ flies using Trizol (GibcoBRL). 50 flies were homogenized in1ml of Trizol in 10flies/100μl sample sizes. Total RNA was isolated using the manufacturer's suggested protocol. The northern blot analysis and probe was done using the manufacture's protocol accompanying the NEB Phototope Kit (New England BioLabs). The template used for making the biotinylated probe was a PCR product obtained from amplifying the 5' end of the *dARC1* coding sequence which is specific to *dARC1* and is not included in the duplication sequence.

Western blot analysis was done using standard procedures (Adolfsen and Littleton, 2001). Affinity purified α-dARC1 was used at 1:1000.

Protein and antibody purification

dARC1 protein was purified using methods previously described (Adolfsen et al., 2004). Antibodies were generated in rabbits to both an N-terminal fragment fused with GST, and a synthetically produced peptide (sequence THSFGGTRDHDVVEEFIG) through Research Genetics (Invitrogen, Inc.). The anitsera obtained was purified to the peptide utilized in the antibody generation on an AKTA FPLC (Amersham Biosciences) as previously described (Adolfsen et al., 2004). In addition, antisera was affinity purified to full-length dARC1 fused to GST in a separate purification. Full length GST-dARC1 was loaded into a 10% polyacrylamide gel and transferred onto nitrocellulose. The nitrocellulose was stained with PonceauS and the band corresponding to the purified fusion protein was cut from the membrane, blocked, and sliced into 1cm x .3cm strips. These strips were incubated with antisera overnight at 4°C. Antibodies bound to the membrane were stripped from the membrane with 50mM glycine-HCl, pH 2.5 (1ml). The solution was re-equilibrated to pH 7 using 1M Tris, pH 9.5. Finally, resultant antibody was concentrated using 10K MWCO Amicon Ultra columns (Millipore, Inc.).

Electrophysiological analysis of dARC1^{ESM18}

Electrophysiological analysis was done as previously described (Montana and Littleton, 2004). Some differences were utilized in the analysis. Electrode resistances used were 20-40MΩ, pulled on a P-30 vertical pipette puller (Sutter Instruments). In analyses using two-electrode voltage clamp, the second electrode was normally 10-20MΩ on a 1X MGU headstage (Axon Instruments).

Only cells which had less than 10nA of leak current were utilized in the analysis, with most having less than 2nA. All stimulus signals were generated through the pCLAMP v8.0 program (Axon Instruments). mEJP recordings were done in CNS-intact animals in 1.5mM Ca^{2+} and 3μM TTX. All recordings were done in HL3 using 4mM or 20mM Mg^{2+} at the indicated Ca^{2+} concentrations (Stewart et al., 1994). Traces in the figures were plotted in Microsoft Excel by exporting the trace values into a spreadsheet. Data was transferred onto a second computer for analysis on pCLAMP v9.0.

Quantification of the electrophysiological recordings

mEJP analysis was done in a semi-automated manner using the event detection analysis in pCLAMP v9.0 using a template obtained from mEJP recordings done in *CantonS* based on 1000+ individual events. EJP analysis was done by averaging ten events in each muscle and counting the average amplitude as one measurement for the genotype assayed. High-frequency vesicle depletion was quantified by dividing the EJP at the designated time point by the first EJP amplitude. Paired-pulse facilitation was quantified by averaging ten paired-pulse events from a single muscle, then dividing the average second EJC by the average first EJC. Post-tetanic potentiation was quantified by averaging 30s of EJCs at 0.5Hz to determine baseline amplitude. All EJC amplitudes graphed are the EJC at the designated time point divided by the baseline EJC amplitude.

Immunohistochemical analysis and imaging

Structural analysis on third instar neuromuscular junctions was done as previously described using α-synaptotagmin 1 antisera at 1:1000 and affinity purified α-dARC1 at 1:500 (Littleton et al., 1993; Montana and Littleton, 2004). Imaging was done on an AxioScope 2 confocal microscope and processed with LSM software (Zeiss). All images shown are taken with a 40X/1.3NA oil-immersion lens (Zeiss).

Statistical analysis of data

Statistical analysis of the data was done in several programs. Student's T-test and ANOVA analysis was done using Microsoft Excel in the Microsoft Office XP Professional Software Suite (Microsoft). KS-test analysis on mEJP distributions was done using the KS-test applet at http://www.physics.csbsju.edu/stats/KS-test.n.plot_form.html. Post-hoc analysis of the ANOVA was done using the Tukey-test applet at http://department.obg.cuhk.edu.hk/ResearchSupport/Least_sig_diff_Tukey.asp in order to determine the least significant difference values.

Behavioral analysis of dARC1

Courtship conditioning assays were done as previously described (Ejima et al., 2005). Similarly, circadian rhythm analysis was done as previously described (Stoleru et al., 2004).

Acknowledgements

We thank Mark Mattaliano, Leslie Griffith, Bill Adolfsen, and Motojiro Yoshihara for helpful discussions about the manuscript. We would also like to thank the Bloomington Stock Center for *Drosophila* strains. This work was supported by grants from the NIH, the Human Frontiers Science Program, the Searle Scholars Program, and the Packard Foundation. J. Troy Littleton is an Alfred P. Sloan Research Fellow.

References

Adolfsen, B., and J.T. Littleton. 2001. Genetic and molecular analysis of the synaptotagmin family. *Cell Mol Life Sci.* 58:393-402.

Adolfsen, B., S. Saraswati, M. Yoshihara, and J.T. Littleton. 2004. Synaptotagmins are trafficked to distinct subcellular domains including the postsynaptic compartment. *J Cell Biol.* 166:249-60.

Allada, R., P. Emery, J.S. Takahashi, and M. Rosbash. 2001. Stopping time: the genetics of fly and mouse circadian clocks. *Annu Rev Neurosci.* 24:1091-119.

Bader, M.F., F. Doussau, S. Chasserot-Golaz, N. Vitale, and S. Gasman. 2004. Coupling actin and membrane dynamics during calcium-regulated exocytosis: a role for Rho and ARF GTPases. *Biochim Biophys Acta.* 1742:37-49.

Bailey, C.H., E.R. Kandel, and K. Si. 2004. The persistence of long-term memory: a molecular approach to self-sustaining changes in learning-induced synaptic growth. *Neuron.* 44:49-57.

Blitz, D.M., K.A. Foster, and W.G. Regehr. 2004. Short-term synaptic plasticity: a comparison of two synapses. *Nat Rev Neurosci.* 5:630-40.

Bogdanik, L., R. Mohrmann, A. Ramaekers, J. Bockaert, Y. Grau, K. Broadie, and M.L. Parmentier. 2004. The Drosophila metabotropic glutamate receptor DmGluRA regulates activity-dependent synaptic facilitation and fine synaptic morphology. *J Neurosci.* 24:9105-16.

Daniels, R.W., C.A. Collins, M.V. Gelfand, J. Dant, E.S. Brooks, D.E. Krantz, and A. DiAntonio. 2004. Increased expression of the Drosophila vesicular glutamate transporter leads to excess glutamate release and a compensatory decrease in quantal content. *J Neurosci.* 24:10466-74.

Davis, G.W., A. DiAntonio, S.A. Petersen, and C.S. Goodman. 1998. Postsynaptic PKA controls quantal size and reveals a retrograde signal

that regulates presynaptic transmitter release in Drosophila. *Neuron*. 20:305-15.

Davis, G.W., and C.S. Goodman. 1998a. Genetic analysis of synaptic development and plasticity: homeostatic regulation of synaptic efficacy. *Curr Opin Neurobiol*. 8:149-56.

Davis, G.W., and C.S. Goodman. 1998b. Synapse-specific control of synaptic efficacy at the terminals of a single neuron. *Nature*. 392:82-6.

Davis, G.W., C.M. Schuster, and C.S. Goodman. 1996. Genetic dissection of structural and functional components of synaptic plasticity. III. CREB is necessary for presynaptic functional plasticity. *Neuron.* 17:669-79.

Donai, H., H. Sugiura, D. Ara, Y. Yoshimura, K. Yamagata, and T. Yamauchi. 2003. Interaction of Arc with CaM kinase II and stimulation of neurite extension by Arc in neuroblastoma cells expressing CaM kinase II. *Neurosci Res*. 47:399-408.

Ejima, A., B.P. Smith, C. Lucas, J.D. Levine, and L.C. Griffith. 2005. Sequential learning of pheromonal cues modulates memory consolidation in trainer-specific associative courtship conditioning. *Curr Biol*. 15:194-206.

Elkins, T., B. Ganetzky, and C.F. Wu. 1986. A Drosophila mutation that eliminates a calcium-dependent potassium current. *Proc Natl Acad Sci U S A*. 83:8415-9.

Frey, N., T.A. McKinsey, and E.N. Olson. 2000. Decoding calcium signals involved in cardiac growth and function. *Nat Med*. 6:1221-7.

Gailly, P. 2002. New aspects of calcium signaling in skeletal muscle cells: implications in Duchenne muscular dystrophy. *Biochim Biophys Acta*. 1600:38-44.

Guzowski, J.F., G.L. Lyford, G.D. Stevenson, F.P. Houston, J.L. McGaugh, P.F. Worley, and C.A. Barnes. 2000. Inhibition of activity-dependent arc protein expression in the rat hippocampus impairs the maintenance of long-term potentiation and the consolidation of long-term memory. *J Neurosci*. 20:3993-4001.

Hall, J.C. 1994. The mating of a fly. *Science*. 264:1702-14.

Jackson, F.R., J. Gitschier, G.R. Strichartz, and L.M. Hall. 1985. Genetic modifications of voltage-sensitive sodium channels in Drosophila: gene dosage studies of the seizure locus. *J Neurosci*. 5:1144-51.

Joiner MI, A., and L.C. Griffith. 1997. CaM kinase II and visual input modulate memory formation in the neuronal circuit controlling courtship conditioning. *J Neurosci*. 17:9384-91.

Konopka, R.J., and S. Benzer. 1971. Clock mutants of Drosophila melanogaster. *Proc Natl Acad Sci U S A*. 68:2112-6.

Lanahan, A., and P. Worley. 1998. Immediate-early genes and synaptic function. *Neurobiol Learn Mem*. 70:37-43.

Leinwand, L.A. 2001. Calcineurin inhibition and cardiac hypertrophy: a matter of balance. *Proc Natl Acad Sci U S A*. 98:2947-9.

Littleton, J.T., H.J. Bellen, and M.S. Perin. 1993. Expression of synaptotagmin in Drosophila reveals transport and localization of synaptic vesicles to the synapse. *Development*. 118:1077-88.

Lyford, G.L., K. Yamagata, W.E. Kaufmann, C.A. Barnes, L.K. Sanders, N.G. Copeland, D.J. Gilbert, N.A. Jenkins, A.A. Lanahan, and P.F. Worley. 1995. Arc, a growth factor and activity-regulated gene, encodes a novel cytoskeleton-associated protein that is enriched in neuronal dendrites. *Neuron*. 14:433-45.

Maier, B., S. Medrano, S.B. Sleight, P.E. Visconti, and H. Scrable. 2003. Developmental association of the synaptic activity-regulated protein arc with the mouse acrosomal organelle and the sperm tail. *Biol Reprod*. 68:67-76.

Malenka, R.C., and M.F. Bear. 2004. LTP and LTD: an embarrassment of riches. *Neuron*. 44:5-21.

Moga, D.E., M.E. Calhoun, A. Chowdhury, P. Worley, J.H. Morrison, and M.L. Shapiro. 2004. Activity-regulated cytoskeletal-associated protein is

localized to recently activated excitatory synapses. *Neuroscience*. 125:7-11.

Montana, E.S., and J.T. Littleton. 2004. Characterization of a hypercontraction-induced myopathy in Drosophila caused by mutations in Mhc. *J Cell Biol*. 164:1045-54.

Nedivi, E., S. Fieldust, L.E. Theill, and D. Hevron. 1996. A set of genes expressed in response to light in the adult cerebral cortex and regulated during development. *Proc Natl Acad Sci U S A*. 93:2048-53.

Nishimura, M., K. Yamagata, H. Sugiura, and H. Okamura. 2003. The activity-regulated cytoskeleton-associated (Arc) gene is a new light-inducible early gene in the mouse suprachiasmatic nucleus. *Neuroscience*. 116:1141-7.

Paradis, S., S.T. Sweeney, and G.W. Davis. 2001. Homeostatic control of presynaptic release is triggered by postsynaptic membrane depolarization. *Neuron*. 30:737-49.

Phelps, C.B., and A.H. Brand. 1998. Ectopic gene expression in Drosophila using GAL4 system. *Methods*. 14:367-79.

Rikhy, R., M. Ramaswami, and K.S. Krishnan. 2003. A temperature-sensitive allele of Drosophila sesB reveals acute functions for the mitochondrial adenine nucleotide translocase in synaptic transmission and dynamin regulation. *Genetics*. 165:1243-53.

Schuster, C.M., G.W. Davis, R.D. Fetter, and C.S. Goodman. 1996a. Genetic dissection of structural and functional components of synaptic plasticity. I. Fasciclin II controls synaptic stabilization and growth. *Neuron*. 17:641-54.

Schuster, C.M., G.W. Davis, R.D. Fetter, and C.S. Goodman. 1996b. Genetic dissection of structural and functional components of synaptic plasticity. II. Fasciclin II controls presynaptic structural plasticity. *Neuron*. 17:655-67.

Shinozaki, K., K. Maruyama, H. Kume, H. Kuzume, and K. Obata. 1997. A novel brain gene, norbin, induced by treatment of tetraethylammonium in rat hippocampal slice and accompanied with neurite-outgrowth in neuro 2a cells. *Biochem Biophys Res Commun*. 240:766-71.

Steward, O. 2002. mRNA at synapses, synaptic plasticity, and memory consolidation. *Neuron*. 36:338-40.

Steward, O., C.S. Wallace, G.L. Lyford, and P.F. Worley. 1998. Synaptic activation causes the mRNA for the IEG Arc to localize selectively near activated postsynaptic sites on dendrites. *Neuron*. 21:741-51.

Steward, O., and P. Worley. 2002. Local synthesis of proteins at synaptic sites on dendrites: role in synaptic plasticity and memory consolidation? *Neurobiol Learn Mem*. 78:508-27.

Stewart, B.A., H.L. Atwood, J.J. Renger, J. Wang, and C.F. Wu. 1994. Improved stability of Drosophila larval neuromuscular preparations in haemolymph-like physiological solutions. *J Comp Physiol [A]*. 175:179-91.

Stoleru, D., Y. Peng, J. Agosto, and M. Rosbash. 2004. Coupled oscillators control morning and evening locomotor behaviour of Drosophila. *Nature*. 431:862-8.

Suri, V., J.C. Hall, and M. Rosbash. 2000. Two novel doubletime mutants alter circadian properties and eliminate the delay between RNA and protein in Drosophila. *J Neurosci*. 20:7547-55.

Tan, A., R. Moratalla, G.L. Lyford, P. Worley, and A.M. Graybiel. 2000. The activity-regulated cytoskeletal-associated protein arc is expressed in different striosome-matrix patterns following exposure to amphetamine and cocaine. *J Neurochem*. 74:2074-8.

Tompkins, L., R.W. Siegel, D.A. Gailey, and J.C. Hall. 1983. Conditioned courtship in Drosophila and its mediation by association of chemical cues. *Behav Genet*. 13:565-78.

Ying, S.W., M. Futter, K. Rosenblum, M.J. Webber, S.P. Hunt, T.V. Bliss, and C.R. Bramham. 2002. Brain-derived neurotrophic factor induces long-term potentiation in intact adult hippocampus: requirement for ERK activation coupled to CREB and upregulation of Arc synthesis. *J Neurosci*. 22:1532-40.

Zucker, R.S., and W.G. Regehr. 2002. Short-term synaptic plasticity. *Annu Rev Physiol*. 64:355-405.

Future Directions

Future directions

The analysis we have performed has provided the groundwork for using *Drosophila* as a model system to study diseased states of human cardiac and skeletal muscle. This model system is not only amenable to large-scale genetic screens for dissecting the gene network underlying muscle function, but also provides a cellular model for understanding diseased states and how the cell responds to genetic mutations which affect muscle function. The following experiments will help in elucidating the mechanisms activated in response to hypercontraction-induced myopathy in *Drosophila*.

Review of the results

We have described the isolation and characterization of a *Drosophila* mutant which causes a hypercontraction-induced myopathy. This myopathy included a degradation of the IFM in adult flies. These mutants harbor mutations in the *Mhc* locus, which encodes all isoforms of the muscle-specific type II myosin motor. The mutations mapped onto the ATP binding/hydrolysis domain of the protein, suggesting an alteration in the ATP cycle of Mhc. The genetic interactions of Mhc^{S1} and Mhc^{S2} with known muscle mutants revealed that the mutations led to hypercontraction defects, rather than decreasing contractile activity, altering the dosage of Mhc protein in the muscle, or leading to developmental defects in the architecture of the sarcomere.

Interestingly, these mutations were isolated based upon a temperature-dependent behavioral defect, showing temperature-dependent seizures in adult animals. Electrophysiological analysis of this behavior showed that these seizures were correlated with abnormal activity in the giant fiber flight system and were dependent upon neuronal activity. It is likely that these seizures occur in the muscle, but require nerve activity to trigger them. Further, analysis of the third instar muscle 6/7 neuromuscular junction revealed no changes in the synaptic structure, nor alterations in the functional activity of the synapse. However, this analysis revealed spontaneous muscle contractions that were independent of presynaptic input and external Ca^{2+}.

From the data, we hypothesized that these mutations lead to a stabilization of an intermediate of the contractile cycle, causing contraction to occur spontaneously. In addition, this stabilization could potentially lead to higher contraction forces in the muscle, compromising the structural integrity. Interestingly, we found that all hypercontraction mutants that we assayed exhibited temperature-dependent seizure activity. This activity may be due to alterations in the regulation of contraction which could lead to changes in the intracellular Ca^{2+} through buffering of Ca^{2+} by the troponin complex. Further, this suggests the possibility that hypercontraction alters the overall state of the muscle. This state may be similar to states resulting from hypertrophic cardiomyopathies and muscular dystrophies.

Based upon the characterization of the *Mhc* mutants, we began a study of the altered muscle state in hypercontraction mutants. Given the strong parallels

between the genetics of hypertrophic cardiomyopathies and the genetics of flight behavior in *Drosophila*, we hypothesized that the cellular response to these mutations may be likewise conserved. Therefore, *Drosophila* may provide a model system in which to study diseases caused by contractile dysfunctions.

In order to gain insight into this altered muscle state, expression analysis was done. By analyzing changes in the transcriptional profile, we may begin to understand the functional differences between normal and diseased muscle states. Two important observations were made in this study. The first observation is that, like the genetic data, the transcriptional response to hypercontraction is similar to transcriptional responses found in diseased states of human cardiac and skeletal muscles. This strengthened the hypothesis that conservation exists in how the muscle responds to changes in contractile function. This response includes the upregulation of genes in adult muscle which are normally developmentally regulated, the upregulation of genes which function in immune responses, and the downregulation of genes involved in energy and metabolism.

The second observation was that the predominant response to hypercontraction-induced myopathy was an upregulation of genes which regulate and support the actin cytoskeleton. These genes most likely act at three key structural sites in the muscle which include the nuclear membrane, the Z-line, and the plasma membrane. This may indicate a remodeling of the structural architecture which underlies muscle support utilized to both withstand the forces generated during contraction and to provide leverage with which to transduce

forces. Interestingly, several of the genes identified as upregulated in this analysis have been previously identified in mammals. These genes, *dARC1*, *MSP-300*, and *dNeurochondrin* have been shown to be regulated in response to neuronal activity at excitatory synapses in the mammalian CNS.

The identification of these genes supported the idea of conserved muscle response to mutation-induced changes in muscle function. Ca^{2+} has been implicated as an important mediator of both muscle diseases and activity-dependent synaptic strengthening. This overlap in identified genes suggests that not only is the response to muscle dysfunction conserved, but the signaling pathway underlying this response may also be utilized in different contexts.

Although the identification of differentially-regulated transcripts gives a genomic view of how muscles respond to dysfunction, the functional implications of this altered regulation remain unclear. Studying the loss-of-function phenotype of these genes individually and in context of muscle dysfunction is important in understanding the consequences of differential regulation. Given that at least a subset of these genes seem to play roles in both synaptic plasticity and muscle remodeling, understanding the roles within both contexts can give a more comprehensive picture of the functional roles of the proteins these genes encode.

To this end, we began by studying the loss-of-function phenotype of the most upregulated gene identified in the expression analysis, *dARC1*, in the context of activity-dependent synaptic modulation. The analysis revealed that *dARC1* does not mediate an integral role of synaptic function on several levels.

These include basal synaptic transmission, high-frequency induced vesicle recycling, short-term plasticity, and postsynaptic glutamate receptor trafficking and clustering. In addition, *dARC1* does not likely underlie critical roles in the learning and memory of courtship conditioning, or circadian rhythm. These results suggest that either *dARC1* does not play a central role in these processes, or mediates subtle aspects of these processes that are undetectable by the assays.

The following chapter is a suggestion on the path I feel the project should go in the future. There are two large questions that need to be answered, and though these questions are difficult, these experiments can begin to address them in the *Drosophila* myopathy model. The first question is, "Does the Ca^{2+} dysregulation that has been suggested and implied exist in *Drosophila,* and if so, is it similar to that found in mammalian muscle disease?" The second, "What is the functional consequence of differential gene regulation and how does it occur in response to a single point mutation in *Mhc*?"

The importance of Ca^{2+} in hypercontraction-induced myopathy

Although the electrophysiological characterization of Mhc^{S1}/+ flies suggested a dysregulation of Ca^{2+}, more experiments towards direct visualization of the intracellular Ca^{2+} will determine whether this is the case. These experiments can be done in the third instar body wall muscles, as these muscles are relatively large and easily imaged for this type of analysis. Utilizing Fura-2 to

quantitatively assay the intracellular Ca^{2+} concentration of muscles at rest, direct comparisons between wildtype and hypercontracted muscles may be made. Imaging of the muscle may reveal several possibilities. The first possibility is that there is no quantitative difference in the intracellular Ca^{2+} between normal and hyperconcontracted muscle, suggesting that the spontaneous contractions are caused by Ca^{2+}-independent mechanisms. The second is that Ca^{2+} concentrations are constitutively higher in mutant muscles. This would indicate a chronic overload of Ca^{2+} in the muscle, affecting all Ca^{2+}-dependent processes throughout the cell. Finally, imaging could reveal Ca^{2+} concentrations oscillating over time, which would lead to slow contraction waves as seen in third instar neuromuscular junction recordings.

It may also be the case that Ca^{2+} is affected in an excitation-dependent manner. Therefore, imaging of muscles before, during and after presynaptic activation may yield additional insights into Ca^{2+} homeostasis in mutant muscles. Indeed, in mouse models of hypertrophic cardiomyopathy, Ca^{2+} transient decays during muscle activation have been shown to be significantly prolonged (Kim et al., 1999). In addition, results in the mouse *mdx* model of muscular dystrophy have shown that 20% of *mdx* fibers have a 10- to 30-fold increase in Ca^{2+} influx (De Backer et al., 2002). These experiments will determine whether Ca^{2+} dysregulation occurs in hypercontraction mutants. Further, if dysregulation occurs, imaging will determine whether this is a constitutive, oscillatory, or excitation-dependent alteration in Ca^{2+} homeostasis.

Pharmacological studies of Ca^{2+} homeostasis

Another avenue to pursue in Ca^{2+} homeostasis is to use pharmacological compounds to modify the defects associated with hypercontraction. Several drugs have been characterized to alter Ca^{2+} handling processes in the cell. Diltiazem acts as an inhibitor of L-type Ca^{2+} channels. Mice harboring the R403Q mutation in *α-MHC* have decreases in the SR Ca^{2+}, SR Ca^{2+} buffer calsequestrin, and decreases in ryanodine receptors prior to the morphological changes associated with hypertrophy. However, early administration of diltiazem prevented these Ca^{2+}-related defects as well as the pathological defects (Semsarian et al., 2002). Treatment of *Drosophila* with diltiazem may alter the effects of hypercontraction mutations. In addition, calcineurin inhibiting drugs have likewise been utilized to prevent hypertrophy in mice (Sussman et al., 1998). Assessing the effect of calcineurin-modulating compounds on the *Drosophila* hypercontraction phenotype may yield insights into the conservation of mechanism shared between flies and mammals, and may help in understanding how Ca^{2+} plays a role in muscle dysfunction.

Revisiting the transcriptional regulation in hypercontraction mutants

The transcriptional profile of the *Mhc* mutants has revealed a potential conservation of the response to muscle dysfunction, including the upregulation of developmentally-regulated sarcomeric genes and immune-response related

genes, and the downregulation of energy and metabolism genes. Although we have complete genomic view of the transcriptional response to muscle dysfunction in *Drosophila*, it is important to understand the functional consequences of this differential regulation. To this end, comprehensive characterization of the gene set identified will help direct future experiments in interpreting the transcriptional response. This revisiting of the transcriptional profile would occur along two lines of experimentation—1) Multi-layered classification of the gene set to help identify differentially-regulated genes that may yield insights in a reverse-genetic approach, and 2) Bioinformatics-based approach to help identify how these genes are or are not co-regulated and what proteins/molecular pathways mediate this differential regulation. These two lines of experimentation will allow us to identify WHAT are the important players and their functions (both endogenously and in context of a hypercontraction), WHERE are they localized, and HOW are they co-regulated.

Classification of the dataset includes the identification of the expression patterns of the differentially-regulated genes. This analysis can be done in a high-throughput manner in wildtype and mutant *Drosophila* embryos. Many of the genes which may represent a remodeling response in the microarray remain uncharacterized. We analyzed the expression pattern for a small subset of these genes in embryos. Our data suggests that a large proportion of the genes may be expressed in the muscle. Performing *in situ* hybridization experiments on all of the differentially-regulated genes will help in identifying which of the genes are expressed differentially in the muscle, and which are expressed in other tissues.

Comparing this expression pattern in mutant embryos may further identify which of the genes that are expressed in the muscle are specifically upregulated in mutant muscle. This analysis can help in narrowing the gene list to a smaller subset for further study.

The second analysis that can be done in large numbers is to characterize the subcellular localization and RNAi defects of genes in cultured *Drosophila* S2 cells. RNAi analysis has been done previously with a large number of genes (~90) which putatively function in the regulation of actin in the context of lamellae formation (Rogers et al., 2003). In addition, we have performed a preliminary analysis of the localization of a small number of genes when overexpressed in S2 cells as GFP fusion proteins. Using these methods, we can begin to classify genes based upon localization and RNAi phenotype in S2 cell cultures. From previous studies, we expect at least eight classes of defects from RNAi in *Drosophila S2* cells: 1) stellate morphology, 2) failure to spread with actin accumulation at the cortex, 3) failure to spread with actin throughout the cell, 4) increased width of lamellae, 5) increased membrane ruffling, 6) thin process formation, 7) cytokinesis failure, and 8) no effect. Further, the GFP fusion constructs will allow us to classify genes based upon subcellular localization.

Potential regulators of transcription

A bioinformatics-based analysis can be done with the data obtained from the microarray to identify potential regulatory sequences which may mediate the

transcriptional response seen in muscle dysfunction. Identifying the upstream regulatory sequences which may participate in the differential regulation will help in discovering which proteins mediate the gene regulation. This approach begins with a primary gene set that is consistently upregulated across all hypercontraction mutants assayed in the expression analysis. Genes which have known or potential roles in regulating cytoskeletal structure *in vivo* are prime candidates for the initial seed set with which to do the following analysis.

First, a list of all potential enhancer sites within 2kb upstream of the ORF as well as within the first exon and intron of the gene is composed. These sites can be determined by two ways. First, all characterized regulatory sequences are placed into this list obtained from the TRANSFAC database (Wingender et al., 1997). Second, from the initial seed set sequences, three algorithms can be used to search for motifs which include AlignACE, MEME, and MotifSampler (Bailey and Elkan, 1995; Hughes et al., 2000; Thijs et al., 2002). These algorithms search for sequence motifs which occur more often in the seed set as compared to the entire genome using position weight matrices. Position weight matrices estimate the binding specificities of the motifs based upon the specific sequence of any single predicted motif as compared to the frequency distribution of the nucleotides in each position across all related motifs. These matrices assume independence between positions of a particular motif, and thus do not account for potential position interactions. Therefore, they provide a first-order approximation of the binding interaction energies between the theoretical

transcription factor and the particular instance of the motif, providing more stringency than simple consensus sequence analysis.

After identification of all known and potential enhancer sites, a search for modules of motifs can be done. Modules are defined by the occurrence of two to four motifs bound by the following rules: 1) the maximum distance between motifs is equal to a predefined distance (25, 50, 100, and 200 bp), 2) if two motifs overlap in sequence, then the maximal overlap can be no more than half the length of a single motif, 3) the module must be present in at least 4 genes within the initial seed set, and 4) the module must be enriched within the initial seed set when compared with the frequency of occurrence across the entire genome. For the fourth criteria, it is required that the module must appear at least as frequently or more frequently within the seed set of sequences as it does within the entire genome. This type of analysis has previously been done on genes which are integral to anterior-posterior axis formation in *Drosophila* (Kreiman, 2004). Using this analysis in context of the microarray can lead to identification of sequences which are important to the regulation of the genes in the microarray. In addition, these sequences can be further utilized to isolate factors which may potentially bind them *in vivo*. However, bioinformatics approaches tend to return a lot of background "noise," along with biologically-relevant information. Therefore, as a first test of stringency, *in situ* hybridization anaysis can be done on gene sets controlled by the same regulatory modules. In this manner, gene sets can be identified that contain sequences which potentially co-regulate them, and that this regulation may occur in the muscle of *Drosophila*.

Functional studies of the genes identified as differentially-regulated

Reverse-genetic studies of the genes identified in the transcriptional profile will aid in our understanding of the functional relevance of these genes. Analysis has begun with the most upregulated transcript identified, *dARC1*. Several of the genes identified in the microarray have been previously identified in mammals to be regulated by neuronal activity. Understanding the roles of these proteins in both cellular contexts can provide a more thorough picture of the functions these genes may mediate. Our analysis has shown that in *Drosophila*, *dARC1* does not seem to play a role in synaptic function and plasticity. However, the analysis did not assay its function in sensitized backgrounds, nor did it investigate a potential role for *dARC1* in modulation of these processes. Studying the role of *dARC1* in sensitized backgrounds may reveal subtle aspects of function.

In addition, we did not study the roles of *dARC1* in muscle dysfunction. Although overexpression studies suggest that it may act on sarcomeric structures, the subcellular distribution of endogenous dARC1 remains unclear. Structural analysis of *dARC1* mutant muscle may show subtle defects in the ultrastructural properties of the sarcomere. Further, analysis of *dARC1* mutants in the context of hypercontraction backgrounds may reveal defects that remain obscured in normal backgrounds.

Finally, based upon data from the experiments outlined above, additional reverse-genetic analyses can be done on novel genes based upon the resulting classifications obtained. The multi-layered classification of the differentially-regulated gene set will allow for more informed decisions on which of the differentially-regulated genes should be further studied.

Genetic interaction studies with hypercontraction mutants

The advantage of *Drosophila* is its ability to be used for large-scale forward-genetic screens in identifying novel components of characterized pathways. Screening for modifiers of *Mhc* mutants may identify novel genes involved in hypercontraction-induced myopathies. Indeed, many genes have already been identified by screening for flight-defective mutants and modifiers of this behavior (Ferrus et al., 2000; Homyk et al., 1980; Mogami and Hotta, 1981; Vigoreaux, 2001). However, the TS defects of hypercontraction mutants provide a novel behavior to screen for new interactions. Already, we have identified two dominant TS mutations which show genetic interactions with the *Mhc* hypercontraction mutants. These include *Swing* and *Breakdance* (Montana and Littleton, 2004). These mutants map to cytological regions 42A and 88F based upon recombination mapping of the TS behavior and non-complementation for recessive lethality with characterized deficiencies. Screening for additional interactions, as well as cloning the genes mutated in *Swing* and *Breakdance* will

aid in identifying the underlying molecular and genetic components in muscle function.

In addition to screening for new mutations, testing the ability of known genes to modify different aspects of the *Mhc* phenotype can help determine whether previously identified genes play a role in *Drosophila*. Inducing mutations in the components of the calcineurin complex, as well as utilizing previously isolated mutations in genes such as the L-type Ca^{2+} channel, calmodulin, and CamKII may provide a parallel method in which to study the role of Ca^{2+} in hypercontraction muscles (Gellon et al., 1997; Nelson et al., 1997). Recently, overexpression of the human gene myosin-binding protein C (*MYBPC3)* in *Drosophila* was shown to cause flightless behavior (Manh et al., 2005). Mutations in *MYBC3* can cause hypertrophic cardiomyopathies in humans (Bonne et al., 1995). Interestingly, calmodulin was upregulated in these overexpression flies and mutations in calmodulin acted as dominant suppressors of the flightless defect (Manh et al., 2005). Therefore, using forward- and reverse- genetic techniques will allow for the identification of novel genes involved in diseased states of the muscle, as well as help in our understanding of how the muscle compensates for or responds to changes in sarcomeric structure and function.

Concluding remarks

We have identified and characterized a model system for human muscle diseases in *Drosophila*. The characterization has revealed general parallels between hypercontraction-induced myopathies, human cardiomyopathies and muscular dystrophies. In addition to these parallels, a novel muscle remodeling response which acts upon the actin cytoskeleton and its support structures has been revealed. This response may represent a functional compensation of the muscle in response to altered contractile properties.

However, despite the similarities and parallels, it is still unclear whether a mutation in *Mhc* triggers a conserved signaling response which results in the altered transcriptional profile. Alternatively, contractile dysfunction in both cardiac muscle and *Drosophila* flight muscles activates unrelated signaling events. However, through necessity of functional compensation, a convergence occurs within the altered transcriptional output. The future experiments outlined above can begin to dissect the conservation of signaling within these two systems.

Finally, this model system may provide two promising avenues in which to expedite our understanding of muscle dysfunction. It provides a system to use forward-genetic screens to identify novel genes required in the proper functioning of muscles. This system is well established and is continually providing new insights into the genetic components required in the muscle. Second, it provides a cellular model in which to understand the pathways and signaling events which are activated in response to contractile dysfunction caused by mutation. Further characterization of this model may lead to a platform in which to identify novel

compounds for the treatment of muscular dystrophies and cardiomyopathies, bridging basic research with direct application to real-world problems.

References

Bailey, T.L., and C. Elkan. 1995. The value of prior knowledge in discovering motifs with MEME. *Proc Int Conf Intell Syst Mol Biol.* 3:21-9.

Bonne, G., L. Carrier, J. Bercovici, C. Cruaud, P. Richard, B. Hainque, M. Gautel, S. Labeit, M. James, J. Beckmann, and et al. 1995. Cardiac myosin binding protein-C gene splice acceptor site mutation is associated with familial hypertrophic cardiomyopathy. *Nat Genet.* 11:438-40.

De Backer, F., C. Vandebrouck, P. Gailly, and J.M. Gillis. 2002. Long-term study of Ca(2+) homeostasis and of survival in collagenase-isolated muscle fibres from normal and mdx mice. *J Physiol.* 542:855-65.

Ferrus, A., A. Acebes, M.C. Marin, and A. Hernandez-Hernandez. 2000. A genetic approach to detect muscle protein interactions in vivo. *Trends Cardiovasc Med.* 10:293-8.

Gellon, G., K.W. Harding, N. McGinnis, M.M. Martin, and W. McGinnis. 1997. A genetic screen for modifiers of Deformed homeotic function identifies novel genes required for head development. *Development.* 124:3321-31.

Homyk, T., Jr., J. Szidonya, and D.T. Suzuki. 1980. Behavioral mutants of Drosophila melanogaster. III. Isolation and mapping of mutations by direct visual observations of behavioral phenotypes. *Mol Gen Genet.* 177:553-65.

Hughes, J.D., P.W. Estep, S. Tavazoie, and G.M. Church. 2000. Computational identification of cis-regulatory elements associated with groups of functionally related genes in Saccharomyces cerevisiae. *J Mol Biol.* 296:1205-14.

Kim, S.J., K. Iizuka, R.A. Kelly, Y.J. Geng, S.P. Bishop, G. Yang, A. Kudej, B.K. McConnell, C.E. Seidman, J.G. Seidman, and S.F. Vatner. 1999. An alpha-cardiac myosin heavy chain gene mutation impairs contraction and relaxation function of cardiac myocytes. *Am J Physiol.* 276:H1780-7.

Kreiman, G. 2004. Identification of sparsely distributed clusters of cis-regulatory elements in sets of co-expressed genes. *Nucleic Acids Res.* 32:2889-900.

Manh, T.P., M. Mokrane, E. Georgenthum, J. Flavigny, L. Carrier, M. Semeriva, M. Piovant, and L. Roder. 2005. Expression of cardiac myosin-binding protein-C (cMyBP-C) in Drosophila as a model for the study of human cardiomyopathies. *Hum Mol Genet*. 14:7-17.

Mogami, K., and Y. Hotta. 1981. Isolation of Drosophila flightless mutants which affect myofibrillar proteins of indirect flight muscle. *Mol Gen Genet*. 183:409-17.

Montana, E.S., and J.T. Littleton. 2004. Characterization of a hypercontraction-induced myopathy in Drosophila caused by mutations in Mhc. *J Cell Biol*. 164:1045-54.

Nelson, H.B., R.G. Heiman, C. Bolduc, G.E. Kovalick, P. Whitley, M. Stern, and K. Beckingham. 1997. Calmodulin point mutations affect Drosophila development and behavior. *Genetics*. 147:1783-98.

Rogers, S.L., U. Wiedemann, N. Stuurman, and R.D. Vale. 2003. Molecular requirements for actin-based lamella formation in Drosophila S2 cells. *J Cell Biol*. 162:1079-88.

Semsarian, C., I. Ahmad, M. Giewat, D. Georgakopoulos, J.P. Schmitt, B.K. McConnell, S. Reiken, U. Mende, A.R. Marks, D.A. Kass, C.E. Seidman, and J.G. Seidman. 2002. The L-type calcium channel inhibitor diltiazem prevents cardiomyopathy in a mouse model. *J Clin Invest*. 109:1013-20.

Sussman, M.A., H.W. Lim, N. Gude, T. Taigen, E.N. Olson, J. Robbins, M.C. Colbert, A. Gualberto, D.F. Wieczorek, and J.D. Molkentin. 1998. Prevention of cardiac hypertrophy in mice by calcineurin inhibition. *Science*. 281:1690-3.

Thijs, G., K. Marchal, M. Lescot, S. Rombauts, B. De Moor, P. Rouze, and Y. Moreau. 2002. A Gibbs sampling method to detect overrepresented motifs in the upstream regions of coexpressed genes. *J Comput Biol*. 9:447-64.

Vigoreaux, J.O. 2001. Genetics of the Drosophila flight muscle myofibril: a window into the biology of complex systems. *Bioessays*. 23:1047-63.

Wingender, E., A.E. Kel, O.V. Kel, H. Karas, T. Heinemeyer, P. Dietze, R. Knuppel, A.G. Romaschenko, and N.A. Kolchanov. 1997. TRANSFAC,

TRRD and COMPEL: towards a federated database system on transcriptional regulation. *Nucleic Acids Res*. 25:265-8.

Appendix

Contained within this appendix are two tables to supplement Chapter 3. These tables represent the complete list of genes identified in the expression analysis as determined by the criteria we set. Genes are grouped according to known functions or putative functions as determined by BLAST analysis through NCBI. In addition, there are also two tables which summarize the electrophysiological studies described in Chapter 4.

Supplemental Table I. Upregulated genes in the *Samba* mutants

Muscle Structure and Function

Gene	CS Signal	CS SD	Mutant Signal	Mutant SD	Average Signal FC	Samba SLR Average	Samba2 SLR Average	SAM FC	Algorithm
CG12505	579.33	473.21	3353.40	950.89	5.79	3.00	3.00	5.79	ABCD
CG5797	3160.75	1297.21	22587.27	3160.28	7.15	2.95	2.61	7.15	ABCD
Act88F	10493.42	5568.01	46679.65	4187.62	4.45	2.25	2.06	4.45	ABCD
CG5775	11088.03	2289.31	45266.90	4213.05	4.08	2.10	2.01	4.08	ABCD
Mlp60A	1224.45	228.54	5334.03	1359.00	4.36	2.14	1.69	4.36	ABCD
Msp-300	51.25	6.06	216.33	99.80	4.22	2.44	1.73	3.52	ABCD
CG9025	681.72	163.60	1353.00	137.30	1.98	0.92	0.86	1.98	ABCD
CG2471	1747.93	110.18	2697.70	325.83	1.54	0.81	0.66	1.54	ABCD
Act57B	36098.75	3998.79	63933.40	8460.42	1.77	0.74	0.73	1.77	ABCD
flw	1542.88	346.60	2914.55	793.42	1.89	1.04	0.97		ABC
CG18242	25.17	19.90	60.45	50.53	2.40	1.04	0.92		ABC
Ket	824.38	245.79	1956.93	735.75	2.37	1.33	1.05		ABC
CG13941	63.37	10.11	634.60	167.74	10.01	3.15	3.08	10.01	ACD
sqh	5915.50	300.85	8105.55	1250.23	1.37	0.85	0.43		AB
BcDNA:LD24380	2484.60	149.96	3768.85	373.77	1.52	0.85	0.36	1.52	BD
BG:DS00180.8	3368.77	437.94	5163.53	694.75	1.53	0.58	0.42	1.53	BD
CG2330	1732.22	290.35	4316.98	1700.51	2.49	1.02	0.53		B
CG6972	1003.53	365.06	2027.10	569.87	2.02	0.89	0.56		B
CG3397	1146.35	262.79	1837.82	412.87	1.60	1.05	0.32		B
Mlp84B	10213.85	2175.26	13503.95	2411.89	1.32	0.72	0.16		B
CG5080	3773.05	434.98	5810.40	2137.56	1.54	0.69	0.17		B
CG13311	1023.70	294.95	1722.98	444.21	1.68	1.04	0.45		B
CG16743	2764.35	516.68	3091.07	829.46	1.12	0.69	0.36		B
CG10420	381.52	85.20	587.03	124.80	1.54	0.91	0.60		B
CG10732	682.28	158.19	1358.20	478.58	1.99	0.85	0.61		B
CG5600	921.72	322.79	1436.57	271.83	1.56	0.87	0.39		B
CG6831	1285.95	255.85	1864.32	532.21	1.45	0.65	0.27		B
CG5010	4339.55	1490.98	6745.40	2017.47	1.55	0.61	0.56		B
CG18061	2908.05	413.85	3550.10	385.37	1.22	0.47	0.19		B
CG13124	5648.97	1278.30	7262.42	1263.31	1.29	0.43	0.14		B
CG8679	39.73	17.30	209.45	19.82	5.27	1.85	1.67	5.27	D
CG6238	2558.80	308.93	3621.90	277.15	1.42	0.20	0.30	1.42	D
CG6416	20587.03	68.51	24181.48	1498.94	1.17	0.20	0.30	1.17	D
CG6718	170.57	46.14	163.90	58.36	0.96	0.38	-0.34	1.57	D
CG3652	2323.30	158.46	2702.08	71.00	1.16	-0.07	-0.01	1.16	D

Serine Proteases

Gene	CS Signal	CS SD	Mutant Signal	Mutant SD	Average Signal FC	Samba SLR Average	Samba2 SLR Average	SAM FC	Algorithm
CG18180	4379.40	537.32	23790.50	8986.28	5.43	1.54	2.48	5.43	ABCD
CG10745	960.72	192.83	2530.70	633.35	2.63	1.36	1.12	2.63	ABCD
Ser99Dc	4669.30	669.59	8698.35	1328.14	1.86	0.93	1.17	1.86	ABCD
Ser6	445.65	144.90	1921.50	572.37	4.31	1.75	1.76	4.31	ACD
CG6639	27.67	15.00	829.10	658.37	29.96	5.45	2.22		AB
CG8329	3900.40	312.80	6232.42	1890.38	1.60	0.89	0.30		AB
CG2229	22230.53	6991.20	41123.38	13910.11	1.85	0.39	0.97		AC
Ser99Da	56990.73	8839.46	89887.33	20472.99	1.58	0.32	0.88		AC
gammaTry	28654.15	633.03	35385.27	4746.18	1.23	0.27	0.45		AC
CG16705	5639.75	856.41	8179.75	3364.38	1.45	0.80	-0.04		B
CG18436	2064.77	283.49	2787.40	366.24	1.35	0.79	0.26		B
CG16713	3384.73	503.97	4158.73	984.89	1.23	0.68	0.14		B
CG3088	4043.72	367.26	4919.88	1719.49	1.22	0.51	-0.02		B
Ser99Db	34900.18	9205.45	43105.52	15530.74	1.24	0.04	0.56		C
Ser4	18174.18	9936.79	33237.58	11891.70	1.83	0.43	0.67		C
CG10475	2838.75	827.32	4147.27	1362.13	1.46	0.13	0.91		C
CG18030	321.67	162.74	596.48	227.27	1.85	0.41	1.16		C
CG8869	34348.27	9060.19	45841.03	7184.86	1.33	0.21	0.58		C
CG3380	402.08	334.00	697.70	189.33	1.74	1.16	1.29		C
epsilonTry	13451.20	3180.71	16101.92	5311.16	1.20	0.05	0.59		C
Ser99Db	34900.18	9205.45	43105.52	15530.74	1.24	0.04	0.56		C
CG16996	3841.93	258.50	5726.92	585.73	1.49	0.42	0.23	1.49	D
CG6457	30226.00	188.57	37404.23	2723.29	1.24	0.35	0.38	1.24	D
CG11836	646.47	57.90	850.35	66.52	1.32	0.23	0.26	1.32	D

Unknown

Gene	CS Signal	CS SD	Mutant Signal	Mutant SD	Average Signal FC	Samba SLR Average	Samba2 SLR Average	SAM FC	Algorithm
CG6183	8031.15	1705.86	24253.92	5889.10	3.02	1.77	1.56	3.02	ABCD
CG10912	7068.80	758.75	15842.45	1486.85	2.24	1.12	1.08	2.24	ABCD
CG16844	38055.23	4334.78	70761.65	11536.91	1.86	1.17	0.77	1.86	ABCD
CG14245	16259.58	2452.59	29025.40	2621.06	1.79	0.75	0.78	1.79	ABCD
CG15067	7377.00	1609.21	16408.32	3410.20	2.22	1.32	0.62	2.22	ABCD
CG14109	1980.05	188.63	3695.03	719.93	1.87	0.82	0.58	1.87	ABCD
CG1054	815.18	188.53	1869.23	741.63	2.29	1.42	0.99		ABC
CG16836	10103.85	2971.50	20738.35	7988.03	2.05	1.42	0.79		ABC
CG14688	3971.33	810.32	8682.10	2776.22	2.19	1.33	0.70		ABC
CG18067	11302.30	1197.82	27972.00	11626.79	2.47	1.59	0.84		ABC
CG15065	38819.95	7129.63	72595.70	22546.34	1.87	1.24	0.57		ABC
CG13482	3534.52	1221.88	5608.17	657.02	1.59	0.56	0.71		ABC
CG13323	8670.60	601.78	12579.53	2776.76	1.45	0.59	0.39	1.34	ABD
CG13905	433.25	156.59	1250.85	421.65	2.89	1.86	1.53		AB

CG18279	3254.65	846.27	7272.50	3740.34	2.23	1.28	0.49		AB
CG15825	4883.15	826.49	7317.65	1275.03	1.50	0.98	0.48		AB
CG5676	8141.20	2690.70	13057.85	2257.59	1.60	0.76	0.46		AB
CG13323	8670.60	601.78	12579.53	2776.76	1.45	0.59	0.39	1.34	AB
CG15043	1708.73	378.12	2831.10	634.56	1.66	0.64	0.92		AC
CG6043	3188.65	469.35	5231.17	726.72	1.64	0.93	0.40	1.64	BD
CG14292	10967.47	1740.98	21028.72	3456.51	1.92	0.40	0.71	1.92	CD
CG15066	1381.92	419.48	5336.48	3080.70	3.86	2.50	0.83		B
CG5778	10584.92	2383.18	21682.93	8150.02	2.05	1.15	0.38		B
CG5791	15083.83	2203.28	27492.90	14182.89	1.82	1.35	0.03		B
CG14401	2809.55	624.93	4714.98	1498.27	1.68	0.98	0.36		B
BG:DS01759.2	6750.08	2837.57	9565.88	2646.58	1.42	0.82	0.19		B
CG9928	5092.72	1323.17	6936.98	3164.13	1.36	0.86	-0.16		B
CG15893	1383.17	551.37	2642.20	1505.38	1.91	1.09	0.34		B
CG1572	2530.32	562.56	3973.38	589.81	1.57	0.89	0.36		B
CG9691	16512.90	1500.13	20503.27	2766.71	1.24	0.52	0.21		B
CG9192	282.52	59.83	873.57	543.83	3.09	2.20	0.53		B
CG9616	180.70	129.18	379.30	176.75	2.10	1.68	0.63		B
CG13324	1664.70	395.07	2565.07	476.43	1.54	0.70	0.49		B
BG:DS00810.3	23848.50	8805.53	33557.88	5766.11	1.41	0.67	0.44		B
CG14998	1337.10	395.15	1892.53	322.07	1.42	0.67	0.39		B
CG16971	1001.00	197.70	1566.00	540.63	1.56	0.70	0.18		B
CG10911	33529.75	2661.42	46719.45	9434.27	1.39	0.49	0.36		B
CG13249	1363.70	439.91	1728.65	463.03	1.27	0.42	0.33		B
CG6981	3719.48	864.56	4127.85	1060.39	1.11	0.51	0.10		B
CG15068	41245.75	8593.22	48850.27	4937.07	1.18	0.38	0.19		B
CG7418	6005.42	1024.38	9276.67	3778.28	1.54	0.34	1.00		C
CG4363	8822.42	2258.81	12990.33	4383.57	1.47	0.11	0.84		C
CG11671	762.55	222.91	1079.05	383.76	1.42	0.09	0.86		C
CG2081	426.05	117.82	690.92	203.71	1.62	0.36	0.93		C
CG18170	58.88	38.71	226.02	36.78	3.84	1.66	1.94	3.84	D
CG13641	183.85	113.41	1084.20	318.83	5.90	2.42	2.61	5.90	D
CG14428	2017.05	321.18	3413.68	472.31	1.69	0.48	0.40	1.69	D
CG16707	3330.02	640.53	5061.60	337.79	1.52	0.51	0.40	1.52	D
CG10103	2766.40	450.54	3879.60	140.62	1.40	0.20	0.11	1.40	D
EcDNA:GH08385	568.15	113.89	953.02	122.76	1.68	0.51	0.43	1.68	D
CG17025	126.83	17.07	260.00	52.37	2.05	0.90	0.61	2.05	D
CG14052	41.33	17.79	126.60	29.48	3.06	1.63	1.01	3.06	D
CG9038	3102.00	199.59	3915.18	325.79	1.26	0.36	0.26	1.26	D
CG12868	915.58	175.96	1422.78	169.41	1.55	0.43	0.50	1.55	D

Chaperones

Gene	CS Signal	CS SD	Mutant Signal	Mutant SD	Average Signal FC	Samba SLR Average	Samba2 SLR Average	SAM FC	Algorithm
CG14207	5914.20	261.78	15925.72	1255.96	2.69	1.55	1.17	2.69	ABCD
CG9434	1150.88	430.45	2604.60	531.05	2.26	1.40	1.14	2.26	ABCD
l(2)efl	8818.33	993.11	17085.28	5677.13	1.94	1.16	0.43		ABC
CG7409	5338.63	1048.63	8019.98	898.07	1.50	0.59	0.58		ABC
Hsp22	1117.85	228.99	3863.95	1026.84	3.46	1.05	1.50	3.46	CD
CG7033	987.67	225.75	1323.05	580.45	1.34	0.67	0.22		B
CG6489	247.25	117.63	413.20	258.84	1.67	-0.62	1.63		C
CG4461	18238.48	3071.19	23275.53	4541.44	1.28	0.10	0.45		C

Nuclear Biology

Gene	CS Signal	CS SD	Mutant Signal	Mutant SD	Average Signal FC	Samba SLR Average	Samba2 SLR Average	SAM FC	Algorithm
CG10910	1754.30	344.36	5687.00	3933.69	3.24	0.57	2.33		AC
CG12040	1775.32	193.15	2498.35	426.09	1.41	0.52	0.28		B
CG3308	3484.42	996.67	5526.85	877.99	1.59	0.89	0.54		B
CG8547	2688.25	1001.73	4548.43	1114.29	1.69	0.97	0.41		B
CG11878	3630.65	814.91	4254.25	1478.98	1.17	0.51	-0.08		B
EG:EG0007.7	467.30	22.05	643.65	50.34	1.38	0.56	0.36	1.38	D
CG16859	1229.30	116.03	1858.65	193.98	1.51	0.62	0.55	1.51	D
CG5740	615.40	72.85	934.45	96.52	1.52	0.48	0.56	1.52	D
CG11504	177.88	52.17	542.90	133.08	3.05	1.77	1.03	3.05	D
CtBP	834.00	164.72	1349.53	146.40	1.62	0.37	0.32	1.62	D
NTX1	982.58	179.54	1491.30	157.48	1.52	0.42	0.41	1.52	D
CG9989	57.35	6.42	328.65	126.02	5.73	2.95	1.53	5.73	D
Dhh1	148.10	40.76	267.75	35.11	1.81	0.81	0.57	1.81	D

Metabolism and Energy

Gene	CS Signal	CS SD	Mutant Signal	Mutant SD	Average Signal FC	Samba SLR Average	Samba2 SLR Average	SAM FC	Algorithm
Uro	3828.03	760.87	8116.85	795.42	2.12	1.24	1.02	2.12	ABCD
CG6188	12266.75	2062.73	23569.90	5114.61	1.92	1.22	0.72	1.92	ABCD
CG11089	2243.70	175.73	4336.67	960.90	1.93	0.65	0.68	1.93	ABCD
CG11796	9900.67	1540.84	14411.35	1400.83	1.46	0.55	0.51	1.46	ABCD
CG2708	723.50	279.40	1280.53	166.20	1.77	0.82	0.93		ABC
CG9468	3016.10	769.88	5890.05	1863.52	1.95	1.05	0.88		ABC
ade3	4453.10	1071.10	7857.55	1743.49	1.76	0.77	0.90		ABC
CG9466	200.90	122.29	186.25	27.86	0.93	0.48	0.01		ABC
Amy-d	27624.03	3184.90	45391.60	11084.16	1.64	0.43	0.71		ABC
CG14935	2033.30	596.79	2767.45	560.51	1.36	0.85	0.54		ABC
Ahcy13	5150.63	187.58	6185.53	654.23	1.20	0.49	0.48		ABC
CG17560	5582.40	520.83	8421.58	1403.62	1.51	0.59	0.48		AB
Hn	8903.10	1409.41	12669.20	1628.46	1.42	0.56	0.38		AB

ade5	7518.70	416.44	10628.00	2393.16	1.41	0.64	0.63		AC
Ugt35b	1888.28	213.64	3228.03	403.64	1.71	0.77	0.48	1.71	BD
Ef1alpha100E	1536.72	179.23	2451.50	401.82	1.60	0.81	0.44	1.60	BD
CG6687	2222.85	471.36	3341.50	900.79	1.50	1.03	0.27		B
Aats-asp	2270.40	130.40	3759.95	1029.67	1.66	0.84	0.36		B
CG10638	1254.60	273.48	1826.77	287.11	1.46	0.62	0.49		B
CG3011	2799.02	460.53	3726.50	670.58	1.33	0.77	0.25		B
CG8913	2248.50	340.39	3144.80	855.79	1.40	0.76	0.18		B
Cyp6w1	1559.75	388.99	1900.42	921.76	1.22	0.76	-0.19		B
CG7627	543.72	253.19	968.27	490.13	1.78	1.53	0.56		B
CalpB	1382.60	265.71	2177.20	394.85	1.57	0.88	0.50		B
CG9463	634.95	87.87	867.73	327.63	1.37	0.81	0.49		B
Gs1	1110.65	301.47	1716.90	478.96	1.55	0.73	0.43		B
Nmdmc	1619.50	516.78	2506.95	508.25	1.55	0.65	0.41		B
CG6283	4915.75	515.61	5421.15	871.09	1.10	0.48	0.45		B
CG6767	6199.08	995.31	8859.13	1652.35	1.43	0.55	0.28		B
CG18658	2908.60	626.05	3538.18	816.96	1.22	0.53	0.24		B
CG9480	2389.15	690.66	2902.00	751.31	1.21	0.66	0.11		B
CG5191	1329.05	141.55	1815.93	246.60	1.37	0.54	0.23		B
Transferrin	22609.23	1952.56	30755.90	10355.19	1.36	0.71	0.03		B
aralar1	2741.75	190.33	3453.27	657.61	1.26	0.51	0.22		B
CG5802	3106.85	634.45	3872.35	791.09	1.25	0.56	0.15		B
timp	3713.50	725.22	4371.08	966.72	1.18	0.53	0.16		B
MtnB	532.92	121.80	679.82	406.70	1.28	0.73	-0.19		B
Cyp6a23	1204.03	402.87	1522.25	1134.95	1.26	-0.52	0.79		C
LysP	1147.68	476.16	2787.98	1285.71	2.43	1.21	1.04		C
CG6910	3645.40	837.40	6365.37	1397.35	1.75	0.69	0.70		C
CG3168	9541.95	1422.48	12109.57	1391.13	1.27	0.28	0.54		C
CG17531	257.97	204.76	310.47	186.90	1.20	-0.49	1.08		C
CG6640	1018.52	607.81	1260.65	917.06	1.24	-0.68	0.94		C
CG10622	2656.10	80.74	3115.77	90.32	1.17	0.16	0.28	1.17	D
CG9164	74.83	35.79	265.57	46.14	3.55	1.51	1.88	3.55	D
6-phosphofructo-2-kinase	5466.00	406.12	7274.90	471.70	1.33	0.42	0.46	1.33	D
CG1753	577.35	72.03	1004.45	135.29	1.74	0.39	0.54	1.74	D
CG1827	2294.13	70.94	2588.20	79.20	1.13	0.14	0.19	1.13	D
CG15093	3619.52	261.12	4498.65	202.75	1.24	0.28	0.33	1.24	D
CG8773	758.97	74.97	1088.70	103.40	1.43	0.19	0.34	1.43	D
eIF-4E	5260.95	544.21	6897.50	504.38	1.31	0.29	0.17	1.31	D
ade2	2163.47	287.51	3331.93	447.19	1.54	0.53	0.60	1.54	D
Adhr	383.45	46.38	544.15	52.98	1.42	0.30	0.37	1.42	D
CG3376	820.15	132.11	1270.23	168.68	1.55	0.39	0.10	1.55	D
CG18377	295.22	46.88	455.53	56.35	1.54	0.45	0.48	1.54	D

Immune and Defense Response

Gene	CS Signal	CS SD	Mutant Signal	Mutant SD	Average Signal FC	Samba SLR Average	Samba2 SLR Average	SAM FC	Algorithm
CG15231	42427.40	4856.65	75557.53	14440.08	1.78	0.90	0.64	1.78	ABCD
CG14746	5759.40	1111.98	10329.65	2163.06	1.79	0.51	0.94		ABC
CG18108	5831.07	2335.65	15167.02	5451.39	2.60	1.73	0.94		ABC
CG8577	1668.35	596.13	2728.55	630.73	1.64	0.54	0.90		ABC
CG9681	3371.15	918.21	5122.70	451.33	1.52	0.54	0.75		ABC
CG14745	3775.27	515.56	5103.78	526.67	1.35	0.53	0.66		ABC
Phas1	10208.55	1738.05	16501.80	2244.29	1.62	0.75	0.50	1.62	ABD
Drs	9503.17	5971.63	23327.32	13848.53	2.45	2.18	0.38		AB
IM2	3524.10	546.78	10114.92	4443.20	2.87	1.69	0.68		AB
Ag5r2	2235.52	281.23	4516.30	957.22	2.02	0.90	0.58	2.02	BD
CG13422	5253.40	2096.48	8299.97	3481.58	1.58	1.12	-0.08		B
CG4740	3523.00	3511.75	3747.17	1560.92	1.06	0.90	0.03		B
CG14027	978.63	329.45	1498.07	472.07	1.53	0.56	0.21		B
drongo	1705.80	117.61	2129.80	113.28	1.25	0.21	0.13	1.25	D
CG17352	848.95	27.44	1208.45	151.21	1.42	0.15	-0.01	1.42	D

Signaling

Gene	CS Signal	CS SD	Mutant Signal	Mutant SD	Average Signal FC	Samba SLR Average	Samba2 SLR Average	SAM FC	Algorithm
CG2656	686.60	120.30	1651.00	417.40	2.40	1.07	0.90	2.40	BD
grk	419.63	121.11	860.22	220.53	2.05	0.91	0.49		B
CG8242	4159.95	800.24	4652.40	432.34	1.12	0.59	0.32		B
puc	563.32	181.77	980.85	263.22	1.74	0.86	0.51		B
Lk6	1638.00	491.59	2329.38	397.69	1.42	0.72	0.47		B
cact	2460.58	150.21	2833.92	799.24	1.15	0.49	0.14		B
CG9311	1678.82	158.36	1721.63	331.92	1.03	0.24	0.01	1.41	D
CG1900	845.63	56.61	1111.63	93.70	1.31	0.65	0.38	1.31	D

Other

Gene	CS Signal	CS SD	Mutant Signal	Mutant SD	Average Signal FC	Samba SLR Average	Samba2 SLR Average	SAM FC	Algorithm
CG12844	1776.85	403.16	4827.25	1585.35	2.72	1.68	1.05		ABC
CG5597	3465.58	542.23	6448.83	1645.75	1.86	0.97	0.59		ABC
BcDNA:GH05741	441.17	52.90	2125.75	1768.73	4.82	2.98	0.52		AB
AnnIX	3932.25	595.35	6769.00	1654.79	1.72	0.94	0.42		AB
CG12843	2555.70	93.63	4542.40	836.14	1.78	0.66	0.42	1.78	BD
CG7874	17192.10	1575.76	29292.35	5132.68	1.70	0.25	0.66	1.70	CD
CG8791	269.48	168.57	607.88	91.08	2.26	1.78	1.50		B
CG4250	3010.40	920.01	7131.32	4525.69	2.37	1.14	0.46		B
CG3246	2525.77	146.87	2888.42	705.42	1.14	0.54	0.14		B
BcDNA:LD19727	785.75	314.96	1339.07	580.91	1.70	1.22	0.40		B

Prcot	9484.95	999.35	11448.53	1792.35	1.21	0.43	0.20		B
CG14499	929.72	384.93	2767.92	2105.51	2.98	-0 08	2.40		C
CG16775	959.00	166.45	1843.38	147.49	1.92	0.85	1.09	1.92	D
CG12838	171.73	93.05	571.65	129.05	3.33	1.51	1.39	3.33	D
Ela	631 97	323.32	1579.57	222.07	2.50	1 60	1.13	2.50	D
CHES-1-like	452.58	31.34	572.45	38.55	1.26	0.35	0.28	1 26	D

Supplemental Table II. Downregulated genes in the *Samba* mutants

Metabolism and Energy

Gene	CS Signal	CS SD	Mutant Signal	Mutant SD	Average Signal FC	Samba SLR Average	Samba2 SLR Average	SAM FC	Algorithm
CG12628	40046.32	5281.32	27545.22	3004.29	0.69	-0.65	-0.55		ABC
CG12628	40046.32	5281.32	27545.22	3004.29	0.69	-0.65	-0.55		ABC
CG15434	4219.42	881.60	1877.30	541.16	0.44	-1.41	-0.79		ABC
Mgstl	21549.15	3907.22	15155.70	2230.68	0.70	-0.51	-0.50		ABC
CG12400	25448.63	3043.79	18197.50	2507.09	0.72	-0.52	-0.33		ABC
CG12374	19916.60	8451.89	11086.25	4505.97	0 56	-1 00	-0.79		ABC
CG14576	11247.50	2303.17	7904.58	1195.02	0.70	-0.52	-0.45		ABC
CG7712	10417.05	2126.08	7878.10	1142.33	0.76	-0.50	-0.29		ABC
CG14482	33671 85	4673.78	25256.77	5790.02	0.75	-0.65	-0.26		AB
CG9090	28831.00	6283.12	16693.35	6255.57	0.58	-1.27	-0.21		B
CG2022	7045.95	379.48	4422.15	1294.19	0.63	-0.95	-0 33		B
CG15328	19217.72	2040.59	13859.22	4234.36	0.72	-0 72	-0 18		B
CG9240	1890.20	386.20	1193.60	240.63	0.63	-0.71	-0.48		B
Qcr9	41777 98	9827.63	30038 05	5466.72	0.72	-0.57	-0.21		B
Cyt-c2	27063 40	6308 54	19258.72	3957.62	0.71	-0.72	-0 25		B
CG5703	10545.20	1417.29	7586.15	1537.12	0.72	-0.74	-0.21		B
CG4769	20515 48	3605.84	15480.70	2848.26	0 75	-0.63	-0 21		B
Gapdh1	58771 30	11677.69	43830.82	9477.04	0.75	-0.60	-0.20		B
Qcr9	41777.98	9827.63	30038.05	5466.72	0.72	-0.57	-0.21		B
CG12233	9882 03	963 76	7467.67	1309 87	0.76	-0.62	-0.16		B
porin	21333 23	1907.80	15700.53	1478.96	0.74	-0.46	-0.27		B
CoVa	42068.97	6625.01	32941.30	7144.13	0.78	-0.62	-0.13		B
Oscp	38607.57	6437 13	30420.60	7824.83	0 79	-0.57	-0 17		B
Pgk	12577 42	1376.53	9327.48	960.10	0.74	-0.47	-0 25		B
CG6666	8758.80	949 57	6485.82	1227.35	0.74	-0.55	-0.18		B
ATPsyn-b	20596 48	3940 70	15723 88	2977.87	0.76	-0.52	-0.19		B
CG4169	23846.32	2924.41	18031 63	2377 30	0 76	-0 47	-0.22		B
Pgi	17812.80	3061.81	14165.20	2117.98	0.80	-0.50	-0.18		B
ATPsyn-d	31379 77	3251 80	25902.75	6004.82	0.83	-0.57	-0 09		B
CG7580	64617 90	7294 97	52665.52	5725.21	0.82	-0.42	-0.19		B
ATPsyn-gamma	31854.50	7345.81	24783.53	4515.92	0.78	-0.44	-0.16		B
CG17280	48800 60	9680.91	39793 63	7554.27	0.82	-0.48	-0.11		B
CG3861	14424 13	1611 36	11938.30	4012.94	0.83	-0 50	0.04		B
CG18323	52029 70	6656.23	46846.13	6673.83	0.90	-0.39	-0.01		B
CG6733	2095.52	304 56	2410.40	1185 69	1.15	-0 52	0.49		B
CG3944	6689.63	1713.51	5083.22	1107.71	0.76	-0.62	-0.28		B
ATPsyn-Cf6	20446 35	3390.73	14854.85	1720.31	0.73	-0.64	-0.23		B
CG8689	2673 55	217 76	1905.38	575.28	0.71	-0.51	-0 34		B
Scs-fp	10672 78	2299 04	7778.25	809.45	0.73	-0.59	-0 26		B
Lectin-galC1	4716.75	1370.15	3276.40	279.60	0.69	-0.55	-0.29		B
SdhB	17539.33	1964.58	13496 55	2650.93	0.77	-0.58	-0.24		B
CG7361	8822.63	1287 43	7261 27	1800.38	0.82	-0.55	-0.27		B
CG1274	5352.38	732.59	3893.80	554.69	0.73	-0.41	-0.39		B
CG18624	12437 97	2218 86	8899.35	1396.22	0.72	-0.57	-0.23		B
CG3214	8238 00	1198 12	5905.52	487 97	0.72	-0 51	-0.27		B
CG9140	11373.07	1787.74	9009.45	1476.11	0.79	-0.60	-0.17		B
CG9032	18658.85	4602 01	13868.05	2908.16	0 74	-0.55	-0.18		B
CG11015	41741 80	8831 34	34190 05	6234.65	0.82	-0.47	-0 26		B
Eno	23768.02	2840.71	18408.20	2225.28	0.77	-0.42	-0.27		B
CG10664	52932.25	8397 34	40890.17	6379.92	0 77	-0.46	-0.21		B
CG8708	2530 07	561.02	1801 65	116.14	0.71	-0.46	-0.22		B
CG9172	12964.38	2196.28	10427.65	1146.43	0.80	-0.45	-0.22		B
CG9244	24883.25	6474 12	20157.00	4441 11	0.81	-0.60	-0.05		B
CG7430	7598.95	676 01	5812.90	623 38	0.76	-0.44	-0.23		B
CG5028	11147.13	1516.68	9085.63	2087.80	0.82	-0.56	-0.09		B
ND75	9112.75	1194 53	7301 55	219.17	0.80	-0 49	-0.17		B
GlyP	14248 05	4784 69	12670.58	1529.47	0.89	-0.36	-0 28		B
CG1746	1143.20	265 94	1151.35	362.13	1.01	-0.10	0.02		B
CG10219	14958.43	1867 67	12789 85	2809.62	0.86	-0.45	-0 17		B
CG12203	3704 13	681 46	2992.68	570 66	0 81	-0.47	-0.13		B
CG7181	33129.50	5670 61	25859.35	3041.98	0.78	-0.41	0.18		B
BG:DS09217 1	7614 13	1399 66	5940.98	803.79	0 78	-0 49	-0.09		B
CG9297	12649.13	2005 65	14321 58	3411.33	1.13	-0 36	0.01		B
blw	47047.68	6800 21	40110.13	9242.82	0.85	-0.43	-0.10		B
CG14235	27217.30	3162 60	25431.00	6783.57	0.93	-0 43	-0 09		B
Dbi	30056.48	5282 07	25688.93	6812.89	0.85	-0 43	-0.04		B
CG3321	39531.58	11335.00	34695.02	11314.41	0.88	-0.45	0.01		B
Argk	26293.68	3563 36	21866 40	4171 14	0 83	-0 42	-0.03		B
CG11876	11637 13	1282 75	9644 42	1653.46	0.83	-0.31	-0.11		B
Ald	62193.67	6455.36	57974.38	9460.64	0.93	-0.34	-0.04		B
CG9306	17856.97	459 41	15507.93	1888 51	0.87	-0.37	-0.01		B
CG3731	24015.40	2578 59	20501 50	3432.51	0 85	-0 34	0.01		B
CG1787	3004.35	214.78	2103.60	478.62	0.70	-0.41	-0.71		C
Cyp6a17	868.45	64 26	812.18	369 84	0.94	0.06	-1 01		C
Atpalpha	3081 55	436.94	2391.30	420 31	0 78	-0.46	-0.76		C
CG5932	3173.70	1112.19	2566.38	1201.43	0.81	-0.12	-0.67		C
CG10361	2222.60	117.33	1839.67	38.88	0.83	-0.19	-0.08	0.83	D

Muscle Structure and Function

Gene	CS Signal	CS SD	Mutant Signal	Mutant SD	Average Signal FC	Samba SLR Average	Samba2 SLR Average	SAM FC	Algorithm
CG14022	5774.52	585.28	3454.55	1142 12	0.60	-1.05	-0.47		ABC

Ca-P60A	34574.30	4200.06	26608.38	5156.32	0.77	-0.48	-0.09	B
CG6514	2489.32	293.14	2070.82	413.95	0.83	-0.39	-0.11	B
fln	6678.17	1837.91	5141.45	1520.69	0.77	-0.63	0.15	B
CG15306	18707.78	3201.35	17391.75	6728.25	0.93	-0.48	0.13	B
TpnC41C	16283.97	5267.47	13494.35	3284.33	0.83	-0.46	0.14	B

Other

Gene	CS Signal	CS SD	Mutant Signal	Mutant SD	Average Signal FC	Samba SLR Average	Samba2 SLR Average	SAM FC	Algorithm
Lsp1beta	1436.38	219.23	296.77	144.24	0.21	-2.70	-1.68	0.21	ABCD
Lsp2	28329.52	4154.80	9717.88	2277.85	0.34	-2.09	-1.45	0.34	ABCD
CG11853	7114.35	2400.95	1325.10	347.53	0.19	-2.33	-2.90		ABC
nAcRbeta-64B	1099.90	53.82	743.55	88.14	0.68	-0.67	-0.56	0.68	ABD
CG7630	42247.10	4527.39	31987.65	5240.01	0.76	-0.59	-0.30		AB
CG7592	1882.27	403.47	1101.27	561.63	0.59	-1.37	-0.13		B
CG15304	35859.13	5797.78	29066.00	4856.57	0.81	-0.46	-0.16		B
CG6749	1160.35	175.22	704.85	269.36	0.61	-0.74	-0.97		B
CG9399	9768.10	1524.34	8053.63	1419.23	0.82	-0.50	-0.31		B
CG11218	18924.30	2149.33	16201.00	1328.51	0.86	-0.32	-0.18		B
Rac1	1405.63	523.26	1122.32	327.85	0.80	-0.19	-0.19		B
CG8496	1119.38	317.97	676.40	378.14	0.60	-0.28	-1.33		C
CG11797	2738.30	444.30	1799.82	230.25	0.66	-0.37	-0.79		C
CG14259	1176.93	97.92	765.70	171.84	0.65	-0.26	-0.76		C
CG10812	7035.38	1196.93	5465.17	1188.63	0.78	-0.33	-0.63		C
Sdic	6142.97	493.50	4497.48	831.80	0.73	-0.17	-0.69		C
CG3739	11828.82	2588.32	8902.35	3309.73	0.75	-0.10	-0.70		C
CG1839	705.30	57.34	470.88	46.09	0.67	-0.20	-0.53	0.67	D
spt6	1068.67	84.91	738.75	30.32	0.69	-0.18	-0.12	0.69	D
polo	2545.85	281.46	1649.55	102.78	0.65	-0.42	-0.44	0.65	D
CG5213	2144.78	120.52	1333.35	245.85	0.62	-0.52	-0.48	0.62	D
CG9135	667.67	67.23	455.03	18.46	0.68	-0.28	-0.04	0.68	D

Unknown

Gene	CS Signal	CS SD	Mutant Signal	Mutant SD	Average Signal FC	Samba SLR Average	Samba2 SLR Average	SAM FC	Algorithm
CG15353	9515.38	1117.45	6773.77	543.46	0.71	-0.40	-0.48	0.66	ABCD
BG:DS07851.4	9993.45	1278.10	6089.98	2091.39	0.61	-0.43	-1.07		ABC
CG13328	31256.57	8132.46	23416.58	2622.74	0.75	-0.40	-0.27		ABC
CG11373	7720.90	969.49	6011.07	1604.33	0.78	-0.57	-0.20		B
CG11752	9877.10	830.46	7273.65	1614.27	0.74	-0.51	-0.25		B
CG16826	55492.75	9188.67	45744.08	7860.30	0.82	-0.31	-0.21		B
CG10513	5395.08	1044.05	3552.60	1003.73	0.66	-0.45	-0.74		C
CG17763	1518.35	436.28	1009.30	68.61	0.66	-0.45	-0.63		C
CG13026	3859.23	1048.24	3008.17	255.21	0.78	-0.29	-0.46		C
CG5773	2703.80	793.56	2566.43	920.65	0.95	-0.15	0.58		C
CG12057	5184.75	2135.89	5416.20	2492.86	1.04	0.45	-0.41		C
CG10514	10446.47	574.22	7180.58	753.81	0.69	-0.34	-0.41	0.69	D
CG12821	184.02	8.08	132.92	8.65	0.72	-0.11	0.02	0.72	D

Table S3: Summary of the Electrophysiological Data in the Mutant Analysis of *dARC1*

Genotype	*n* (muscles)	Resting Potential (mV)	EJP Amplitude (mV)	$[Ca^{2+}]_{ext}$ (mM)
w; dARC1 ^{ESM115}	**11**	**-65.74 ± 2.65**	**1.73 ± 0.28**	0.1
w; dARC1 ^{ESM18}	10	-64.39 ± 1.82	1.96 ± 0.31	
w; dARC1 ^{ESM295}	**12**	**-63.45 ± 1.32**	**18.70 ± 1.85**	0.2
w; dARC1 ^{ESM18}	15	-66.41 ± 1.32	14.86 ± 1.34	
w; dARC1 ^{ESM295}	**8**	**-68.32 ± 2.37**	**31.33 ± 1.76**	0.4
w; dARC1 ^{ESM18}	10	-66.25 ± 1.69	29.56 ± 1.05	
w; dARC1 ^{ESM115}	**17**	**-70.04 ± 1.74**	**42.22 ± 1.05**	1.5
w; dARC1 ^{ESM18}	18	-71.49 ± 1.86	42.82 ± 1.53	

**Data expressed as value ± SEM*

Control
Mutant

Table S4: Summary of the Electrophysiological Data in the Overexpression Analysis of *dARC1*

Genotype	*n* (muscles)	Resting Potential (mV)	EJP Amplitude (mV)	$[Ca^{2+}]_{ext}$ (mM)
w;UAS-dARC1/+	10	-69.49 ± 2.25	3.60 ± 1.02	
C155/w	9	-62.72 ± 3.34	4.30 ±0.74	
w;Mhc-GAL4/+	8	-60.35 ± 2.20	2.17 ± 0.77	0.1
C155/w; UAS-dARC1/+	10	-65.00 ± 2.09	3.46 ± 0.95	
w; Mhc-GAL4,+/+,UAS-dARC1	8	-66.76 ± 2.55	1.76 ± 0.16	
w;UAS-dARC1/+	9	-66.72 ± 1.16	21.36 ± 1.09	
C155/w	9	-70.63 ± 1.98	25.81 ± 2.40	
w;Mhc-GAL4/+	8	-63.21 ± 1.80	19.23 ± 2.38	0.2
C155/w; UAS-dARC1/+	8	-68.82 ± 2.28	22.78 ± 2.36	
w; Mhc-GAL4,+/+,UAS-dARC1	9	-67.34 ± 1.42	23.11 ± 3.09	
w;UAS-dARC1/+	8	-72.02 ± 1.44	38.19 ± 1.54	
C155/w	10	-76.45 ± 1.75	42.76 ± 1.41	
w;Mhc-GAL4/+	8	-74.27 ± 2.48	40.74 ± 2.83	0.4
C155/w; UAS-dARC1/+	8	-71.94 ± 1.59	39.42 1.43	
w; Mhc-GAL4,+/+,UAS-dARC1	9	-74.05 ± 1.67	41.71 ± 1.89	

**Data expressed as value ± SEM*

Control
Mutant